PhD Program in Bioengineering and Robotics

Curriculum: Bionanotechnology

Emulsion technology for the development of novel Alginate-based composite materials for controlled drug delivery applications

Student: Setti Chiara

Cycle: XXXI

Tutors:
Athanassia Athanassiou
Ilker S. Bayer
Giulia Suarato

To my family

A scientist in his laboratory is not a mere technician: he is also a child confronting natural phenomena that impress him as though they were fairy tales. (M. Curie)

Table of Contents

List of Figures and Tables

Figure 2.11: Antiseptic drug release profiles from various alginate- MaterBi® matrices, for release periods of (a) 60 minutes, (b) 5 hours, and (c) 2days. Each data point is an average of at least triplicate measurements.

Figure 2.12: Atomic Force Microscope images depicting the surface topography of eosin-loaded fabricated matrices, before the drug release experiment (a, d) and after 1 hour of release in PBS (b, e). SEM images shown in (c,f) confirm formation of pits seen in (b,e). The reported matrices were composed of (a-c) 50wt.% alginate – 50wt.% MaterBi® and (d-f) 100% MaterBi® White arrows are indicating the "pitting" phenomenon, suggesting the liberation of the drug from the matrices. Scale bar 10 μm.

Figure 2.13: SEM images of (a) 100% MaterBi®, (b) 90wt.% MaterBi®– 10wt.% alginate, (c) 80wt.% MaterBi® – 20wt.% alginate, (d) 70wt.% MaterBi® – 30wt.% alginate, (e) 60wt.% MaterBi® – 40wt.% alginate and (f) 50wt.% MaterBi® – 50wt.% alginate after 1 week.

Figure 2.14: Effect of Calcium Chloride concentration on drug release (%) of the hydrophilic model drug from pure alginate films.

Figure 2.15: Effect of the crosslinking on 100% alginate, 50 wt.% alginate–50 wt.% MaterBi® and 30 wt.% alginate – 70 wt.% MaterBi® films. Increase in percent decrease in release due to cross-linking indicates slower and lower amount release. The decline in percent decrease in release after reaching its maximum indicates that the release rate starts to catch up with the un-crosslinked films. If the percent decrease in release does not decline but remains steady after reaching the maximum, the crosslinked matrix could not release more than the un-crosslinked film. See Fig. 2.20 for a schematic demonstration. Each data point is an average of at least triplicate measurements.

Figure 2.16: Effect of the calcium crosslinking treatment on the hydrophilic, antiseptic drug (eosin) release from (a) 100% alginate film, (b) 50wt.% alginate – 50wt.% MaterBi®, and (c) 30wt.% alginate – 70wt.% MaterBi® matrices.

Figure 2.17: Hydrophobic drug (curcumin) release profiles for 60 minutes (a) and 5 hours (b). The release profile is divided in two plots in order to aid inspection of the initial release period. Each data point is an average of at least triplicate measurements.

Figure 2.18: Schematic representation of composite films comprising (a) 30 wt.% alginate-70 wt.% MaterBi® and (b) 50 wt.% alginate-50 wt.% MaterBi®. In the latter, the alginate domains encapsulating curcumin can be easily eroded by the release

List of abbreviations

ACN – Anthocyanin

AFM – Atomic Force Microscopy

BSA – Bovine Serum Albumin

CaAlg – Calcium Alginate

Cur – Curcumin

DAPI – 4'-6-diamino-2-phenylimidale

DNA – deoxyribonucleic acid

EIP - emulsion inversion point

FTIR - Fourier transform infrared

HCl – Hydrochloric Acid

HLB - hydrophilic-lipophilic balance

HPH – High Pressure Homogenizer

IL - interleukin

LSGS - Low Serum Growth Supplement

Mcfe – Concentrated extract from *Prunus mahaleb L.* fruIT

NaOH – sodium hydroxide

PBS - phosphate buffered saline

PIC - phase-inversion composition

PIT – phase-inversion temperature

pKa – logarithm of the acid dissociation constant

PCL – poly-eε-caprolactone

PPR - pattern recognition receptors

RNA – ribonucleic acid

TGA – Thermogravimetric Analysis

TLR - toll-like receptor

SEM– scanning electron microscopy

SIF – Simulated Intestinal Fluid

SGF – Simulated Gastric Fluid

WST1 – (water-soluble tetrazolium salts)-1

Acknowledgments

I want first of all to thank Dr. Athanassia Athanassiou for welcoming me in her laboratory, in which I always found a stimulating, familiar and multidisciplinary environment.
Thanks, Nassia, for always being available for me, kind, but at the same time an excellent leader able to give scientific advice that often allowed me to solve the problems encountered during the course of my research.

I would also like to thank my tutors Dr. Ilker Bayer and Dr. Giulia Suarato for always supporting and enduring me throughout my doctorate. Thank you for teaching me how to do my research at my best and for teaching your expertise, thanks for the advices and for passing on my passion for this job.

I want to thank all the colleagues in my group for these past years together. A special thanks, however, goes to Laura, Francesca, Aldo (Caty), Davide, Gianvito (Dr. Caputo or Gianvi), Luca (Fish), Maria (Maraia), Alex (Sandrino), Doriana, Giammarino, Alice and Simone.
Thank you very much because without you my doctorate would not have been the same. Thanks for the shared moments together, for the laughter that we made in the laboratory, which have lightened the long days of experiments. Thank you for having endured and supported me in difficult moments and for always giving me good advice, scientific and life.
For me you were not just mere colleagues, but you are and will always be good friends. You are all fantastic people and I wish the best to each of you.

I want to thank my family: my parents, my brother Walter, my uncles, aunts and my grandmothers. Thank you for the free love you have always given me. Thanks for always making me not to give up even in the most difficult moments.

Abstract

Emulsions have been used for centuries in many fields, such as pharmaceutical, cosmetic, food, and agriculture industry. Manufacturers of pharmaceutical products have recently shown great attention for multifunctional products in which different active agents can be incorporated, and for controlled drug delivery systems. Emulsion technology is a very simple, inexpensive and easy-to-scale approach. This technique is characterized by high loading capacity and encapsulation efficiency for therapeutic agents, independently from their nature (hydrophobic or hydrophilic). On the other hand, the other advantage is related to the possibility to use emulsion technology, to combine materials with different physiochemical properties.

The aim of my doctoral research was focused on the development of new polymeric Alginate-based composite materials for biomedical applications, specifically, controlled delivery systems for drugs or bioactive molecules.

The idea was to use biocompatible and non-toxic polymers, both of synthetic and natural origin, to produce the above-mentioned constructs. Biopolymers are widely used as scaffolds for biomedical applications, especially in tissue engineering and drug delivery systems due to their excellent properties such as biocompatibility, biodegradability to non-toxic products and bioactivity. In these fields, the biopolymers have been processed in different forms such as films, sponges, beads, hydrogels and capsules.

However, emulsions containing dissolved biopolymers both in the oil and water phases are very scarce. In this thesis, we demonstrate such an emulsion, in which the oil phase contains a hydrophobic biodegradable polymeric material and the water phase is constituted by a sodium alginate solution. Emulsion technology was the main technique employed for the fabrication of composite matrices, constituted of hydrophilic and hydrophobic polymers, and for the encapsulation of model drugs (single and dual delivery of hydrophilic and hydrophobic active principles). Low

cost raw materials and facile methods of fabrication were considered, in order to contain the costs of production, and obtain functional bio-composites easily scalable in an industrial setting. More detailed description about emulsions will be discussed in **Chapter 1**.

In the first part of the thesis, as will be discussed in **Chapter 2**, we used an emulsion solution casting process to fabricate sodium alginate-Mater-Bi® polymer films that can retain both hydrophilic (a cutaneous antiseptic) and lipophilic (curcumin) model drugs. The objective was to achieve a biodegradable and biocompatible material as active dressing to promote and accelerate skin wound healing. The obtained matrices have been characterized in terms of their physio-chemical properties and their ability to release these model drugs individually or simultaneously in vitro.

The novelty in this research was to demonstrate, for the first time the possibility to use Mater-Bi® also in the biomedical field. In fact, this commercial hydrophobic biodegradable polymer composite comprising polycaprolactone (PCL) and thermoplastic starch, obtained by a proprietary compound extrusion method is actively marketed as sustainable food packaging material as well as biodegradable material for perishable food containers.

In the second part of the thesis, as will be discussed in **Chapter 3**, calcium alginate-Beeswax microbeads have been fabricated by a solvent free emulsion gelation technique. The objective of this study was to formulate an all-natural oral-controlled delivery system for a natural hydrophilic compound, a concentrated extract from *Prunus mahaleb L.* fruit (here named as *mcfe*) rich in anthocyanins, optimizing its encapsulation and assessing in vitro its release under simulated gastrointestinal conditions. The obtained microbeads were investigated for their morphology and physico-chemical properties under the different pH conditions that characterize the gastrointestinal tract. The novelty in this research was to demonstrate, for the first time the possibility to use Beeswax as wall material, acting as retardant in drug release of phenolic compounds.

Chapter 4 summarizes the conclusions made throughout this study and suggests the fulfilment of future works.

Publications and conferences

Publications

- **C.Setti**, G.Suarato, G.Perotto, A.Athanassiou and I.Bayer, *Investigation of in vitro hydrophilic and hydrophobic dual drug release from polymeric films produced by sodium alginate-MaterBi® drying emulsions*, European Journal of Pharmaceutics and Biopharmaceutics, Volume 130,2018, Pages 71-82,ISSN 0939-6411.

- M. E. Genovese, G. Caputo, G. Nanni, **C.Setti**, M.Bustreo, G.Perotto, A.Athanassiou, and D.Fragouli, *Light Responsive Silk Nanofibers: An Optochemical Platform for Environmental Applications*, ACS Applied Materials & Interfaces 2017 9 (46), 40707-40715.

Conferences

- C.Setti, G. Suarato, A.Athanassiou and I.Bayer, *Hydrophilic and lipophilic dual model drug release from bio-polymeric matrices produced by sodium alginate - MaterBi® emulsions*, "Merck Young Chemists Symposium", Rimini (Italy), October 25th-27th 2017.

- C.Setti, G. Suarato, A.Athanassiou and I.Bayer, *Emulsion technology for the development of bio-based materials for controlled drug delivery applications*, 4th International Society for Biomedical Polymers and

Polymeric Biomaterials (ISBPPB) conference and exposition, July 15-18, 2018, Krakow, Poland.

Workshop participation

The Future of Medicine Starts Now, How Science and New Technology are reshaping Health Science, Genoa (Italy), June 29th-30th 2017 at Palazzo della Meridiana, Organised by: ISTITUTO GIANNINA GASLINI, Promoted by Fondazione Internazionale Menarini.

Schools

INTERNATIONAL SCHOOL OF BIOPHYSICS «ANTONIO BORSELLINO» 43rd Course: *Nanoscale biophysics: focus on methods and techniques*, http://www.ccsem.infn.it, Duration 5 days, (from 17th to 24th April 2016.

Chapter 1
Introduction

1.1.Biodegradable polymers in drug delivery devices

Over the last decades, drug delivery has become one of the most interesting and rapidly expanding scientific areas to overcome the limitations associated with the traditional administration of drugs. The conventional pharmaceutic preparations, administrated by different routes (i.e. oral, parenteral, subcutaneous, topical, intravenous, intramuscular, etc.) need to be repeatedly distributed to maintain their therapeutic concentration within the body. This causes plasma fluctuations of the drug, with spikes in concentration upon administration, followed by rapidly decreasing concentration until below its therapeutic effect. Main objectives of a drug delivery device are (1) to improve the delivery of the pharmaceutical compound at the desired target within the body, (2) to maintain the drug concentration within the therapeutic window over the desired time, (3) to protect the drug against degradation, and (4) to increase patient compliance due to the reduced frequency of drug application[1-3]. In this context, different biomaterials have been investigated for the development of these systems, such as metals, ceramics, glasses, and polymers[4]. The most important features of biomaterials intended for biomedical devices are: non-immunogenicity, biocompatibility, controllable biodegradability, biofunctionality, mechanical flexibility and structural integrity[5-6]. Among the different classes of

biomaterials, polymers have been extensively investigated as biomaterials in biomedicine[7-10].

In drug delivery, polymers are classified based upon the following characteristics: origin (synthetic, natural, or a combination of both), chemical nature (polyester, polyanhydride, protein-based, cellulose derivatives, etc.), backbone stability (biodegradation or non-biodegradability), and water solubility (hydrophilic, hydrophobic)[11-13]. However, some of these properties may lead to usage limitations. Natural polymers are difficult to extract from their sources and purify, while synthetic polymers have high immunogenicity, which limits their long term-usage. However natural polymers have the advantage, respect to the synthetic ones, to be biodegradable.

In fact, non-biodegradable polymers need to be surgically removed after they release the drug at the target site, in comparison to biodegradable polymers that degrade into the body and not need a second surgical procedure to be removed.

In this thesis work, the selection of the polymeric matrix has been based mainly on the requirements of the application. The general characteristic features that makes the polymer a potential candidate for drug delivery include safety, efficacy, water solubility, absence of immunogenicity, biological inertia, sufficient pharmacokinetics, and the presence of functional groups for covalent conjugation of drugs, targeting moieties, or formation of copolymer[14]. Polymeric materials may be found in a variety of forms such as membranes, films, fibers, gels, hydrogels, capsules, spheres, particles and 3D-structures (scaffolds)[15]. The work developed in this thesis has focused on the use of natural origin polymers in particular alginate and therefore, in the next section, this material will be further described.

1.2. Alginate

1.2.1. Sources of alginates

Alginates are a class of polysaccharides produced by *Brown Algae* and bacteria. They occur as structural components of marine brown seaweeds, localized in the intracellular mucilage and algae cell walls. Alginate found in the intracellular matrix exists of an insoluble gel containing a mixture of salt of various cations found in sea water, such as calcium, magnesium, potassium, strontium, barium and sodium ions[16]. Commercially available alginates are derived primarily from different *Brown Algae* species[16-17], including *Laminaruia Hyperboria Macrocystis Pyriera, Laminaria Diagitata, Ascophyllus Nodosum, Laminaria Japonica, Eclonia Maxima, Lessonia Nigrescense, Durvillea Antarcitica,* and *Sargassum Spp.* In all of these species, alginate is the most abundant polysaccharide, comprising up to 40% of the dry weight, conferring mechanical strength and flexibility to the marine plant, and acting at the same time as a water reservoir to prevent dehydration of the seaweed when exposed to the air. In addition, alginate is also produced by some species of bacteria, *Azotobacter vinelandii*, and several *Pseudomonas* species. They harvest alginate as an extracellular polymer, during their vegetative growth phase, with biological functions related to the specie. In *Azotobacter vinelandii* it acts as a structural element protecting the cyst from desiccation and unfavorable environmental conditions. In *Pseudomonas aeruginosa* strains, alginate is associated with pathogenicity, acting as the causative agent of cystic fibrosis[18].

Alginates produced by bacterial biosynthesis, similar in both species, have more defined chemical structures and physical properties, if compared to the ones derived from algae[19-20]. Their biosynthetic pathway comprises four different steps:

1. synthesis of precursor substrate,
2. polymerization and cytoplasmic membrane transfer,
3. periplasmic transfer and modification,
4. export through the outer membrane.

The knowledge of the metabolic pathway and the possibility to modify easily bacteria, may permit the production of high-quality bacterial alginate with tailor-made characteristics that can be used for biomedical application in future.

1.2.2. Alginate extraction from seaweeds

The commercial production of various type of alginate are obtained from algal material. The alginate extraction process (Fig.1.1) consists mainly in three major steps:

1. Pre-extraction
2. Neutralization
3. Precipitation/Purification

The first step involves an acidic treatment with HCl of the powdered algal mass to extract alginic acid and, at the same time, to allow the removal of impurities potentially present. These include counter ions (Ca^{2+}, Na^{+}, Mg^{2+}, Sr^{2+}, etc.) and contaminants (fucoidans, laminarins, proteins and polyphenols) present in the kelp. This pretreatment is often repeated several times to ensure full extraction of alginic acid. At the end of this process, the supernatant (residual algal particles) is eliminated. In the neutralization step the insoluble alginic acid is treated with an alkaline solution by using sodium carbonate (Na_2CO_3) or sodium hydroxide (NaOH), leading to a pH=9-10. This process allows the conversion of insoluble alginic acid

into the water-soluble sodium alginate. The final step is the precipitation of alginate solution to obtain its water-soluble powder as sodium alginate, calcium alginate or alginic acid by the addition of alcohol, typically ethanol, calcium chloride and hydrochloric acid, respectively[16].

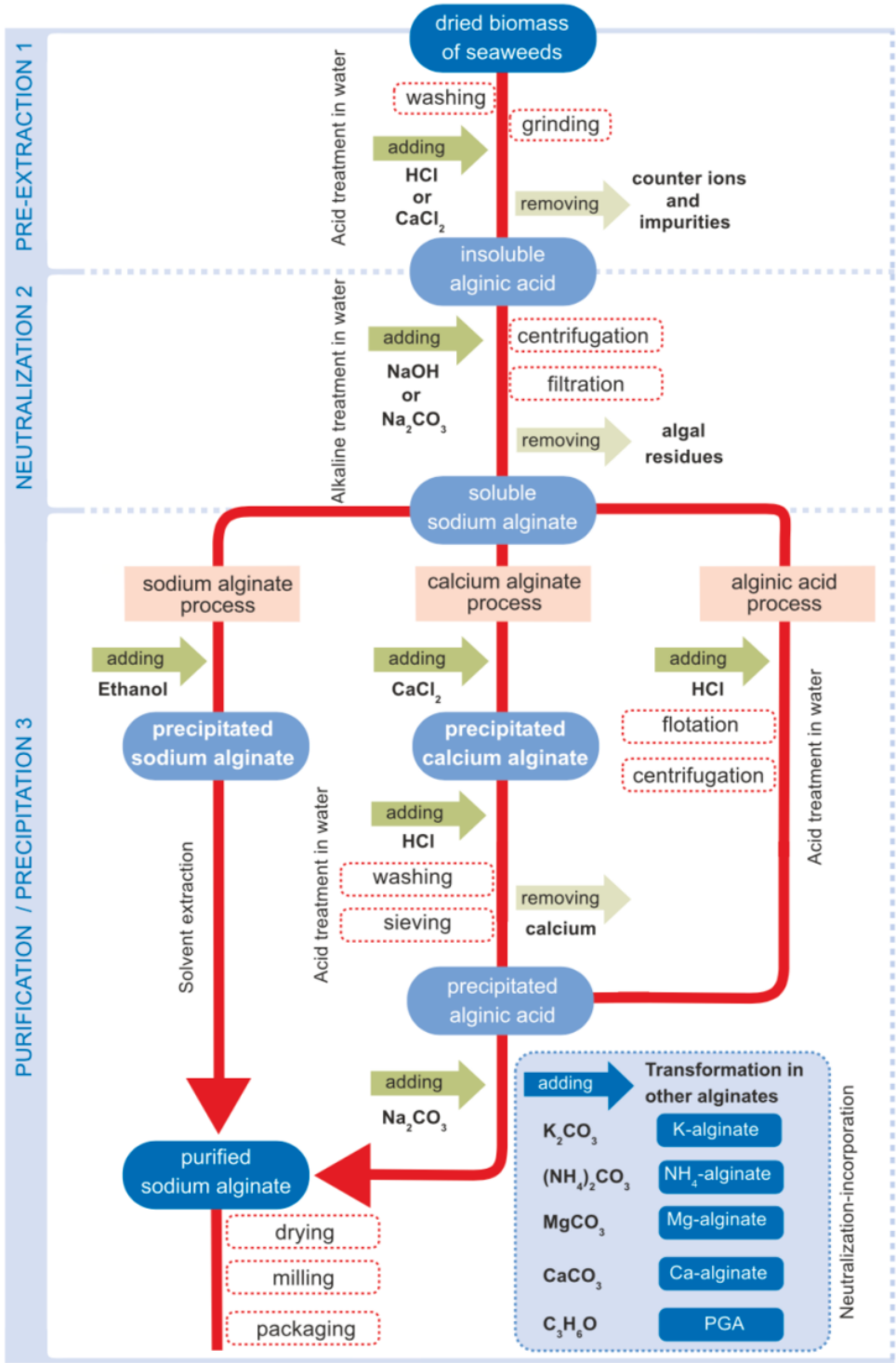

Figure 1.1: Schematic representation of the extraction process of alginates from seaweeds[16].

1.2.3. Chemistry

Structurally speaking, alginates are a family of linear, unbranched binary polysaccharides containing blocks of monomers of β-D-mannuronic acid (M) and α-L-guluronic acid (G) residues joined together by (1,4)-glycoside linkages. The monomers can be composed of G-G, M-M and G-M blocks (Fig. 1.2)[21-23].

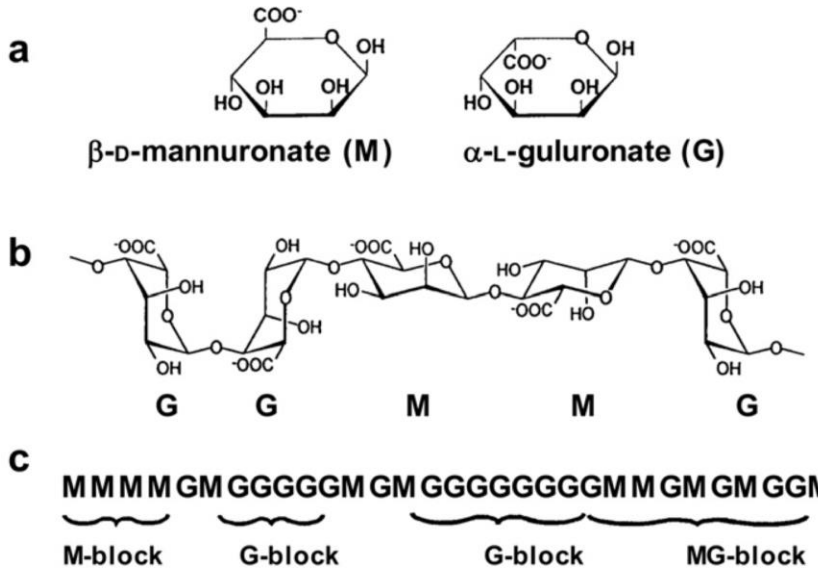

Figure 1.2: Structural characteristics of alginates: (a) alginate monomers, (b) chain conformation, (c) block distribution[23].

The M and G contents, the extent of the sequences and the molecular weight give different physical and chemical properties to the alginates. The molecular variability is dependent on the organism, the algae tissues from which the alginates are isolated from the algae, and the time of year when it is harvested[16]. For these reasons, different types of alginates exist in nature. One of the main characteristics of alginate physical features is the ion-binding property, with an affinity against multivalent cations such as Ca^{2+}, Sr^{2+}, or Ba^{2+} inducing the formation of a crosslinked gel[24-26]. Responsible of this process are the G-blocks of alginate, able to participate in

intermolecular cross-linking with divalent cations to form hydrogels. This process is based on the substitution of sodium ions of the G residues by calcium ions, resulting in the formation of the so-called *"egg-box gel"* as depicted in Fig.1.3, whose strength is dependent on the concentration of divalent ions. In this model, calcium ions are packed in the cavity between two diaxially linked glucuronic acid residues[27].

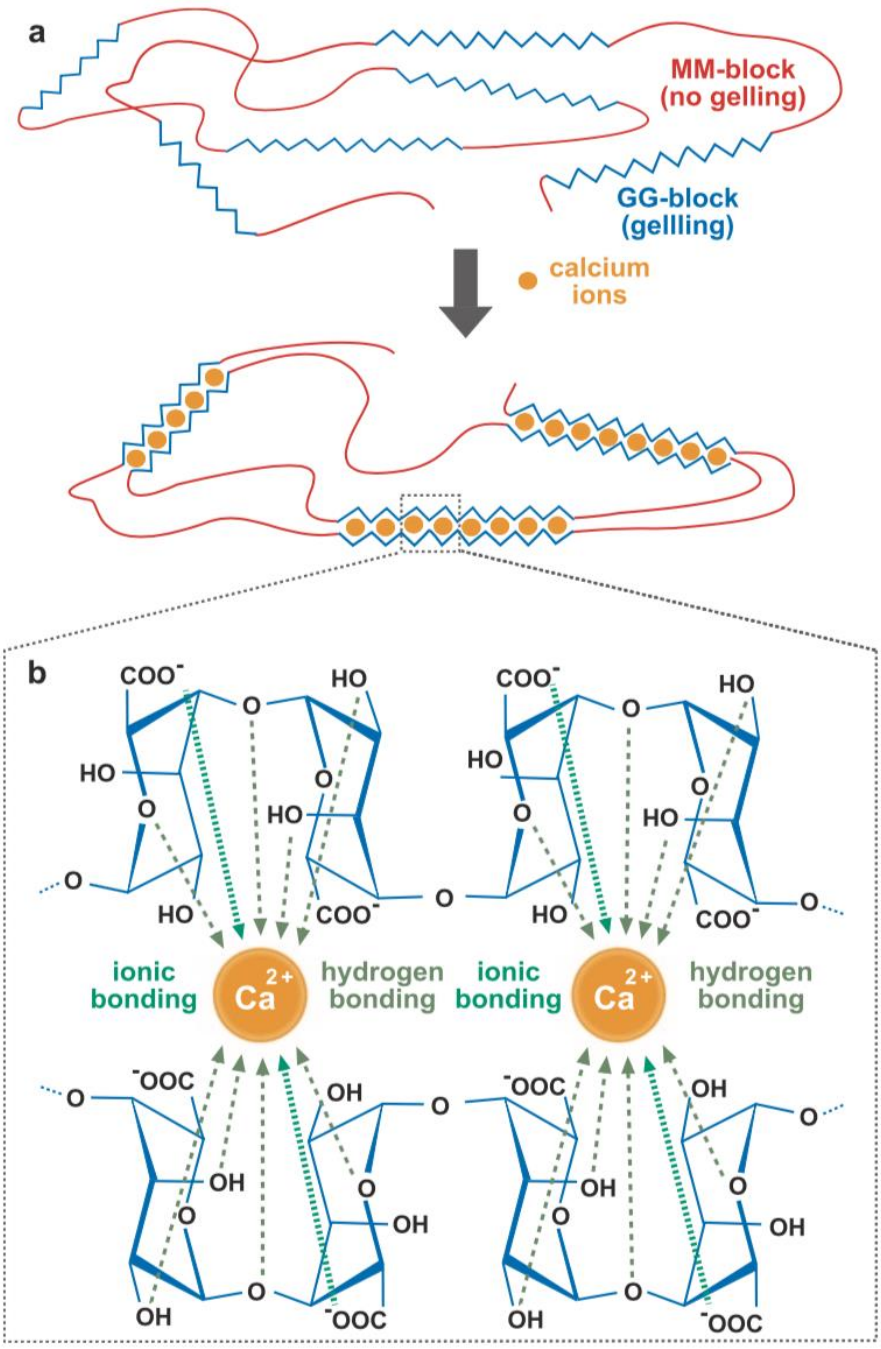

Figure 1.3: Schematic representation of the egg-box model for calcium alginate gelation. (a) Drawing of the binding of polymer chains and (b) the formation of junction zones in alginate gels[16].

1.2.4. Alginate as biomaterial

Alginate is a polymer approved by the Food and Drug Administration (FDA) for human use as food and medical grade material. Because of its properties of biocompatibility, low toxicity, non-immunogenicity, biodegradability, hydrophilicity and relatively low cost, alginates have been widely applied as biomaterials for multiple biomedical and pharmaceutical applications. However, the chemical composition and the mitogenic contaminants found in alginates are the two main contributors to its immunogenicity. Alginate biocompatibility have been analyzed and confirmed by *in vitro* cytotoxicity assays together with *in vivo* experiments, after injection or implantation of the polymer[28]. The biocompatibility characteristics are influenced by the concentration of G and M residues. Moreover, it has been described that alginates with high M-block content are directly connected to the stimulation of inflammatory reaction increasing cytokines production[29], especially tumor necrosis factor alpha (TNF- α) and interleukin 1 (IL-1) and 6 (IL-6)[30]. In this regard, pattern recognition receptors (PPR's), especially toll-like receptors TLR4 or TLR 2 together with CD14[31] are involved. The immunologic potential of poly-mannuronate has also been registered in several *in vivo* animal models[32]. On the contrary, alginates with high G content don't induce inflammatory responses and consequently are used for *in vivo* research[33]. In addition, the immunogenic reaction can be attributed to impurities residual (i.e. heavy metals, endotoxins, proteins, polyphenolic compounds) that could be present in the alginate[43]. Therefore, purification is assumed to eliminate contaminants that can cause an undesirable immuno-response, ensuring very high purity of alginate, that was reported to not induce any significant foreign body reaction when implanted[35] or subcutaneously injected into animals[36]. Moreover, properties such as solubility, hydrophobicity and physico-chemical and biological characteristics may be modified by forming alginate derivatives through functionalizing available hydroxyl and carboxyl groups.

The above-mentioned properties of alginate have contributed to diffuse its use in many fields, particularly in the *food, pharmaceutical and biotechnological industries*. Alginate has been, and still is, widely studied and has numerous industrial application[37]. Different aspects of its properties had been exploited, namely, alginate's stabilizing, viscosity-enhancing, emulsifying, gelling and film-forming properties[38-39]. As biomaterial, alginate have been used for different biomedical applications, due to its biocompatibility and low cost. Different alginate structures can be obtained by processing the biopolymer into fibers, films, foams, hydrogels, nanoparticles and microspheres, have been proposed based for the wide range of uses[40-41]. Several commercial alginate-based products have been marketed especially as wound dressings (e.g Algicell® (Derma Sciences), AlgiSite M® (Smith & Nephew), Comfeel Plus® (Coloplast), Kaltostat® (ConvaTec), Sorbsan® (UDL Laboratories), and Tegagen® (3M Healthcare)), as the material provides a moist environment that could aid wound healing. Alginate dressings are mainly commercially available in freeze-dried porous sheet or fibrous non-woven form. The dry form of the dressing will enable the absorption of the wound exudate hereby providing a physiological moist environment while concurrently preventing infection at the wound site[40]. However, other commercial products have been developed for *oral applications*, such as Gastrotuss®, Algicid®, Gaviscon Double Action Liquid® or tablets®. These formulations are available as syrups, tablets and suspensions. In oral formulations, alginate acts creating a mechanical barrier between the stomach and the esophagus which prevents the reflux, recurrent symptoms of respiratory, choking, dysphagia, heartburn, belching, irritability; accelerating gastric movement, regenerating mucous membranes of the esophagus and ensuring its protection[42]. In *tissue engineering*, several studies report the application of alginate for the regeneration of various tissues and organs such as liver, pancreas, nerve bone, cartilage, skin and muscle[43]. In *pharmaceutical applications*, this polysaccharide has been employed both alone and in combination

with other material, as a matrix for drug delivery. The possibility to modify alginate properties in order to regulate the kinetics of the drug release has been the main interest in some researches. The interaction of alginate with the respective drugs and also the physical properties that affect the manner in which the drug is released were investigated[40].

Besides the above-mentioned applications, alginate has been investigated as a model system for the encapsulation of mammalian cell culture for biomedical study purposes. Stable cultures in alginate beads have been achieved with a number of cell types including chondrocytes, bone- marrow stromal cells, islets, myoblasts, fibroblasts, Schwann cells, kidney cells, epithelial cells, and hepatocytes. However, due to the lack of cell-binding sequence in alginate, RGD-modified alginate is primarily utilized for cell-culture substrate purposes nowadays[44].

1.3. Emulsions

1.3.1. Emulsion definition

An emulsion is a heterogeneous system consisting of two immiscible liquids, combined together to form a semi-stable mixture. Generally, the immiscible liquid phases in an emulsion consist of an organic (oil) phase and an aqueous (water) phase. In an emulsion, one liquid is dispersed, in the form of droplets, in a second liquid continuous phase. The dispersed phase is referred as the internal (disperse) phase and the continuous phase as the external one[45-47].

Emulsions can be classified based on the nature of the external and internal phases as oil-in-water (O/W) or water-in-oil (W/O). However, more complex systems referred to as "double emulsions" or "multiple emulsions" can be made. These systems present an emulsion as the dispersed phase in a continuous phase and they can be either water-in-oil-in-water ($W_1/O/W_2$) or oil-in-water-in-oil ($O_1/W/O_2$). These emulsions are usually prepared using a two-stage process to obtain the final emulsion (Fig.1.4).

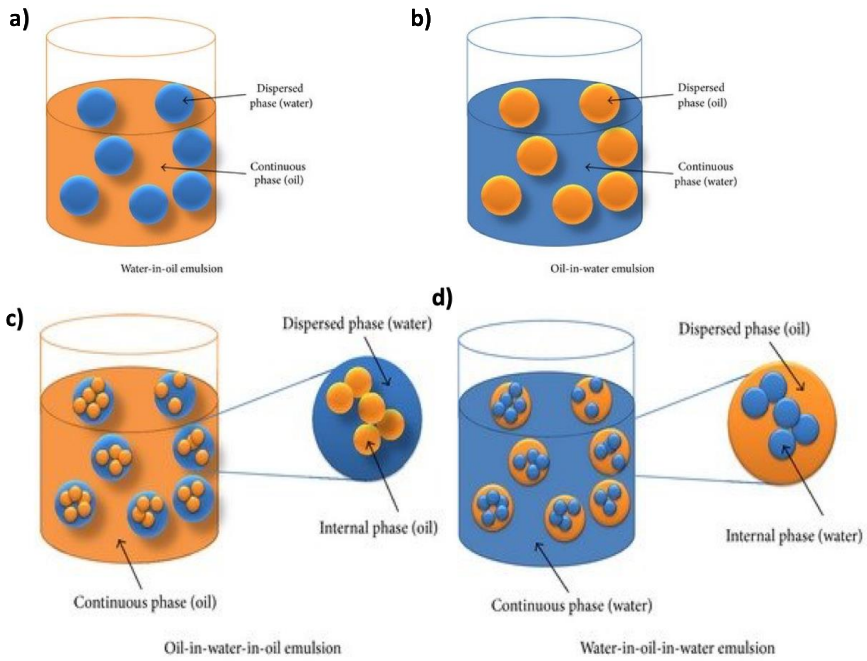

Figure 1.4: Emulsion classification according to the distribution of the internal and external phase: (a) water-in-oil, (b) oil-in-water, (c) oil-in-water-in-oil and (d) water-in-oil-in-water emulsions. Readapted from[48].

Emulsions can be also classified with respect to droplet size in[49-50]:

1. *Macroemulsions O/W and W/O:* These systems usually have a size (of what?) range of 0.1–5 μm with an average of 1–2 μm. These systems are usually opaque or milky due to the large size of the droplets and the significant difference in refractive index between the oil and water phases.
2. *Nano-emulsions*: These systems usually have a size range 20–100 nm. Similarly to macroemulsions, they are only kinetically stable. They can be transparent, translucent or opaque, depending on the droplet size, the refractive index difference between the two phases and the volume fraction of the disperse phase.
3. *Microemulsions* These systems usually have the size ranging from 5 to 50 nm. They are thermodynamically stable and strictly speaking they should not

be described as emulsions. A better description is “swollen micelles” or “micellar systems”.

1.3.2. Emulsifiers

Emulsions are thermodynamically unstable systems, which tend to complete phase separation due to droplet coalescence. For this reason, during emulsions formulation, a third component is necessary to make these systems kinetically stable, the emulsifier. Emulsifiers are ‘amphiphilic’ and ‘surface active’ materials[51-52] which are not only able to facilitate droplet break-up, thus lowering the oil-water interfacial tension[53], but they also create a protective layer around the oil droplets, in order to prevent them to coalescing[54].

Surfactants are generally classified according to the nature of the hydrophilic group. The hydrophilic regions can be anionic, cationic, or nonionic[55]. Among them, non-ionic surfactants, mainly Tweens and Spans, are widely used in the food and pharmaceutical industries. In addition, some surfactants possess both positively and negatively charged groups, and can exist in either or both anionic or cationic state, depending on the pH of the solution and the pK_a of the ionizable groups on the surfactant. These surfactants are known as ampholytic compounds.

The past two decades have seen the introduction of a new class of surface-active substance, so-called “polymeric surfactants” or “surface-active polymers”, which result from the association of one or several macromolecular structures exhibiting hydrophilic and lipophilic characters, either as separated blocks or as grafts. They are now very commonly used in formulating products as different as cosmetics, paints, foodstuffs, and petroleum production additives[56]. To select the surfactant during emulsion formulation, the hydrophilic-lipophilic balance (HLB number) is used. It is a dimensionless scale, ranging from 0 to 20, developed by Griffin[57]. This system is an indicator of the emulsifying characteristics of an emulsifier, but not its efficiency and takes into account the relative percentage of hydrophilic to lipophilic (hydrophobic) groups in the surfactant molecule. In general,

W/O emulsifiers exhibit HLB values in the range 3–8 while O/W emulsifiers have HLB values of about 8–18. So, the higher the HLB value of an emulsifying agent, the more hydrophilic it is[58].

The average HLB number may be calculated as follow:

$$HLB = x_1HLB_1 + x_2HLB_2$$

where x_1 and x_2 are the weight fractions of the two surfactants with HLB_1 and HLB_2.

1.3.3. Emulsion stability

An emulsion can be defined stable when its properties remain unchanged over a certain period of time. However, emulsions are thermodynamically unstable, and changes of their properties will generally occur over time. Moreover, the more slowly the properties change, the more stable the emulsion is. For this reason, in important to understand the causes of instability to select suitable components to form stable emulsions and to distinguish thermodynamic stability and kinetic stability. Thermodynamics gives information about processes taking place during emulsification or at quiescent conditions. Kinetics gives information about the rate at which these processes occur. There are many phenomena of physical instability that can alter emulsion properties as creaming/sedimentation, coalescence, flocculation, Ostwald Ripening and phase inversion, some of which may occur simultaneously[59-61] (Fig. 1.5). In addition, chemical instabilities could occur, i.e. oxidation of the oil phase, microbiological contamination and adverse storage conditions[62].

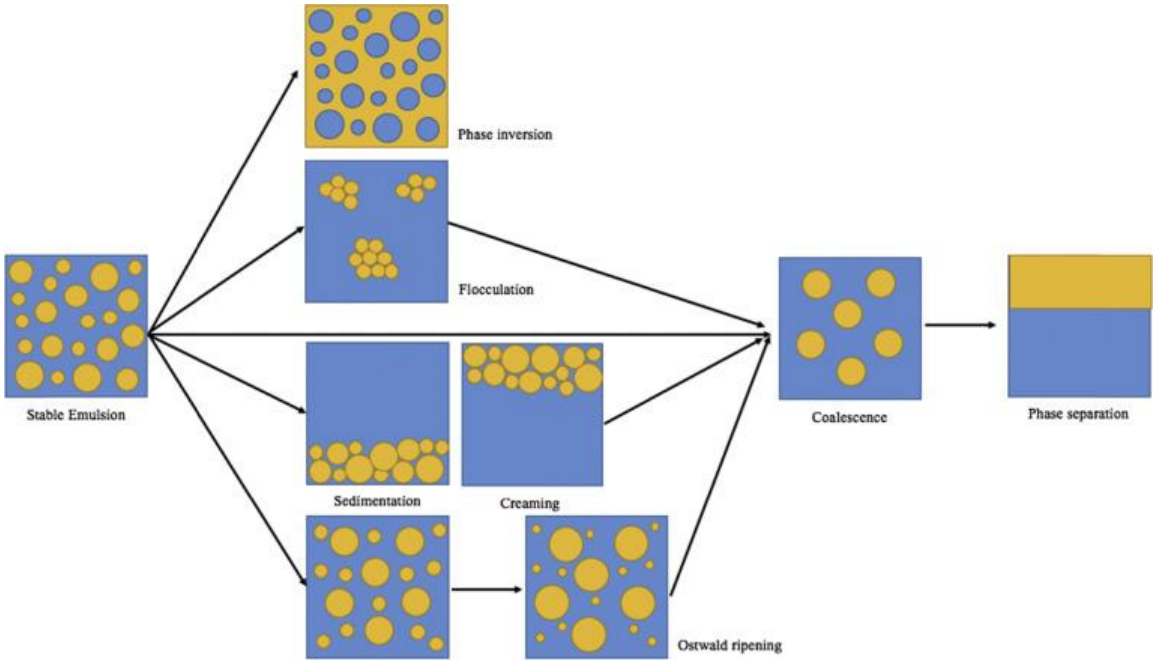

Figure 1.5: Overview of the instability phenomena in the emulsion system[61]

1.3.3.1. Creaming/Sedimentation

Creaming/Sedimentation results from external forces, usually gravitational or centrifugal. Creaming occurs when dispersed droplets rise to the top of the continuous phase, in the case of o/w emulsions, and it is characterized by a whitish/yellowish layer at the top of an emulsion. On the contrary, sedimentation occurs when dispersed droplets sink the bottom of the continuous phase, in the case of w/o emulsions, where in general the oil phase has a lower density than the water phase and characterized by a layer that appears at the bottom of an emulsion. However, while this process is not considered as serious instability, because can be reversed by gently mixing or shaking of the formulation, it may lead to coalescence of the dispersed phase.

Creaming or sedimentation processes occurring in emulsion can be easily assessed by optical observations. Creaming/sedimentation rate can be determined by measuring the volume of cream/sediment in the emulsion with time. This may be

done by placing the emulsion in a calibrated beaker or tube and measuring the height of the cream/sediment every second, minute etc. In some cases, visual observations are not accurate enough to measure the creaming/sedimentation rate; creaming or sedimentation can occur very quickly or the distinction between continuous phase and cream/sediment layer is difficult to visualize. More sophisticated techniques are then used to measure the creaming rate, using light scattering or ultrasonic imaging. Creaming/sedimentation can be minimized by reducing the droplet size, increasing viscosity of the continuous phase, reducing density differences between the two phases and increasing the volume fraction of the dispersed phase[61].

1.3.3.2. Coalescence

Coalescence is also known as breaking of emulsions. This phenomenon occurs when two or more droplets fuse together to form larger droplets, due to thinning and disruption of the liquid film between the droplets. This process results in a considerable change of the droplet size distribution, which shifts to larger sizes. Thus, contrary to creaming, coalescence process is irreversible. The limiting case for coalescence is the complete separation of the emulsion into two distinct liquid phases. The driving force for coalescence is the surface or film fluctuations; this results in a close approach of the droplets whereby the van der Waals forces are strong and prevent their separation. To prevent coalescence, the repulsive forces must exceed the van der Waals attraction, thus preventing film rupture, for example altering the viscosity and/or forming a strong interfacial film, using particulate solids[61].

1.3.3.3. Flocculation

Flocculation refers to droplet aggregation into larger ones, initially without any change in primary droplet size. It is caused by van der Waals attraction which are universal with all disperse systems. It is the result of the van der Waals attractions

which are universal with all disperse systems. Flocculation occurs when there is not sufficient repulsion to keep the droplets apart at distances where the van der Waals attraction becomes very weak. Flocculation may be either strong or weak, depending on the magnitude of the attractive energy involved. Specifically, flocculation occurs when there is not sufficient repulsion to keep the droplets apart at distances where the van der Waals attraction is weak. Flocculation may be "strong" or "weak", depending on the magnitude of the attractive energy involved. In cases where the net attractive forces are relatively weak, an equilibrium degree of flocculation may be achieved (so-called weak flocculation), associated with the reversible nature of the aggregation process. With a strongly flocculated system, one refers to a system in which all the droplets are present in aggregates due to the strong van der Waals attraction between the droplets. Flocculation of droplets it is not a serious stability problem and it can be reversed by gentle mixing or shaking of the emulsion as with creaming. However, it can result in coalescence of the droplets if the emulsifier showed inadequate mechanical resistance.

1.3.3.4. Ostwald Ripening

Ostwald Ripening is a breakdown mechanism that occurs when the droplets are not in direct contact. With emulsions which are usually polydisperse, the smaller droplets will have larger solubility compared to the larger ones (due to the effects of curvature). With time, smaller droplets disappear, and their molecules diffuse to the bulk and become deposited on the larger droplets. With time the droplet size distribution shifts to larger values. A certain solubility of the dispersed in the continuous phase is required for Ostwald ripening to take place and is driven by the difference in Laplace pressure between droplets having different radii. It is possible to stabilize emulsions against Ostwald ripening by adding components of high molecular weight that reduce the rate of diffusion of molecules within the dispersed species[61,63-64].

1.3.3.5. Phase inversion

Phase inversion refers to the process whereby there will be an exchange between the disperse phase and the medium. For example, an O/W emulsion changes to a W/O emulsion and *vice versa*. It can be affected by a high concentration of dispersed phase (≥70%) or by changing the hydrophilic/lipophilic properties of the emulsifier by the addition of any additive[65].

1.3.4. Emulsification

The process of producing an emulsion by mixing two immiscible liquids is called emulsification or homogenization and a mechanical device designed to carry out this process in known as homogenizer[66-67]. Considering the nature of the starting materials, this process can be divided into two categories: primary and secondary homogenization. In the primary homogenization the creation of an emulsion is directly obtained from two separate liquids. On the contrary, secondary homogenization occurs when droplets of an already existing emulsion are reduced in size[63]. The size of the droplets produced by a homogenizer depends on a balance between two physical processes: *droplet disruption* and *droplet coalescence.* Droplet disruption involves the disruption of larger droplets into smaller ones and is determined by a balance between interfacial forces and disruptive forces [59,68].

Interfacial forces are responsible to keep a droplet in a spherical shape and are characterized by the Laplace pressure (ΔP_L), which acts across the oil–water interface toward the center of the droplet so that there is a larger pressure inside the droplet than outside of it:

$$\Delta P_L = 4\,\gamma\,/\mathrm{d}$$

The equation indicates that the pressure required to disrupt a droplet increases as the interfacial tension (γ) increases or as the droplet size (d) decreases. The nature of the disruptive forces responsible of the droplet break-up during emulsification depends on the hydrodynamic conditions, i.e. the flow regime (laminar, turbulent, or cavitational) that takes place during the mixing process and also on the type of

homogenizer used[69-70]. In order to induce the droplet break up, the disruptive forces must overcome the interfacial forces. The droplet disruption is determined by different flow regimes that are dependent on the type of homogenizer and the features of the fluids. The type of regime is mainly influenced by the type of forces and by the flow type. The forces that act in the droplet separation process are:

1. Frictional (mainly viscous) forces due to the flow of fluid parallel to the surface of the droplets;
2. Inertial forces due to local pressure fluctuations and that act perpendicular to the surface of the droplets.

While, the types of flow are classified as laminar and turbulent depending on the dimensionless Reynolds numbers (Re):

$$\mathrm{Re} = \frac{\nu l \rho}{\eta}$$

where ν is the linear liquid velocity, ρ is the liquid density, η is its viscosity. l is a characteristic length that is given by the diameter of flow through a cylindrical tube and by twice the slit width in a narrow slit. If Re <1000 the flow is laminar, while if Re>2000 the flow is turbulent.

In the case of droplet coalescence, once the droplets are disrupted during homogenization, they are constantly moving, and the frequency of collision is very high due to agitation. These collisions may lead to coalescence, leading to an increase in droplet size. To avoid this phenomenon, the presence of emulsifier in the system, adsorbing at the oil-water interface can create a layer around the droplets that prevents merging. In this context, the concentration of the emulsifier and that time that it requires to adsorb at the interface are two critical parameters. The concertation of the emulsifier as to be high enough to cover the droplet surface, in contrast if is too low droplets may coalesce. The time needed to the emulsifier to soak up at the

interface (τ_{ADS}), compared to the time between the droplet collision (τ_{COL}), has to be τ_{ADS} /τ_{COL} <<1 in order to minimize the coalescence.

Emulsions can be fabricated employing a number of different techniques, which are generally categorized in high energy or low energy methods depending on the energy input requirements[71-75].

1.3.5. High energy methods

High-energy techniques generate intensive disruptive forces able to mix and breakup the oil and the water phases, producing tiny droplets. During this process, the generated disruptive forces have to be higher than the restorative forces, determined by the Laplace pressure, which holds the droplets into spherical shapes. Consequently, the droplets deform, and the specific surface area increases up to the point of disruption. The size of the droplets using high-energy methods depends on the homogenizer type, operating conditions (e.g., energy intensity, duration, and temperature), sample composition (e.g., oil type, emulsifier type, relative concentrations), and physicochemical properties of the phases (e.g., interfacial tension and viscosity). The main advantage of this processes is the possibility to control the size distribution and composition, producing emulsions with desired properties. However, recoalescence can occur during high energy emulsification together with chemical degradation events due to the intense energy generated. Various devices can be used to fabricate the emulsions such as high pressure, rotor-stator, ultrasonic and membrane systems[73-75].

1.3.5.1. High-pressure homogenizers

High-pressure homogenizers (HPH) are devices comprising of a high-pressure pump and a homogenizing nozzle. These systems are efficient in reducing the size of droplets in a coarse emulsion. The emulsion is introduced into the input of the homogenizer and dragged by a pump into a chamber located on the backstroke

of the homogenizer. Later, the pump forces the emulsion through a tight valve at the end of the chamber on its forward stroke. When the emulsion passes across the valve, disruptive forces (turbulence, shear and cavitation) cause the deformation and breakup of the larger droplets into smaller ones. The flow regime responsible of this phenomenon depends on the characteristics of the material being homogenized, the size of the homogenizer, and the design of the homogenization nozzle[68,73-78] (Fig.1.6). A variety of different nozzle designs is available to increase the success of droplet disruption within the homogenizer. For example, for standard and microfluidizer nozzles inertial forces in turbulent flow are responsible of droplet breakup; while for jet dispenser or orifice valves shear forces in laminar elongational flow come into play)[76].

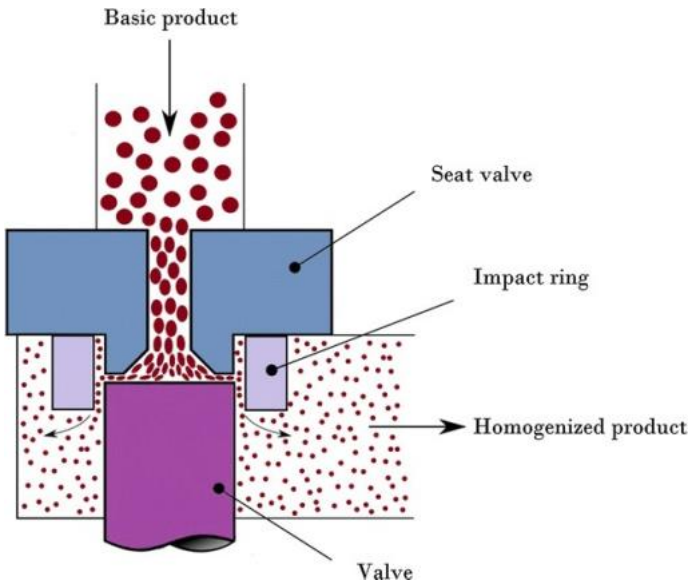

Figure 1.6: Schematic of high-pressure homogenizer device[79]

1.3.5.2. Rotor-stator

In the rotor-stator system, emulsification is carried out under very high shear rate (up to 10^7 s^{-1}) in a very narrow gap (*e.g.* 0.1 mm) between a high-speed rotor and stator surface. Rotor-stator systems are used to produce emulsion operating discontinuously or continuously. Usually, for discontinuous or quasi-continuous operating systems, agitators of different geometry or gear-rim dispersing machines are used. Here, the effective breakup energy is registered in the form of forces of inertia and shearing in turbulent flow. On the other hand, colloid mills with smooth or toothed rotors and stators, gear-rim dispersing machines and intensive mixers are employed for continuous process. When the surfaces of the rotor and stator are smooth the dominant droplet disruption mechanism is laminar shear flow, but when the surfaces are roughened or toothed it is turbulence. The liquids enter at the bottom through suitable tubes and then flow through the narrow slit between the stator and the rotor and finally leave the system. In the dispersing zone of these machines droplets of a premix are deformed and disrupted[80-81](Fig.1.7).

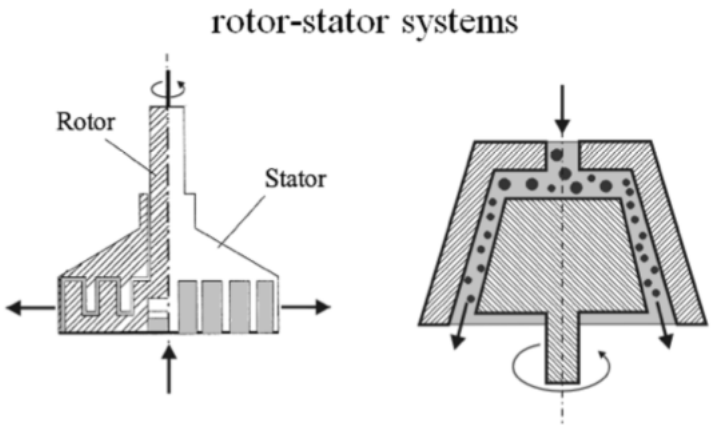

Figure 1.7: Schematic of Rotor-stator device[80]

1.3.5.3. Ultrasonic homogenizers

Ultrasonic systems employ high intensity ultrasonic waves (> 20kHz) to form an emulsion containing very tiny droplets. The ultrasonic waves generate intense

shear and pressure gradient within the material, determining droplet breakup mainly thanks to cavitation and turbulent effects[82]. The main features regulating the efficiency of ultrasonic homogenizers are the intensity, duration and frequency of the ultrasonic waves[54,83-84]. This technique can be used both to generate an emulsion homogenizing separate oil and water phases or to reduce the droplet size of a pre-existing coarse emulsion. The ultrasonication can be done both in a continuous or discontinuous way. It is possible to distinguish two different types of sonicators: (1) bench-top and (2) large-scale continuous flow.

Bench top homogenizers are mainly used in research laboratories and are ideal for the preparation of small volume emulsions. It comprises of an ultrasonic probe that contains a piezoelectric crystal enclosed within a protective metal case usually tapped at the end. This kind of homogenizers work as follow: the electrical wave applied to the transducer causes a rapid oscillation of the piezoelectric crystal inside it, which generates ultrasonic waves. As the probe is immersed into the sample, the ultrasonic wave generates intense disruptive forces at its tip (cavitation, turbulence and interfacial waves) determining the disruption of the liquid sample into smaller fragments (Fig.1.8).

Large-scale continuous-flow homogenizers are generally used for the continuous production of emulsions. In these devices, the sample to be homogenized flows through a channel and impacting on a sharp-edged blade causes the rapid vibration of the blade which generates intense ultrasonic waves capable to breakup any droplet in its immediate vicinity thanks to a combination of turbulence, shear and cavitation.

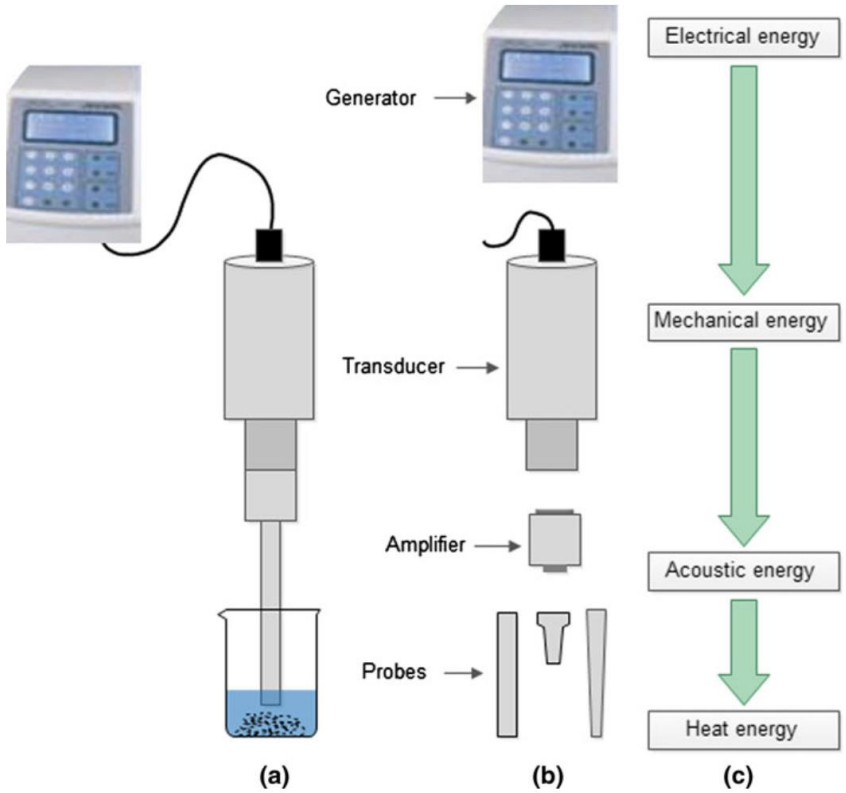

Figure 1.8: Ultrasonic setup (a) batch-type ultrasonic setup, (b) components of batch-type ultrasonic setup[84].

1.3.5.4. Microfluidizer homogenizers

Microfluidizers consist of a fluid inlet, a pumping device and an interaction chamber comprising two channels through which the fluids are made to flow and interact with each other. In particular, the fluid (pre-existing coarse emulsion or individual water and oil phases) is pushed within the system under high pressure. Once into the interaction chamber the fluid is split into two streams that collide to each other generating intense disruptive forces and causing the mix of the fluids and the droplets breakup allowing the emulsion formation. In order to increase the

efficiency of this process, different channel types have been designed, such as straight or zig-zag channels[54,74,85] (Fig.1.9).

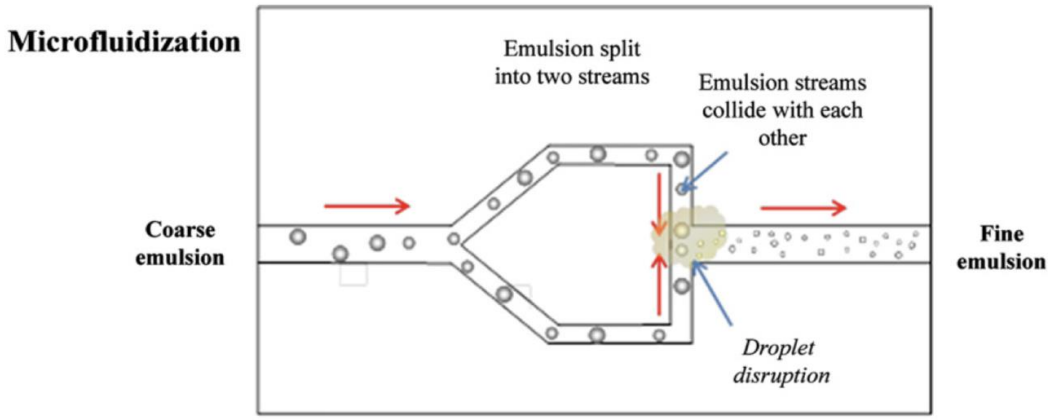

Figure 1.9: Schematic of Microfluidization[71]

1.3.5.5. *Membrane and microchannel homogenizers*

In a membrane homogenizer, an emulsion is formed by pushing the disperse phase through the pores of a membrane into the continuous phase. During this process, that could be in batch or continuous, the disperse phase is constrained perpendicular to the membrane, while the continuous phase flows tangential to the membrane. In general, the membrane has a shape of an hallow cylinder and through it the dispersed phase is pressed from outside, while the continuous phase is pumped through the cylinder[86-87] (Fig.1.10). Several parameters influence the droplet size: membrane properties, transmembrane pressure and fluxes[88]. The membrane pore size distribution influences the diameter of the formed droplets. Different membranes with several pore dimensions can be manufactured leading to the production of emulsions with different mean droplet size[89]. When the pore density is too large, coalescence between the formed drops can occur, while, if the pore density is too low, the production rate is insufficient. Preferably, to have a monodisperse emulsion, the membrane should have pores with a narrow size distribution, even if practically the pore size distribution of a membrane produces usually droplets more or less polydisperse[90].

The second important property of the membrane to take into account is its polarity, which determines the type of emulsion produced. Hydrophobic membranes are needed to produce water-in-oil emulsions, whereas hydrophilic membranes are needed to produce oil-in- water emulsions[87]. Also the pressure applied to the dispersed phase have to be sufficient high to achieve drop formation. This pressure should be at least of the order of magnitude of the Laplace pressure of a drop of diameter equal to the pore diameter. In general, high pressure promotes large drops formation or dispersed phase jet, while low pressure decreases the production rate; for this reason, a compromise between these two situations is needed[88,91]. The membrane must be sufficiently robust so that it is not broken by the pressures applied to the fluids during homogenization and for this reason are commonly made of microporous glass or of ceramic materials. The main advantage of this process is the low stress induced to the product, so that this method is suitable for sensitive products.

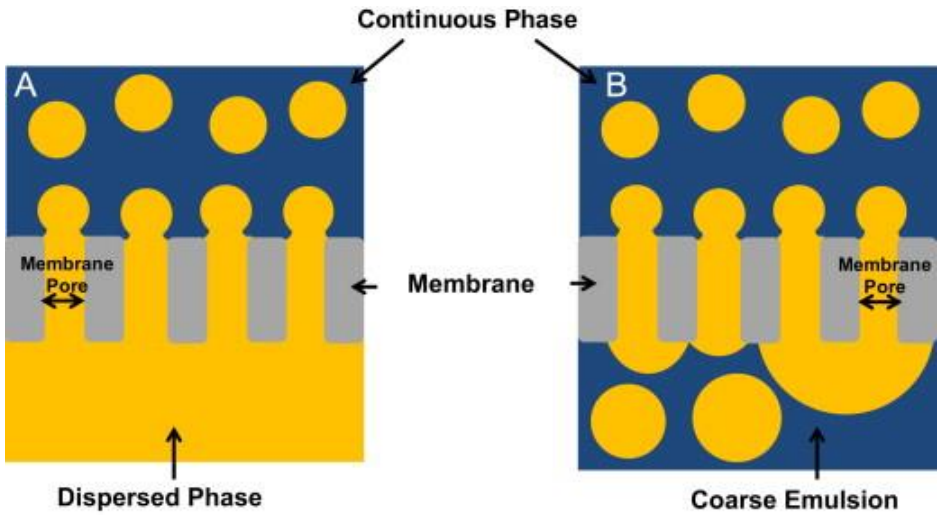

Figure 1.10: Particles production by direct and premix membrane emulsification. (A) Direct membrane emulsification and (B) Premix membrane emulsification[87].

Microchannel emulsification is a technique similar to membrane emulsification by using the same principle of force out the dispersed phase into the continuous phase[92-95]. However, in this system, the dispersed phase is pushed through microfabricated channels with well-defined geometries, which influence droplet size. As in the case of membrane emulsification, also for microchannel homogenization, the emulsion type is dependent on the polarity of the channel: hydrophilic to produce O/W emulsions and hydrophobic for W/O emulsion type. The emulsification process can be followed by using high-speed camera and a microscope. During this process (Fig.1.11), the phase to be dispersed is driven across a hole in the center of the plate so that it flows through the microchannels onto a relative flat area, called terrace, where the droplet can expand to a disk-like-shape. Upon extra swelling, the disk reaches the end of the terrace and drops into the deeper well, in which spontaneous detached of the droplet takes place. The mechanism of droplet detachment is due to the Laplace instability mechanism. This technique has demonstrated to be very helpful for generating droplets with very narrow particle size distributions.

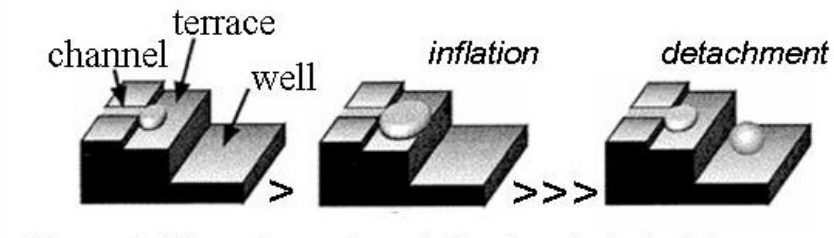

Figure 1.11: Schematic representation of droplet formation process in microchannel emulsification[93]

1.3.6. Low-energy approaches

Low energy methods for emulsion formation, rely on the spontaneous formation of small and uniform droplets within the oil-water-surfactant systems under specific environmental conditions (i.e. stirring, temperature and composition). These methods are mainly dependent on the physicochemical properties of the

surfactant and the oil phase. They are advantageous because they can avoid the disruption or damage of encapsulated molecules by using low quantity of energy to generate the emulsions. However, the main drawback is the requirement of large amounts of surfactants and in addiction polysaccharides or proteins cannot be used. Different techniques to prepare emulsions are based on low-energy methods, including: phase inversion and spontaneous emulsification[70,96-97].

1.3.6.1. Phase inversion emulsification

Phase-inversion methods are based on the induction of a phase inversion in emulsions from W/O to O/W and *vice versa*. Among these approaches it is possible to distinguish: phase-inversion temperature (PIT), phase-inversion composition (PIC) and emulsion inversion point (EIP) methods[73,75]. Phase inversion Temperature relies changes in the optimum curvature (molecular geometry) or relative solubility of non-ionic surfactants with changing the temperature. The molecular geometry of a surfactant can be described considering the packaging parameter (p) expressed as the ratio between the cross-sectional area of the lipophilic tail group (a_T) and the hydrophilic head-group (a_H) present within the surfactant structure:

$$p = \frac{\mathrm{aT}}{\mathrm{aH}}$$

In water, due to the hydrophobic effect, the surfactant molecules tend to self-assemble creating monolayers with optimum curvatures that permits the most effective packing of the molecules[95]. The driving force of the PIT method is the changes in the physicochemical properties (packing parameter or solubility) of the surfactant with Temperature. The temperature at which the inversion of the emulsion occurs is known as phase inversion temperature (PIT). At T< PIT -30 °C, the surfactant is soluble in water and its packing parameter is p<1, determining an optimum curvature that is convex and tend to favor the formation of O/W emulsions. When the temperature reached the PIT, the packing parameter is p=1, monolayers with zero curvature are present, with the formation of liquid crystalline or

bicontinuous systems. Finally, when the temperature is higher than the PIT (T> PIT +20 °C) the surfactant is more soluble in oil than in water, and its packaging parameter is p>1, with an optimum concave curvature, supporting the formation of W/O emulsion[73,75,101].

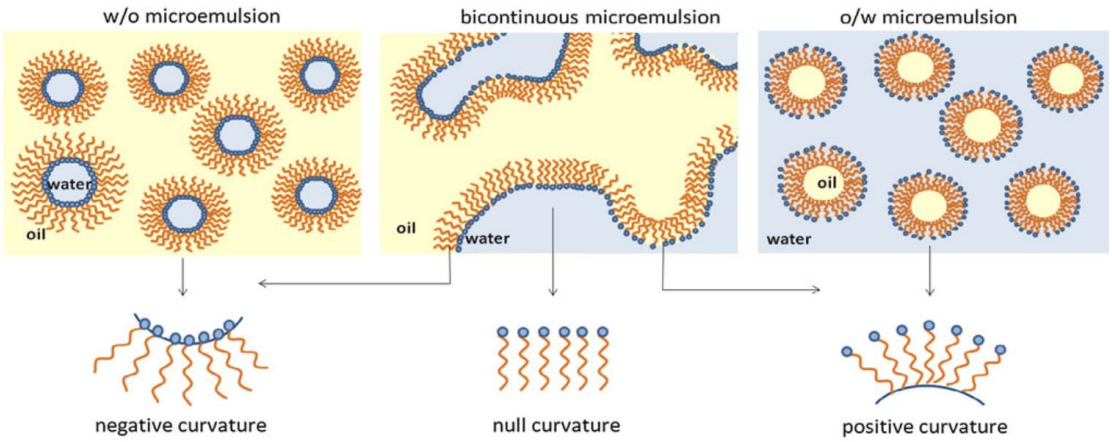

Figure1.12: Monolayer curvature of W/O, bicontinuous and O/W microemulsions[70]

Phase-inversion composition method is rather similar to the PIT method. In this case the optimum curvature of the surfactant is modified by altering the composition of the system, i.e. by adding salt or changing the pH to amend the electrical charge and stability of the emulsion, instead of temperature changes[99].

In both PIT and PIC methods, the conversion of an emulsion type to another is governed by a transitional phase inversion (TPI) which, acting on the formulation variables (temperature, pH or ionic strength), consequently cause an alteration of the surfactant properties. On the other hand, in the emulsion inversion point (EIP) method, the transformation of on type of an emulsion to another is determined by a catastrophic phase inversion (CPI). This phenomenon occurs when the ratio of the oil and water phase is altered, but the surfactant characteristics remain stable, and is caused by increasing or decreasing the volume fraction of the disperse phase of an emulsion above or below some critical level. On the other hand, a catastrophic-phase inversion occurs when the ratio of the oil-to-water phases is

altered while the surfactant proper- ties remain constant. Practically, catastrophic-phase inversion is usually induced by either increasing (or decreasing) the volume fraction of the dispersed phase in an emulsion above (or below) some critical level[100].

1.3.6.2. Spontaneous emulsification

In this method, the emulsion is spontaneously created when a combination of oil, water, surfactants (lipophilic and/or hydrophilic) and a water miscible cosurfactant are mixed together at constant temperature without any phase transitions in the system during the emulsification process[101-102] (Fig.1.13). This technique can be performed in different ways, by varying the compositions of the two phases, the environmental conditions (e.g., temperature, pH, and ionic strength), and/or, the mixing conditions (e.g., stirring speed, rate of addition, and order of addition). In the pharmaceutical field, the systems prepared employing this method are called self-emulsifying delivery systems (SNEDDS).

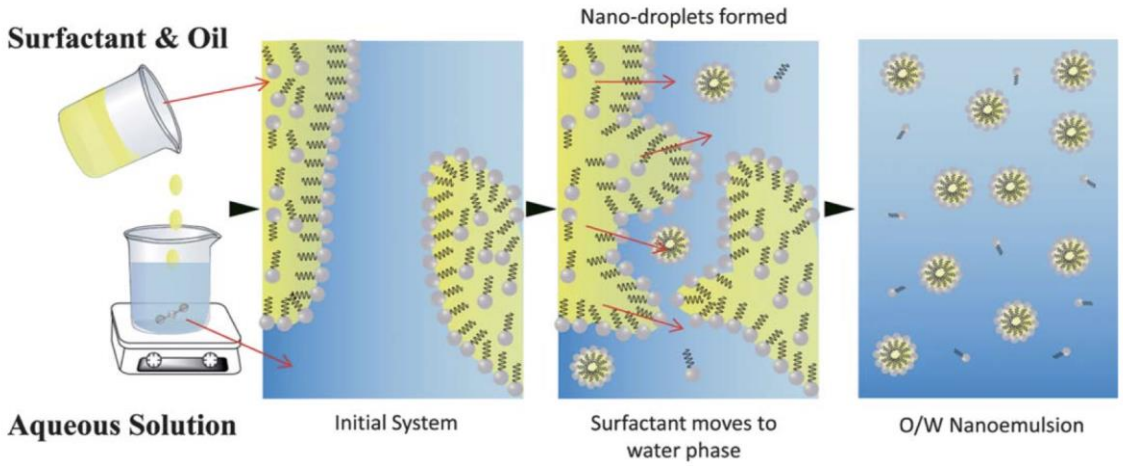

Figure 1.13: Proposed mechanism for spontaneous emulsification[70]

1.3.7. Emulsions Pharmaceutical Applications

Emulsion technology is employed in many industrial applications including food (in which emulsions are by far the most widely used in systems such as

mayonnaise, salad creams, beverages, etc.), agriculture (for formulation of many herbicides and insecticides), cosmetic and personal care products (hand creams, lotions, sunscreens, hair sprays, etc.), pharmaceuticals and others.

More specifically, in the pharmaceutical field, emulsions have been widely used as drug carriers both for hydrophilic and hydrophobic drugs, as they can be delivered by oral, topical, and parenteral routes[103-104]. A more detailed description of these three routes of administration will be discussed in the following sections.

1.3.7.1. Parenteral administration

The term "parenteral" covers different administration routes: intravenous, intramuscular, and subcutaneous. However, among these routes the most important delivery is the intravenous one. These kinds of emulsions are in general O/W emulsions and are suitable systems for the delivery of lipophilic compounds. The mean particle size of this systems ranging from 200 to 500 nm. The have to satisfy a very strict requisite regarding the droplets size because fat particles with a diameter over 5um can cause fat emboli in small capillaries i.e. lung capillaries[105-107]. Parenteral emulsions have been extensively used for parenteral nutrition in patients in a critical nutrition state and also commercialized in most cases for this purpose (i.e. Intralipid, Lipofundin, Liposyn)[108-109]. These emulsions have been also used as carriers for delivering lipophilic drugs intravenously[110].

Lipid emulsions offer numerous advantages as parenteral drug carriers such as solubilization of highly lipophilic drugs, stabilization of labile drugs against hydrolysis or oxidation, sustained release, and drug targeting. There are two different method for drugs incorporation within these systems: (1) *de novo* production or (2) extemporaneous addiction. *De novo* production is usually used for highly oil soluble drugs by dissolving the drug in the oil phase prior to emulsification. On the contrary, extemporaneous addiction of the drug occurs when it is added, with the aid of an organic solvent, in preformed fat emulsions. The main drawback of this process is

related to the possibility to have drug precipitation in the aqueous phase or breaking of the carrier emulsion.

1.3.7.2. Topical administration

Topical drug delivery through the skin is a popular method of drug administration as it is a non-invasive and painless. In this context, emulsions have been used as both dermatological and cosmetic formulations for many centuries. As a topical drug delivery system, emulsions have been formulated in a variety of forms including lotions, creams, foams, sometimes emulsion-gels and emulsion-ointments, used to apply solutions or suspensions of drugs to the skin for therapeutic purposes. These systems are able to delivery either water soluble and insoluble active ingredients that can be used for cosmetic or pharmaceutical applications[111-112]. These kinds of formulations have higher compatibility with the skin if compared with other topical and transdermal dosage forms. For example, in contrast to ointments, emulsions do not block the normal evaporation of moisture and are easy to wash away with water, being less oily. Instead, in comparison to liquid formulations, the viscosity of emulsions can be adjusted to better control the surface area of the application[111-113].

When the emulsion is applied on the skin, the drug delivery process occurs in different steps. First, the drug is released from the formulation, then it partitions into the skin surface and finally the drug diffuses through the skin surface into the underlying tissues[114]. The range of topical emulsion products that use an emulsified form of drug includes[115]:

1. Creams are topical preparations used across a wide range of skin conditions (eczema, psoriasis, acne vulgaris). They can be formulated both as O/W and W/O dosages. Creams hold useful barrier properties which can protect the skin and can also be used as vehicle for drug substances (antibiotics,

antifungal drugs, local anesthetics, anti-inflammatory drugs, antipruritic drugs) when dispersed in a suitable base.

2. Ointment are usually oil-based dosage forms topically applied both on the skin and the mucous membranes. Its dispersion medium or vehicle is referred as its base, which selection depends upon the end use of the ointment. In general, they are used as emollients, for the application of actives to the skin or for protective purposes where occlusion is required.
3. Gel disintegrates on contact with the skin.
4. Paste consists of oil, water and powder. Also described as an ointment with a dispersed powder.
5. Liniment (balm, lotion or embrocation) are not hugely significant for therapeutic use.

1.3.7.3. Oral Administration

Emulsions for oral delivery, as submicron emulsions, microemulsions, multiple emulsions and self-emulsifying drug delivery systems, are formulations in which the active ingredients are solubilized or dispersed in the internal phase of the emulsion. In general, these emulsions are mainly used in the form of O/W type enhancing the oral bioavailability of poorly absorbed drug substances. Oral administration of emulsion based formulations offer numerous advantages, including: increased absorption, prolonged pharmacological effects of drugs with short half-life, decreased toxicity, protection against degradation (hydrolysis or enzymatic) in the GIT [116-119]. For their formulation, all the materials used have to be safe and are in general supplied from the food field in order to overcome toxicity effects. The absorption of O/W formulations mainly depends on many formulation−related parameters, such as drug physical properties, particle size, oil nature, the presence of surfactant and the polarity of the oil droplets.

Among the different emulsions types for oral delivery, self-emulsifying drug delivery systems (SEDDS) are the most used, because when compared with

emulsions, which are sensitive and metastable dispersed forms, SEDDS are physically stable formulations that are easy to manufacture[117]. SEDDS can be orally administered in soft or hard gelatin capsules[118] and form fine relatively stable oil−in−water (O/W) emulsions upon aqueous dilution owing to the gentle agitation of the gastrointestinal fluids.

Four drug products on the pharmaceutical market, Sandimmune® and Sandimmun Neoral® (cyclosporin A), Norvir® (ritonavir), and Fortovase® (saquinavir), present active compounds that have been formulated into specific SEDDS, demonstrating a significant improvement in oral bioavailability for these drugs[120].

1.5. References

1. Harrison, K. Introduction to polymeric drug delivery systems. Biomedical Polymers. Woodhead Publishing, 2007. 33-56.
2. Wen H, Jung H, Li X. Drug Delivery Approaches in Addressing Clinical Pharmacology-Related Issues: Opportunities and Challenges. AAPS J. 2015;17(6):1327-40.
3. Tiwari G, Tiwari R, Sriwastawa B, et al. Drug delivery systems: An updated review. Int J Pharm Investig. 2012;2(1):2-11.
4. Patel, Nitesh R., and Piyush P. Gohil. A review on biomaterials: scope, applications & human anatomy significance. International Journal of Emerging Technology and Advanced Engineering 2.4 (2012): 91-101.
5. Grund, Stefan, Marius Bauer, and Dagmar Fischer. "Polymers in drug delivery—state of the art and future trends." Advanced Engineering Materials 13.3 (2011): B61-B87.
6. Angelova, Nela, and David Hunkeler. Rationalizing the design of polymeric biomaterials. Trends in biotechnology 17.10 (1999): 409-421.
7. Ulery BD, Nair LS, Laurencin CT. Biomedical Applications of Biodegradable Polymers. J Polym Sci B Polym Phys. 2011;49(12):832-864.

8. Nair LS, Laurencin CT. Biodegradable polymers as biomaterials. Prog Polym Sci 2007;32(8-9):762-798.
9. Song, R., Murphy, M., Li, C., Ting, K., Soo, C., & Zheng, Z. (2018). Current development of biodegradable polymeric materials for biomedical applications. Drug design, development and therapy, 12, 3117.
10. Kunduru, Konda Reddy, Arijit Basu, and Abraham J. Domb. Biodegradable Polymers: Medical Applications. Encyclopedia of Polymer Science and Technology (2002): 1-22.
11. Pillai, Omathanu, and Ramesh Panchagnula. Polymers in drug delivery. Current opinion in chemical biology 5.4 (2001): 447-451.
12. Kohane DS, Langer R. Polymeric Biomaterials in Tissue Engineering. Pediatr Res. 2008;63(5):487–491.
13. Liechty WB, Kryscio DR, Slaughter BV, Peppas NA. Polymers for drug delivery systems. Annu Rev Chem Biomol Eng. 2010;1:149-73.
14. Elbert DL, Hubbell JA (1996) Surface Treatments of Polymers for Biocompatibility. Ann Rev Mater Sci 26: 365.
15. Vilar, Gemma, Judit Tulla-Puche, and Fernando Albericio. Polymers and drug delivery systems. Current drug delivery 9.4 (2012): 367-394.
16. Peteiro, César. Alginate Production from Marine Macroalgae, with Emphasis on Kelp Farming. Alginates and Their Biomedical Applications. Springer, Singapore, 2018. 27-66.
17. Norton, I. 2010. Practical food rheology: an interpretive approach, Hoboken, NJ, USA, Wiley-Blackwell.
18. Sabra, W., A-P. Zeng, and W-D. Deckwer. Bacterial alginate: physiology, product quality and process aspects. Applied microbiology and biotechnology 56.3-4 (2001): 315-325.
19. Urtuvia, Viviana, et al. Bacterial alginate production: an overview of its biosynthesis and potential industrial production. World Journal of Microbiology and Biotechnology 33.11 (2017): 198.

20. Rehm, B. H. A., and S. Valla. Bacterial alginates: biosynthesis and applications. Applied microbiology and biotechnology 48.3 (1997): 281-288.
21. Haug, A. 1964. Composition and properties of alginates, Norwegian Institute of Seaweed Research.
22. Stokke, B. T., Smidsroed, O., Bruheim, P. & Skjaak-Braek, G. 1991. Distribution of uronate residues in alginate chains in relation to alginate gelling properties. Macromolecules, 24, 4637-4645.
23. Draget, Kurt I., and Catherine Taylor. Chemical, physical and biological properties of alginates and their biomedical implications. Food Hydrocolloids 25.2 (2011): 251-256.
24. Grant GT, Morris ER, Rees DA, Smith PJC, Thom D (1973) Biological interactions between polysaccharides and divalent cations: the egg-box model. FEBS Lett 32(1):195–198
25. Braccini I, Pérez S (2001) Molecular basis of Ca^{2+}-induced gelation in alginates and pectins: the egg-box model revisited. Biomacromolecules 2(4):1089–1096
26. Plazinski W (2011) Molecular basis of calcium binding by polyguluronate chains. Revising the egg-box model. J Comput Chem 32(14):2988–2995
27. Ionita, G., Ariciu, A. M., Smith, D. K., & Chechik, V. (2015). Ion exchange in alginate gels–dynamic behaviour revealed by electron paramagnetic resonance. Soft matter, 11(46), 8968-8974.
28. Augst, A.D.; Kong, H.J.; Mooney, D.J. Alginate Hydrogels as Biomaterials. Macromol. Biosci. 2006, 6, 623–633.
29. Otterlei M, Ostgaard K, Skjakbraek G, Smidsrod O, Soonshiong P, Espevik T. Induction of cytokine production from human mono- cytes stimulated with alginate. J Immunother 1991;10:286–91
30. Soon-Shiong et al., 1994; Yang, Dong, and Kim S. Jones. Effect of alginate on innate immune activation of macrophages. Journal of Biomedical

Materials Research Part A: An Official Journal of The Society for Biomaterials, The Japanese Society for Biomaterials, and The Australian Society for Biomaterials and the Korean Society for Biomaterials 90.2 (2009): 411-418.

31. Espevik, T., Rokstad A.M., Kulseng, B., Strand, B., Skjåk-Braek, G.: Mechanisms of the host immune response to alginate microcapsules. In: Hallè, J.P., de Vos, P., Rosenberg,L. (eds.) The bioartificial pancreas and other biohybrid therapies, Transworld Research Network (2009): 279-290.
32. Skjåk-Bræk, G., Flo, T., Halaas, Ø., & Espevik, T. (2000). Immune stimulating properties of di-equatorially β (1→ 4) linked poly-uronides. In Bioactive carbohydrate polymers (pp. 85-93). Springer, Dordrecht.
33. Spargo, B.J., Rudolph, A.S., Rollwagen, F.M., Recruitment of Tissue Resident Cells to Hydrogel Composites: in Vivo Response to Implant Materials, Biomaterials 15 (1994) 853-858.
34. Zimmermann, U., Klock, G., Grohn, P., Jangaard, N.O., Wilkinson, C.K., Cell Encapsulation in Alginate: Elimination of Foreign Body Reaction and Microcapsule Volume Minimization, Monsanto Co. Newsletter, 1995.
35. Orive G, Ponce S, Hernandez RM, Gascon AR, Igartua M, Pedraz JL. Biocompatibility of microcapsules for cell immobi- lization elaborated with different type of alginates. Biomaterials 2002;23:3825–31.
36. Lee J, Lee KY. Local and sustained vascular endothelial growth factor delivery for angiogenesis using an injectable system. Pharm Res 2009;26:1739–44.
37. Coviello, T., Matricardi, P., Alhaique, F. Drug delivery strategies using polysaccharidic gels. Expert Opin. Drug Deliv. 3 (3) (2006) 395-404.
38. Cottrell, I. W., Kovacs, P., Alginates, In: Davidson, R. L. (Ed), Handbook of water soluble gums and resins, Kingsport Press (1980).
39. Gacesa, P. Alginates. Carbohydr. Polym. 8 (1988) 161-182.

40. Lee, Kuen Yong, and David J. Mooney. Alginate: properties and biomedical applications. Progress in polymer science 37.1 (2012): 106-126.
41. Szekalska, M., Puciłowska, A., Szymańska, E., Ciosek, P., & Winnicka, K. (2016). Alginate: Current use and future perspectives in pharmaceutical and biomedical applications. International Journal of Polymer Science, 2016.
42. Leiman, D. A., Riff, B. P., Morgan, S., Metz, D. C., Falk, G. W., French, B., & Lewis, J. D. (2017). Alginate therapy is effective treatment for gastroesophageal reflux disease symptoms: a systematic review and meta-analysis. Diseases of the Esophagus, 30(2), 1-8.
43. Sarker, Bapi; Boccaccini, Aldo R. Alginate Utilization in Tissue Engineering and Cell Therapy. In: Alginates and Their Biomedical Applications. Springer, Singapore, 2018. p. 121-155.
44. Suarez-Arnedo, A., Sarmiento, P., Cruz, J. C., Muñoz-Camargo, C., Salcedo, F., Groot, H., & Narváez, D. M. (2018, May). 3D Alginate Hydrogels with Controlled Mechanical Properties for Mammalian Cell Encapsulation. In 2018 IX International Seminar of Biomedical Engineering (SIB) (pp. 1-5). IEEE.
45. McClements, D.J. 2005. Food Emulsion; Principles, Practices, and Techniques, London: CRC press LLC.
46. Sarker, D.K. (2008) Quality Systems and Controls for Pharmaceuticals, John Wiley & Sons Ltd, Chichester.
47. Tadros, Th.F. and Vincent, B. (1983) in Encyclopedia of Emulsion Technology (ed. Becher, P.), Marcel Dekker, New York.
48. Yahaya Khan, M., Abdul Karim, Z. A., Hagos, F. Y., Aziz, A. R. A., & Tan, I. M. (2014). Current trends in water-in-diesel emulsion as a fuel. The Scientific world journal, 2014.
49. Callender, S. P., Mathews, J. A., Kobernyk, K., & Wettig, S. D. (2017). Microemulsion utility in pharmaceuticals: Implications for multi-drug delivery. International journal of pharmaceutics, 526(1-2), 425-442.

50. Sahu GK, Sharma H, Gupta A, Kaur CD (2015) Advancements in Microemulsion Based Drug Delivery Systems for Better Therapeutic Effects. Int J Pharm Sci Dev Res 1(1): 008-015.
51. Dickinson, E. and McClements, D.J., 1995. Advances in Food Colloids, Chapman and Hall, London.
52. Whitehurst,R.J.(2004).EmulsifiersinFoodTechnology.Oxford,UK:Blackwell Publishing Limited.
53. Hsu, C.T., Chang, C.H., and Lin, S.Y. 2000. Study on Surfactant Adsorption Kinetics: Effects of Interfacial Curvature and Molecular Interaction. Langmuir, 16, (3) 1211-1215
54. Jafari SM, He Y, Bhandari B (2007) Effectiveness of encapsulating biopolymers to produce sub-micron emulsions by high energy emulsification techniques. Food Res Int 40:862–873
55. de Guertechin, Louis Oldenhove. "71 Surfactants: Classification." Cosmetic Science and Technology (2009): 769
56. Raffa, P., Wever, D. A. Z., Picchioni, F., & Broekhuis, A. A. (2015). Polymeric surfactants: synthesis, properties, and links to applications. *Chemical reviews*, *115*(16), 8504-8563.
57. Griffin WC, Classification of Surface Active Agents by HLB, Journal of the Society of Cosmetic Chemistry 1(1949):311.
58. McClements, D.J. 2005. Food Emulsion; Principles, Practices, and Techniques, London: CRC press LLC.
59. Walstra, P. (1993) Principles of emulsion formation. Chemical Engineering Science, 48(2), 333–349.
60. Tadros, Tharwat F. Emulsion science and technology: a general introduction. Wiley-VCH Verlag GmbH & Co. KGaA Weinheim, 2009.
61. David Julian Mcclements (2007): Critical Review of Techniques and Methodologies for Characterization of Emulsion Stability, Critical Reviews in Food Science and Nutrition, 47:7, 611-649.

62. McClements, D.J. and Li, Y. (2010) Review of in vitro digestion models for rapid screening of emulsion-based systems. Food and Function, 1(1), 32–59.
63. Taylor, P. "Ostwald ripening in emulsions." Advances in colloid and interface science 75.2 (1998): 107-163.
64. Manoharan C., Basarkar A., Singh J. (2010) Various Pharmaceutical Disperse Systems. In: Kulshreshtha A., Singh O., Wall G. (eds) Pharmaceutical Suspensions. Springer, New York, NY.
65. Billany MR. 2007. Suspensions and emulsions. In: Aulton ME, ed. The Design and Manufacture of Medicine. Philadelphia: Churchill Livingstone, Elsevier 383 - 405.
66. Loncin and Mercer, 1979; Walstra, Pieter. "Principles of emulsion formation." Chemical Engineering Science 48.2 (1993): 333-349.
67. Schubert, Helmar, and Heike Karbstein. Mechanical emulsification. Developments in Food Engineering. Springer, Boston, MA, 1994. 9-14.
68. Walstra, Pieter, and Pauline EA Smulders. Emulsion formation. Modern aspects of emulsion science (1998): 56-99.
69. Walstra, P. (2003). Physical Chemistry of Foods. New York, NY.: Marcel Decker.
70. McClements DJ (2011) Edible nanoemulsions: fabrication, properties, and functional performance. Soft Matter 7:2297–2316
71. Tadros, T., Izquierdo, P., Esquena, J., & Solans, C. (2004). Formation and stability of nano-emulsions. Advances in colloid and interface science, 108, 303-318.
72. Tadros, Tharwat F., ed. Emulsion formation and stability. John Wiley & Sons, 2013.
73. Santana, R. C., F. A. Perrechil, and R. L. Cunha. High-and low-energy emulsifications for food applications: a focus on process parameters. Food Engineering Reviews 5.2 (2013): 107-122.

74. Yang, Y., Marshall-Breton, C., Leser, M. E., Sher, A. A., & McClements, D. J. (2012). Fabrication of ultrafine edible emulsions: Comparison of high-energy and low-energy homogenization methods. Food Hydrocolloids, 29(2), 398-406.
75. McClements, David Julian. Edible nanoemulsions: fabrication, properties, and functional performance. Soft Matter 7.6 (2011): 2297-2316.
76. Stang, Michael, Heike Schuchmann, and Helmar Schubert. Emulsification in high-pressure homogenizers. Engineering in Life Sciences 1.4 (2001): 151-157.
77. Karbstein, H.; Schubert, H., Developments in the Continuous Mechanical Production of Oil-in-Water Macroemulsions, Chem. Eng. Process. 34 (1995) pp. 205-211.
78. Walstra, P., Formation of Emulsions, in: Becher, P., Encyclopedia of Emulsion Technology, Vol.1, Basic Theory, Marcel Dekker, Inc., New York 1983, pp. 57±127.
79. Izadiyan Z, Basri M, Fard Masoumi HR, Abedi Karjiban R, Salim N, Shameli K. Modeling and optimization of nanoemulsion containing Sorafenib for cancer treatment by response surface methodology. Chem Cent J. 2017;11:21.
80. Urban, K., Wagner, G., Schaffner, D., Röglin, D., & Ulrich, J. (2006). Rotor-stator and disc systems for emulsification processes. Chemical Engineering & Technology: Industrial Chemistry-Plant Equipment-Process Engineering-Biotechnology, 29(1), 24-31.
81. Atiemo-Obeng, Victor A., and Richard V. Calabrese. Rotor-stator mixing devices. Handbook of industrial mixing: Science and practice (2004): 479-505.
82. Abismaıl, B., Canselier, J. P., Wilhelm, A. M., Delmas, H., & Gourdon, C. (1999). Emulsification by ultrasound: drop size distribution and stability. Ultrasonics Sonochemistry, 6(1-2), 75-83.

83. Dolatowski, Zbigniew J., Joanna Stadnik, and Dariusz Stasiak. Applications of ultrasound in food technology. Acta Scientiarum Polonorum Technologia Alimentaria 6.3 (2007): 88-99.
84. Abbas, S., Hayat, K., Karangwa, E., Bashari, M., & Zhang, X. (2013). An overview of ultrasound-assisted food-grade nanoemulsions. Food Engineering Reviews, 5(3), 139-157.
85. Mao L, Yang J, Xu D, Yuan F, Gao Y (2010) Effects of homogenization models and emulsifiers on the physicochemical properties of b-carotene nanoemulsions. J Disper Sci Technol 31:986–993
86. Charcosset, C., I. Limayem, and H. Fessi. The membrane emulsification process—a review. Journal of Chemical Technology & Biotechnology: International Research in Process, Environmental & Clean Technology 79.3 (2004): 209-218.
87. Piacentini, Emma, Enrico Drioli, and Lidietta Giorno. Membrane emulsification technology: Twenty-five years of inventions and research through patent survey. Journal of membrane science468 (2014): 410-422.
88. Charcosset, Catherine. Preparation of emulsions and particles by membrane emulsification for the food processing industry. Journal of Food Engineering 92.3 (2009): 241-249.
89. Kandori, Kazuhiko. Applications of microporous glass membranes: membrane emulsification. Food Processing. 1995. 113-142.
90. Williams, R.A., Peng, S.J., Wheeler, D.A., Morley, N.C., Taylor, D., Whalley, M., Houldsworth, D.W., 1998. Controlled production of emulsions using a crossflow membrane, Part II: Industrial scale manufacture. Chem. Eng. Res. Des. 76, 902– 910.
91. Schröder, V., Behrend, O., Schubert, H., 1998. Effect of dynamic interfacial tension on the emulsification process using microporous ceramic membranes. J. Coll. Interf. Sci. 202, 334–340

92. Vladisavljević, G. T., Isao Kobayashi, and Mitsutoshi Nakajima. Production of uniform droplets using membrane, microchannel and microfluidic emulsification devices. Microfluidics and nanofluidics 13.1 (2012): 151-178.
93. S. Sugiura, M. Nakajima, J. Tong, H.Nabetani, M. Seki Preparation of monodispersed solid lipid microspheres using a microchannel emulsification technique J Colloid Interface Sci, 227 (2000), pp. 95-103
94. Mitsutoshi Nakajima. Regular-sized cell creation in microchannel emulsification by visual micro processing method. Journal of the American Oil Chemists' Society 74.3 (1997): 317-321.
95. Kobayashi, I., Wada, Y., Uemura, K., & Nakajima, M. (2010). Microchannel emulsification for mass production of uniform fine droplets: integration of microchannel arrays on a chip. Microfluidics and Nanofluidics, 8(2), 255-262.
96. Solans, Conxita, and Isabel Solé. Nano-emulsions: formation by low-energy methods. Current opinion in colloid & interface science 17.5 (2012): 246-254.
97. Mason TG, Wilking JN, Meleson K, Chang CB, Graves SM (2006) Nanoemulsions: formation, structure, and physical properties. J Phys Condens Matter 18:R635–R666
98. Nagarajan, R. Molecular packing parameter and surfactant self-assembly: the neglected role of the surfactant tail. Langmuir18.1 (2002): 31-38.
99. Anton, Nicolas, and Thierry F. Vandamme. The universality of low-energy nano-emulsification. International Journal of Pharmaceutics 377.1-2 (2009): 142-147.
100. Fernandez P., André V., Rieger J., Kuhnle A., 2004, Nano-emulsion formation by emulsion phase inversion, Coll. Surf. A, 251, 53-58, DOI:10.1016/j.colsurfa.2004.09.029

101. Solans, Conxita, and Isabel Solé. Nano-emulsions: formation by low-energy methods. Current opinion in colloid & interface science 17.5 (2012): 246-254.

102. Juan Carlos López-Montilla, Paulo Emilio Herrera-Morales, Samir Pandey & Dinesh O. Shah (2002) Spontaneous Emulsification: Mechanisms, Physicochemical Aspects, Modeling, and Applications, Journal of Dispersion Science and Technology, 23:1-3,219-268

103. Sahu GK, Sharma H, Gupta A, Kaur CD (2015) Advancements in Microemulsion Based Drug Delivery Systems for Better Therapeutic Effects. Int J Pharm Sci Dev Res 1(1): 008-015.

104. Gilberte Marti-Mestres & Françoise Nielloud (2002): Emulsions in Health Care Applications—An Overview, Journal of Dispersion Science and Technology, 23:1-3, 419-439.

105. Driscoll, David F. "Lipid injectable emulsions: 2006." Nutrition in Clinical Practice 21.4 (2006): 381-386. Hippalgaonkar K, Majumdar S, Kansara V. Injectable lipid emulsions-advancements, opportunities and challenges. AAPS PharmSciTech. 2010;11(4):1526-40. R. J.

106. Prankerd, R. J., and V. J. Stella. "The use of oil-in-water emulsions as a vehicle for parenteral drug administration." *PDA Journal of Pharmaceutical Science and Technology* 44.3 (1990): 139-149.

107. Nielloud, Françoise. Pharmaceutical Emulsions and Suspensions: Revised and Expanded. CRC Press, 2000.

108. Fell GL, Nandivada P, Gura KM, Puder M. Intravenous Lipid Emulsions in Parenteral Nutrition. Adv Nutr. 2015;6(5):600-10.

109. Calder PC, Jensen GL, Koletzko BV, Singer P, Wanten GJ. Lipid emulsions in parenteral nutrition of intensive care patients: current thinking and future directions. Intensive Care Med. 2010;36(5):735-49.

110. Collins-Gold, L. C., R. T. Lyons, and L. C. Bartholow. Parenteral emulsions for drug delivery. Advanced Drug Delivery Reviews5.3 (1990): 189-208.

111. Smith, Eric W., Howard I. Maibach, and Christian Surber. Use of emulsions as topical drug delivery systems. Pharmaceutical emulsions and suspensions (2000): 259-270.

112. Lu, Guang Wei, and Ping Gao. Emulsions and microemulsions for topical and transdermal drug delivery. Handbook of Non-Invasive Drug Delivery Systems. 2010. 59-94.

113. Roberts, M.S., Cross, S.E., Pellett, M.A., 2002. Skin transport. In: Walter, K.A. (Ed.), Dermatological and Transdermal Formulations. Marcel Dekker, New York, pp. 89–195.

114. Sarker, Dipak Kumar, ed. Pharmaceutical emulsions: a drug developer's toolbag. John Wiley & Sons, 2013.

115. Kammona O, Kiparissides C. Recent advances in nanocarrier-based mucosal delivery of biomolecules. J. Control. Release 161, 781–794 (2012).

116. Makadia HA, Bhatt AY, Parmar RB, Paun JS, Tank HM. Self-nano emulsifying drug delivery system (SNEDDS): future aspects. Asian J. Pharm. Res. 3, 21–27 (2013).

117. Tan A, Prestidge CA, Nielsen HM, Müllertz A. Self-nanoemulsifying drug delivery systems for oral insulin delivery: in vitro and in vivo evaluations of enteric coating and drug loading. Int. J. Pharm. 477, 390–398 (2014).

118. Sim, T., Lim, C., Hoang, N. H., Joo, H., Lee, J. W., Kim, D. W., ... & Oh, K. T. (2016). Nanomedicines for oral administration based on diverse nanoplatform. Journal of Pharmaceutical Investigation, 46(4), 351-362.

119. Mohsin K, Shahba AA, Alanazi FK. Lipid based self-emulsifying formulations for poorly water-soluble drugs – an excellent opportunity. Indian J. Pharm. Educ. 46, 88–96 66 (2012).

120. Karamanidou, T., Bourganis, V., Kammona, O., & Kiparissides, C. (2016). Lipid-based nanocarriers for the oral administration of biopharmaceutics. Nanomedicine, 11(22), 3009-3032.

Chapter 2

Investigation of in vitro Hydrophilic and Hydrophobic dual drug release from polymeric films produced by sodium alginate-MaterBi® drying emulsions

2.1. Introduction

Partially taken from Setti, Chiara, et al. "Investigation of in vitro Hydrophilic and Hydrophobic Dual Drug Release from Polymeric Films Produced by Sodium alginate-MaterBi® Drying Emulsions." European Journal of Pharmaceutics and Biopharmaceutics (2018).

Emulsion science and technology is proving to be an indispensable tool for pharmaceutical formulations, in which problems like stabilization of poorly soluble drugs in aqueous media can be circumvented, as well as combination or encapsulation of hydrophilic and hydrophobic drugs can be achieved in a single medium[1-3]. An example is the transformation of injectable lipid emulsions, that are clinically used as a nutritional fatty acid and vitamin source for hospitalized patients, into drug releasing media for the intravenous delivery of lipid soluble therapeutic agents[3-4]. At the same time, alginate emulsions have also evolved, as various

microencapsulation and microfluidic technologies started to align with emulsion-based drug delivery approaches[5-6]. Alginate emulsions are regarded as ideal platforms for the encapsulation of hydrophobic drugs, and for high oil cosmetic or edible grade payloads, such as proteins[5]. For instance, alginates have been shown to boost stability of dairy-protein emulsions[7]. They were also indispensably used as pH-sensitive drug delivery systems[8]. Sodium alginate can be easily cross-linked (*gelatinized*) by various aqueous salt solutions (i.e. calcium chloride) via an *ion exchange* mechanism[9]. Being this property transferable to alginate-based emulsions[10], both hydrophilic and hydrophobic active agents can be effectively encapsulated in the form of macro-[11], micro-[1] or nano-scale emulsified spheres[12], depending on the targeted pharmaceutical application. Moreover, the extent of ion exchange cross-linking can be tuned in order to control the release of the encapsulated agents[13]. In certain cases, cross-linked alginate beads can be coated with other natural biopolymers (such as chitosan), in order to further delay or sustain the release process in different pH environments, such as the intestinal media[14].

In the early 90s, surfactant-laden alginate-polymer emulsions containing hydrophobic biopolymers dispersed in oil phase were developed[15], and, lately, they have been gaining in popularity not only in pharmaceutics but also in the field of food science and technology[16]. Recent works showed that these emulsions could be electrospun to encapsulate drug reservoirs in fibrillar scaffolds[17]. According to Qi *et al.*[17], many new types of functional biomaterials can be designed by combining alginate with various hydrophobic biopolymers in alginate-polymer emulsions, with proper surfactant chemistry. Among these systems, polylactic acid (PLA) polymers deserve special attention, considering their extensive use in biomedics[18-19]. Alginate-PLA emulsions are considered to be a cost effective one-pot synthesis templates for creating porous scaffolds[20-21]. For instance, biodegradable microspheres containing cisplatin (a chemotherapy medication) were formulated by PLA-polycaprolactone (PCL) blends in alginate emulsions as sustained drug delivery systems for the control of restenosis[22]. Liquid extrusion of alginate-polymer emulsions into cross-linking

salt solutions is a highly preferred method of producing functional soft materials due to the fact that, during liquid extrusion, surfactants are indispensable and can maintain micellar stability and phase miscibility. However, production of soft materials from drying emulsions requires continuous phase miscibility, since surfactants lose their function as the emulsions dry out into films or monoliths[23].

In the present study, we propose an alternative hydrophobic biocomposite for the development of alginate-biopolymer emulsions that can host and deliver, in a controlled manner, both hydrophobic and hydrophilic active agents. In particular, we show that aqueous solutions of sodium alginate and organic solvent dispersions of MaterBi® can be emulsified without the use of any surfactants by ultrasonic processing, and, upon drying, novel homogenous polymer films can be obtained. We believe that small thermoplastic starch particles in MaterBi® acted as Pickering emulsion stabilizers[24-26] allowing surfactant-free incorporation of two different model drugs, namely a cutaneous hydrophilic antiseptic and hydrophobic curcumin into the emulsions.

MaterBi® is a proprietary blend based on starch and polyesters, which has characteristics of use and workability very similar to those of traditional plastics. Main aspect of this material is its complete biodegradability by microorganisms, with the production of non-toxic degradation products involving water, CO_2 and methane[27]. This bioplastic has been developed and commercialized by Novamont, that produces four different classes of biodegradable materials under the MaterBi® trademark, all starch-based but differing in synthetic components: A, V, Y and Z.

- Class A is composed by thermoplastic starch complexed with vinylic ethylene alcohol copolymers. Those are biodegradable and non-compostable materials, with a biodegradation time frame of 2 years in a liquid environment. They are mainly used in areas where compostability is not required.
- Class V comprises materials where the content of starch, as thermoplastic plasticized starch, is over 85%. These items are biodegradable, with a

biodegradation time shorter than Z grades, compostable and soluble, used as substitutes of polystyrene packaging foams.

- Class Y includes naturally-derived supplies, such as thermoplastic starch in a dispersed form and cellulose derivatives. They are biodegradable and compostable, with mechanical properties and moldability very close to those of polystyrene. These materials are used for rigid and dimensionally stable injection molded items.
- Class Z encompasses materials with thermoplastic starch and PCL in a 1:1 weight ratio. Materials of this class are biodegradable, with a biodegradation time of 20-45 days in composting conditions. They are used for films and sheets production. The micro-structure of the products belonging to this class can be very different, ranging from thermoplastic starch dispersed in the synthetic component as in the case of MaterBi® ZIOIU, to thermoplastic starch in a semi-continuous phase, as in the case of MaterBi® ZF03U/A.

MaterBi® of class Z was used in this research project. It is completely biodegradable and commercially applied for the fabrication of several biodegradable objects (Fig.2.1) such as bags, gloves, food trays, transparent film, disposable cups and dishes, cotton sticks, diapers, containers for cosmetics, and toys[27-29].

Figure 2.1: MaterBi® applications

Although both PCL and thermoplastic starch have been extensively used in biomedical and pharmaceutical applications, no such applications have been published using MaterBi®[29]. We avoided the use of surfactants to stabilize our emulsions. Despite their useful function in various emulsion systems[30], several *in vitro* assays demonstrated certain severe side effects and cytotoxicity of surfactants on skin[31-34]. Non-ionic surfactants are considered to be the most suitable ones, due to their low irritation potential[35]. Furthermore, interaction of certain surfactants with biological systems can be associated with their ability to penetrate into the biological membranes, resulting in toxic effects and limiting their usage in pharmaceuticals. For example, surfactants can induce phospholipid emulsification, contributing to cellular damage, cytolytic processes and the release of proteins, lysosomal and cytoplasmic enzymes as well as inflammatory mediators[36-39].

We focused our research on the combination of two biopolymers, such as Sodium Alginate (SA) and MaterBi®, to develop a novel biodegradable material able to incorporate and release hydrophilic and hydrophobic drugs simultaneously, for the treatment of skin wounds.

The wound healing process, which is a restorative response to tissue injury, is characterized by four overlapping and interdepended phases: hemostasis, inflammation, proliferation, and remodeling, in which different cellular types (*e.g.* fibroblasts, keratinocytes, macrophages), growth factors and matrix components act together to restore the integrity of the damaged tissue[40-43] (Fig.2.2). With the aim of enhancing the healing process and to counteract several aspects affecting the overall tissue remodeling (*e.g.* excessive inflammation and wound infection), different wound dressings have been developed as vehicles able to deliver drugs or therapeutic agents to the wound site[44-51].

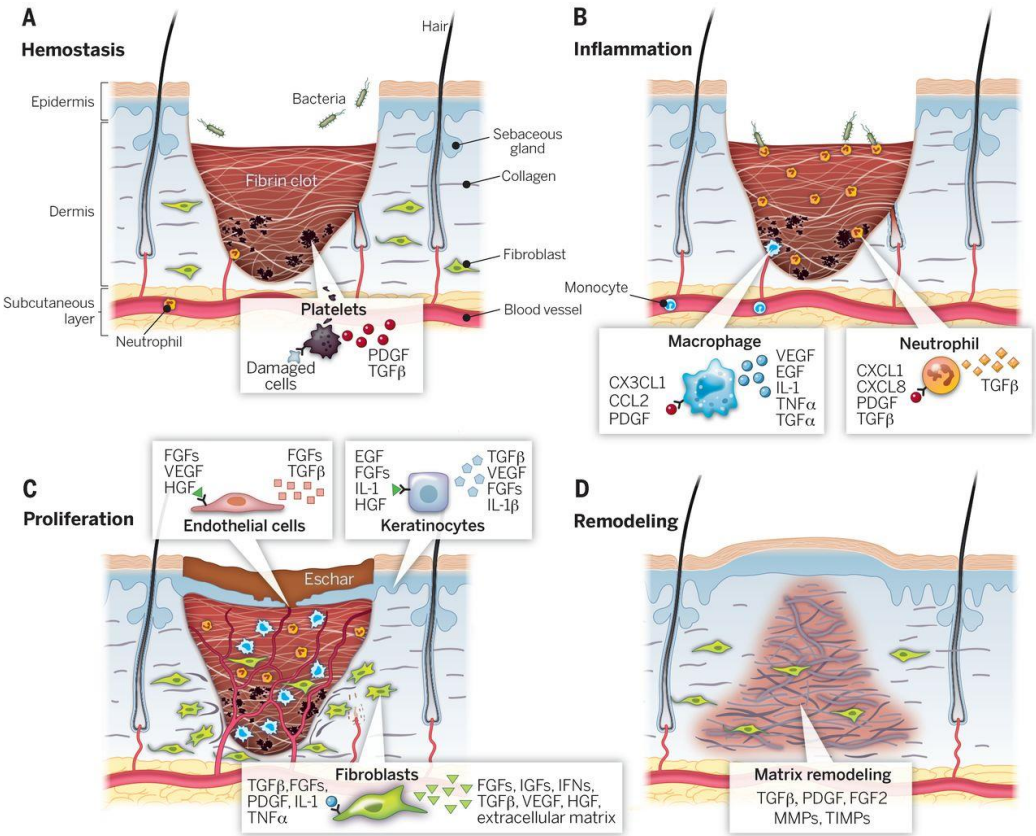

Figure 2.2: Stages characterizing the skin tissue wound healing process[51]

Neomercurocromo®, a commercial drug, was used as cutaneous antiseptic and accelerating healing agent. A standard bottle of 100 mL of this solution contains: chloroxylenol (0.3 g), eosin (2.0 g) and propylene glycol (30.0 g), with trace amounts of ethanol and sodium EDTA. Being not toxic, this product is used for local treatment of wounds, as disinfectant in abrasions, burns and bedsores, by directly applicating few drops (1-2 times a day) on the injured part. Neomercurocromo® is known to be active against gram-positive bacteria (*Staphylococcus aureus*, *Streptococcus pyogenes*, *Propionibacterium acnes*, *Corynebacterium xerosis*), gram-negative bacteria (*Pseudomonas aeruginosa*, *Escherichia coli*, *Klebsiella pneumoniae*), and fungi (*Candida albicans*). The two main components presenting antiseptic functionalities are chloroxylenol and eosin. Chloroxylenol is a chlorinated phenolic compound employed in antiseptic or disinfectant formulations[52-53], listed

by the World Health Organization as model of essential medicines[54]. Thanks to its nature, chloroxylenol may probably exert its effect against a wide range of Gram-positive bacteria by acting on microbial membranes. Eosin (2% in solution) is well-known for topical treatment of several skin complaints. It acts as a bacteriostatic agent against Gram-positive bacteria and fungi; moreover, it is also able to reduce pro-inflammatory cytokines and promote injured skin re-epithelialization[55]. Finally, propylene glycol is extensively used as a solvent in dermatological formulations. This compound was reported to be able to increase the permeation through the skin or the wound site of several active principles, being also employed as co-solvent and vehicle for many enhancers.

Curcumin (Cur) is the principal active ingredient of turmeric, extracted from the rhizomes of the plant *Curcuma longa.* This natural yellow pigment is nowadays considered a therapeutic agent, owning a wide range of pharmacological and medicinal applications, as proven and supported by results from *in vitro* investigations, animal model studies and human clinical trials[56-59]. It exhibits anti-inflammatory, anti-cancer, anti-microbial, anti-oxidant, and wound healing properties[57,59]. Cur is a complex molecule, having pleiotropic activities on various cellular pathways and many molecular targets (i.e. inflammatory molecules, transcription factors, enzymes, protein kinases, protein reductases, carrier proteins, cell survival proteins, drug resistance proteins, adhesion molecules, growth factors, receptors, cell cycle regulatory proteins, chemokines, DNA, RNA and metal ions)[58,60-62]. More specifically, in the wound healing context, Cur has shown efficacy against cutaneous, chronic and excisional wounds, accelerating the healing process[63-65].

Considering the above-mentioned premises and the physicochemical characteristics of the material system under study, we formulated the following hypotheses.

- ***Hypothesis (a):*** the combination of alginate and MaterBi® via emulsion technology can lead to the development of a new biodegradable and biocompatible material with controlled drug release properties.

- ***Hypothesis (b):*** given the hydrophilic and hydrophobic domains of the composite systems two model drugs can be accommodated, either individually or simultaneously. Their respective degradation processes will sustain the drug release profiles.
- ***Hypothesis (c):*** Tuning of the water stability of the hydrophilic component of the polymeric blend through the establishment of an ion cross-linking protocol can finely modulate the release of the drugs from the composite matrices over time.

In order to test our hypotheses, various formulation strategies and characterization methods have been implemented, as presented in detail in the following sections of this Chapter.

2.2. Materials and methods

Partially taken from Setti, Chiara, et al. "Investigation of in vitro Hydrophilic and Hydrophobic Dual Drug Release from Polymeric Films Produced by Sodium alginate-MaterBi® Drying Emulsions." European Journal of Pharmaceutics and Biopharmaceutics (2018).

2.2.1. Materials

Alginic acid sodium salt (sodium alginate), ammonium hydroxide solution (30-33% HN_3 in water), chloroform, phosphate buffered saline (PBS) powder, curcumin powder, ethanol, cell proliferation reagent WST (water-soluble tetrazolium salts)-1 and 2-(4-Amidinophenyl)-6-indolecarbamidine dihydrochloride (DAPI), were purchased from Sigma Aldrich and used as received. A commercial aqueous cutaneous solution known as Neomercurocromo® (Laboratorio Farmaceutico S.I.T. s.r.l. Italy), was purchased from a local pharmacy. Adult Human Dermal Fibroblasts (HDFa), Medium 106, Low Serum Growth Supplement Kit (LSGS Kit), Alexa Fluor 488 Phalloidin and MitoTracker Red were purchased from Thermofisher Scientific. Extruded MaterBi® sheets were purchased from Lavorazione Plastica Srl (Italy).

2.2.2. Preparation of alginate and MaterBi® solutions

In a typical procedure, the alginate solution was prepared by dissolving 1.8 g of sodium alginate powder in a mixture of 5 mL of ammonium hydroxide and 55 mL of distilled water at room temperature under vigorous stirring. Ammonium hydroxide enables extremely rapid solution of sodium alginate in water (within few minutes) and also ensures that the stock solution does not degrade in time (easily noticeable by the lowering of the viscosity) over long periods of storage due to bacterial action. The resultant alginate solution was 3% w/v. The MaterBi® solution was prepared by dissolving 1.8 g of MaterBi® resin in 60 mL of chloroform at room temperature, to obtain a solution with a concentration of 3% w/v. Dissolution was found to be very rapid in chloroform (a few minutes).

2.2.3. Preparation of the emulsions and films

Alginate-MaterBi® composite films were prepared by solvent casting and evaporation from the respective emulsions. Dry films with various sodium alginate-MaterBi® ratios were prepared by blending and emulsifying different amounts of alginate and MaterBi® solutions. Note that no surfactants, emulsifiers or compatibilizers were used in the preparation of the emulsions. Specifically, the following protocol of emulsification was followed. First, appropriate volumes of alginate and MaterBi® were transferred into a glass vial (see Figs. 2.3a and b). The mixture underwent phase separation within few minutes, as seen in Fig.1b. To avoid this phenomenon, the pre-emulsions were ultrasonic processed for 1 min with 40% amplitude (Sonics Vibra-Cell). The processing was done by four consecutive sonication steps each lasting 15 seconds. At the end of each 15-sec processing, the vial was transferred to a vortex mixer and stirred for additional 10 seconds. The schematic representation of the emulsification process is shown in Fig.2.3a. Figure 2.3b shows photographs of alginate (vial 1) and MaterBi® (vial 2) solutions, the

separated phases after vortex mixing (vial 3) and the stable emulsions after ultrasonic processing (vial 4).

Finally, the stable emulsions were poured into Teflon Petri dishes (10 cm in diameter) and were allowed to evaporate slowly at room temperature, while resting on a levelled surface. In order to understand if the relative sodium alginate to MaterBi® ratio in the emulsions affects the stability of the final system, a wide range of ratios between alginate and MaterBi® were considered, as shown in Table 2.1. It was observed that all the emulsions presented in Table 2.1 were stable and suitable for film formation.

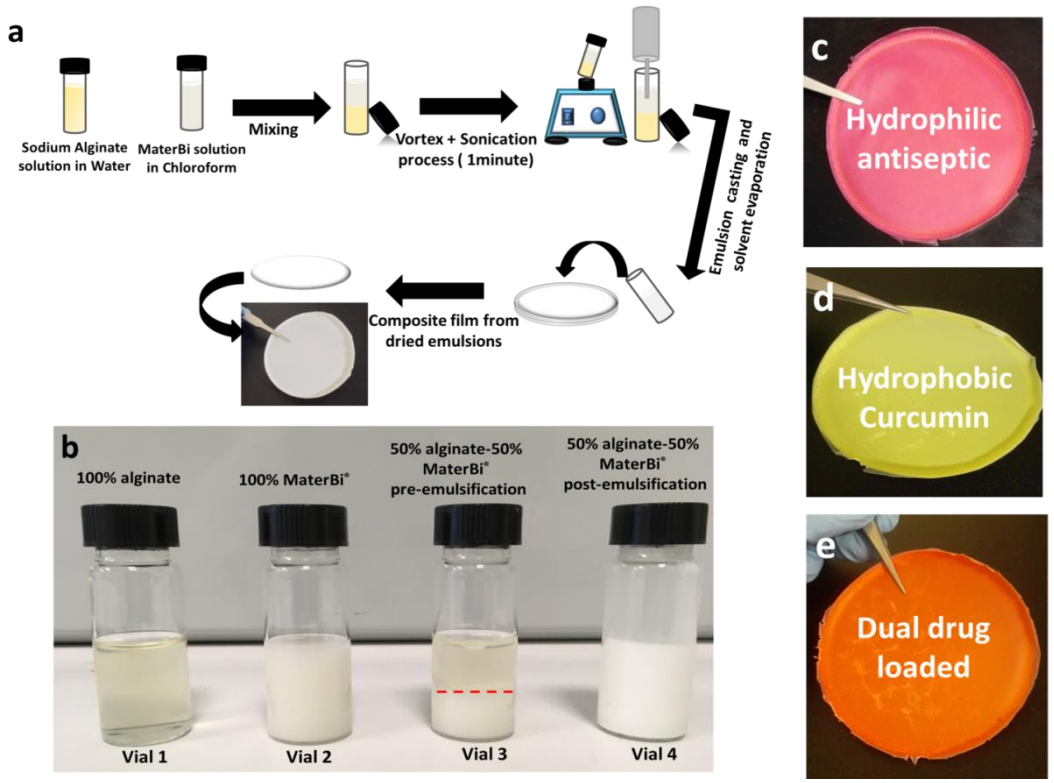

Figure 2.3:(a) Schematic representation of the emulsion preparation protocol; (b) a photograph of the stable, liquid emulsions and (c-e) photographs of the dry composite films loaded with individual or two drugs.

Table 2.1: Emulsions codes and composition

Emulsion Code	Composition (wt. %)
E1	100% alginate
E2	90% alginate – 10% MaterBi®
E3	80% alginate – 20% MaterBi®
E4	70% alginate – 30% MaterBi®
E5	60% alginate – 40% MaterBi®
E6	50% alginate – 50% MaterBi®
E7	40% alginate – 60% MaterBi®
E8	30% alginate – 70% MaterBi®
E9	20% alginate – 80% MaterBi®
E10	10% alginate – 90% MaterBi®
E11	100% MaterBi®

All the compositions reported in Table 2.1 were tested for the hydrophilic model drug release studies. However, only certain selected emulsions, such as the ones containing 30 wt% and 50 wt% alginate with respect to the MaterBi® were used for the hydrophobic model drug release and for dual drug release studies. As an example of emulsion preparation, a composite alginate-MaterBi® film containing 50 wt% alginate was developed by the following process: 7.5 mL of alginate solution was transferred into a vial, followed by the addition of 7.5 mL of MaterBi® solution, in order to have a final volume of 15.0 mL. Note that densities of sodium alginate and MaterBi® are comparable (~1.25 g/cm^3).

2.2.4. Emulsion characterization

In order to determine the type of the different emulsions studied in this work, dilution tests and dye test were performed. The dilution test is based on the sequential addition of one of the two components, until a phase separation is reached and macroscopically observed. For example, if water is added to oil in water (O/W) emulsion, a diluted system will indicate water as the continuous phase. Similarly, if an organic compound is added to water in oil (W/O) emulsion, a diluted system will

indicate oil as the continuous phase. To assess the type of Sodium Alginate-MaterBi® emulsions, a set of two parallel dilution tests were conducted. Briefly, 1 mL of each Sodium Alginate-MaterBi® emulsions previously described in the manuscript was aliquoted in a glass vial. Afterwards, 2 mL of chloroform (the oil phase) were added to each vial. The systems were vortexed for a few minutes and kept undisturbed for 1 hour, prior to visualization and imaging. In a parallel experiment, 2 mL of MilliQ water were added to 1 mL of each Sodium Alginate - MaterBi® emulsions. To further confirm the results, a dye test was carried out. In this case, 200 μL of a hydrophilic dye (Acid Blue 80, Sigma Aldrich, 1,5 x 10^{-3} M in water) were added to 3 mL of each Sodium Alginate – MaterBi® emulsions previously described in the manuscript. The systems were vortexed for a few minutes and kept undisturbed for 1 hour, prior to visualization and imaging.

2.2.5. Model drug loading

The hydrophilic cutaneous antiseptic Neomercurocromo® was premixed into the sodium alginate aqueous solution by dropwise adding 0.05 mL of the aqueous antiseptic solution in 7.5 mL sodium alginate solution before emulsification. The amount of cutaneous antiseptic in the emulsions was always maintained at 0.05 mL (3×10^{-4} M). The hydrophobic curcumin, on the other hand, was first dissolved in chloroform to obtain a concentrated stock solution (1 mg/mL). A certain amount of this stock solution (1 mL) was then added to the 7.5 mL MaterBi® solution. To study the dual drug release, emulsification was performed as described above, by using both solutions containing different drugs. A slightly different protocol was followed in order to emulsify the hydrophilic Neomercurocromo® with the chloroform solution of MaterBi® in the absence of alginate. Specifically, 0.05 mL of the hydrophilic antiseptic was slowly added into 7.5 mL of MaterBi® solution. The antiseptic immediately phase-separated and a first step of homogenization by vortex mixing was needed. Upon emulsification by ultrasonic processing as described above, a very stable water-in-oil emulsion formed. Films casted from this emulsion

were used to measure sustained hydrophilic drug release from 100% MaterBi® films. Similarly, in order to be able to measure the hydrophobic curcumin release from 100% alginate films, 1 mL of curcumin in chloroform solution was slowly added into the aqueous sodium alginate solution under constant stirring. In this case, no ammonium hydroxide, but only water, was used to prepare the alginate solution (3% w/v), in order to avoid the degradation of curcumin.

For the dual drug release study, the hydrophilic cutaneous antiseptic and the hydrophobic curcumin were loaded, upon dispersion in the water or oil phase respectively, using the same amounts encapsulated into the films containing only one of the two drugs. Specifically, 0.05 mL (3×10^{-4} M) of Neomercurocromo® were dispersed in 7.5 mL of sodium alginate, while 1 mL of curcumin from the stock solution was added into 7.5 mL of MaterBi® solution. Afterwards, the two phases were ultra-sonicated in order to obtain double-loaded films. Macroscopic inspection of the resultant films upon drying of the emulsions indicates that dispersion of individual and dual drugs in the films were very homogenous as shown in Fig. 2.3c–e.

2.2.6. Scanning electron and atomic force microscopy

Surface and fracture surface morphology of the alginate-MaterBi® films were analyzed using a JEOL JSM-6490LA scanning electron microscope (SEM), with an accelerating voltage of 10 kV. The films were cut into small pieces and mounted on stubs with double sided adhesive carbon tape. Samples were subsequently sputter-coated with gold (10 nm), to allow SEM imaging. For the atomic force microscopy (AFM) characterization, small pieces of the films were firmly attached on a glass slide by means of double-sided tape. A Park System AFM instrument (XE-100) was used in true non-contact mode. The images were acquired in air on an anti-vibration table (Table Stable TS-150) and within an acoustic enclosure. Single-beam silicon cantilevers tips (PPP- NCHR-10) were used for the data acquisition with about less than 10 nm nominal radius and 42 N/m elastic force constant for high sensitivity.

The resonance frequency was defined around 280kHz. The scan rate was maintained at 0.2 Hz.

2.2.7. Thermogravimetric analysis

The thermal degradation behavior of the films was investigated by a standard thermogravimetric analysis (TGA) method using a TGA Q500 from TA Instruments. Measurements were performed on 3–5mg samples in an aluminum pan under inert N_2 atmosphere with a flow rate of 50 mL/min in a temperature range from 30 to 400 °C with a heating rate of 10 °C/min. The weight loss and its first derivative were recorded simultaneously as a function of time/temperature.

2.2.8. Mechanical stress-strain measurements

Mechanical properties of the films were measured by uniaxial tensile tests on a dual column Instron 3365 universal testing machine. Dog- bone shaped samples (width w = 4 mm, useful length l = 25 mm) were stretched at a rate of 1 mm/min. All the stress-strain curves were re- corded at 25 °C and 44% RH. At least three measurements were conducted for each sample and the results were averaged to obtain a mean value. The Young's modulus E, ultimate strength UTS and elongation at break values were evaluated from the stress-strain curves. For cross- linked samples, the dog-bone samples, cut from films, were crosslinked and measured after drying.

2.2.9. Fourier transform infrared (FTIR) spectroscopy

The chemical analysis of alginate, MaterBi® and alginate-MaterBi® composite films was performed by an attenuated total reflectance (ATR) accessory (MIRacle ATR, PIKE Technologies) coupled to a Fourier transform infrared (FTIR) spectrometer (Equinox 70 FT-IR, Bruker). All spectra were recorded over a range of 4000–400 cm^{-1}, with 4 cm^{-1} resolution (accumulating 128 scans).

2.2.10. In vitro drug release measurements

In vitro drug release measurements were conducted by placing the composite films in aqueous liquid media. The release was quantified by using UV–visible spectroscopy (Cary 6000i-Varian). More specifically, circular films of 8 mm in diameter were cut using a puncher, while weight and thickness of each piece were measured using a sensitive scale and micrometer gauge, respectively. Release profiles of the hydrophilic cutaneous antiseptic (Neomercurocromo®) were obtained by placing individual film pieces in a UV cuvette containing 2.5 mL PBS (pH 7.4) buffer solution. Hydrophobic curcumin release medium was a modified 0.2M PBS solution containing 0.5% Tween surfactant and 10.0% ethanol by weight as described by X.Li et al.[66]. During the release experiments, the cuvettes were continuously stirred in order to ensure full dispersion of the drugs in the medium. Released Neomercurocromo® was quantified by measuring the absorbance at 517 nm, which is the characteristic absorption wavelength of eosin[67-68], while the absorbance peak at 425 nm was used to quantify the release of curcumin[69-70]. At specific time points, changes in absorbance were recorded to obtain release profiles from selected composite films.

2.2.11. Post processing of the films by crosslinking

Calcium chloride was used to induce the gelation/crosslinking process of sodium alginate. The cross-linked films of alginate, or alginate-MaterBi® blends were obtained by soaking them in different concentrated solutions of calcium chloride (1%, 3%, 5% and 15% w/v), for different durations (2, 5 and 10 min). After the crosslinking process, the films were washed with MilliQ water in order to remove any excess of calcium from their surface and oven-dried at 40 °C.

2.2.12. In vitro biocompatibility assay

Human dermal fibroblasts adult (HDFa) were used to investigate the biocompatibility of the alginate-MaterBi® composite films. Cells were cultured in T75 culture flasks with Medium 106 supplemented with LSGS Kit in a humidified incubator at 37 °C and with 5% CO2. When the culture was approximately 80% confluent, the cells were trypsinized and seeded onto 96-well plates at a density of 5000 cells/cm^2, in 0.1 mL of cultured medium for biocompatibility assays. Extraction medium from 100% MaterBi® and from the blends (50% alginate-50% MaterBi® and 30% alginate-70% MaterBi®) were prepared in accordance to the procedure described in ISO10993-5 standard test. The films were sterilized under ultraviolet (UV) light for 40 min (20 min for each side of the matrices). Afterwards, the samples were immersed in cell culture medium for 24 h at 37 °C. After 24 h of culture, the medium was replaced with the extraction one, and the cells were incubated for further 24, 72, and 120 h. The cell viability was determined by the WST-1 assay (0.01 mL for 0.1 mL of culture medium). Briefly, prior to adding the reagent, the extraction media was replaced with the fresh one to avoid alterations during the readings due to the presence of the polymer in the culture medium. All the experiments were performed in triplicate. Results are reported as mean ± standard error.

2.2.13. Cell morphology studies

Cells were grown on 14 mm coverslips into 24-well plate filled with Medium 106, for the controls, or with the extraction media, for the treated samples, for 24, 72, and 120 h. After the incubation period, the media was removed from each well and a pre-warmed staining solution containing MitoTracker probe (300 nM) was added and incubated for 45min under growth conditions. After mitochondria staining, cells were washed with fresh pre-warmed PBS and fixed with 3.7% paraformaldehyde (PFA) in PBS for 15 min. Nuclei staining was obtained incubating the cells with a DAPI solution (2.5 μg/mL) for 15 min in the dark, followed by two

washing with PBS (1x). For the actin fibers staining, samples were first permeabilized with 0.3% Triton X-100 for 8 min and washed 2 times with PBS (1x). After the permeabilization step, to reduce nonspecific background staining, an 1% of bovine serum albumin (BSA) solution in PBS was added and incubated for 20–30 min prior to adding the phallotoxin staining solution. Then Alexa Fluor 488 Phalloidin solution, diluted 1:100 in PBS, was added to each well and incubated for 20 min at room temperature, covered with Al foil. Cell imaging was carried out via confocal microscope Nikon A1 with 401, 488, and 561 lasers and re- corded with 20x and 60x magnifications.

2.2.14. Statistical analysis

All the measured values were expressed as mean ± standard error of the mean (SEM). For *in vitro* biocompatibility tests One-way ANOVA was used to evaluate statistical significance, followed by Bonferroni's post hoc test using GraphPad Prism 5 (GraphPad Software Inc. San Diego, CA, USA). p values less than 0.05 were considered significant.

2.3. Results and discussion

Partially taken from Setti, Chiara, et al. "Investigation of in vitro Hydrophilic and Hydrophobic Dual Drug Release from Polymeric Films Produced by Sodium alginate-MaterBi® Drying Emulsions." European Journal of Pharmaceutics and Biopharmaceutics (2018).

2.3.1. Emulsion stability and emulsion type characterization

The emulsions were monitored for stability and remained stable up to 10 days without additional stirring or sonic processing (Fig. 2.4).

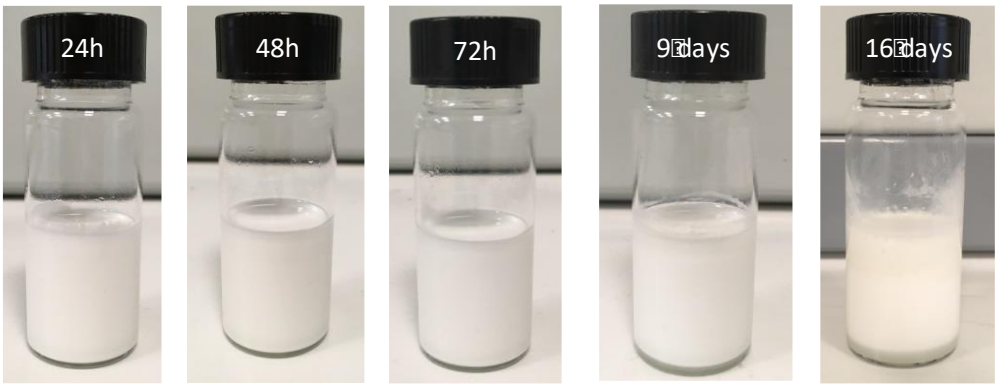

Figure 2.4: Emulsion stability over two weeks.

To evaluate the type of sodium alginate-MaterBi® emulsions by changing the components respective weight ratios, dilution test (Fig.2.5A-B) and dye test (Fig.2.6) were performed.

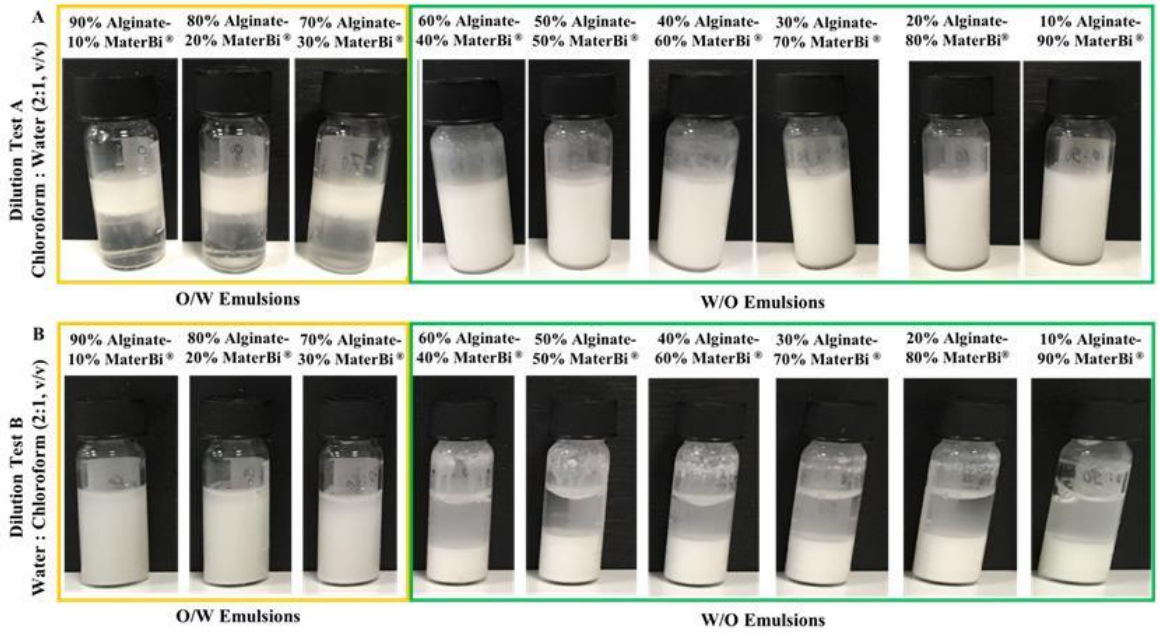

Figure 2.5: Dilution tests: (A) addition of chloroform, and (B) addition of MilliQ water to the emulsions. Systems comprising of 90 wt%, 80 wt%, and 70 wt% of Alginate are type O/W emulsions, while the other Sodium Alginate - MaterBi® systems appeared to be type W/O emulsions.

The dilution test is based on the sequential addition of one of the two components, until a phase separation is reached and macroscopically observed. To assess the type of Sodium Alginate-MaterBi® emulsions, a set of two parallel dilution tests were conducted. In Figure 2.5A, by the adding chloroform to the emulsions we observed that emulsions containing up to 90 wt.%, 80 wt.%, and 70 wt.% of sodium alginate presented a visible phase separation (W/O type of emulsions), while good dispersion and mixing was present in the remaining samples (O/W type of emulsions). Figure 2.5B shows the systems resulting from the addiction of water to the emulsions: from 90 wt.% to 70 wt.% of sodium alginate, water is the predominant phase (O/W emulsions), while a phase separation appears visible starting the emulsion containing from 60 wt.% sodium alginate - 40 wt.% MaterBi®, indicating the transition to the O/W emulsion type.

Outcomes of the dye test are reported in Fig.2.6. The addition of Acid Blue, a hydrophilic dye, allows the determination of the water phase within the emulsion. In the 100 wt.% sodium alginate solution the dye appears completely dissolved. Up to an addition of 30 wt.% of MaterBi®, no phase separation is visible, and the dye is well dispersed, indicating that water is the predominant phase and O/W emulsions types are formed. Lastly, the hydrophilic dye separates when the organic phase is the predominant one and W/O emulsions are formed. The emulsion inversion was again confirmed for the emulsion 60 wt.% sodium alginate - 40 wt.% MaterBi®.

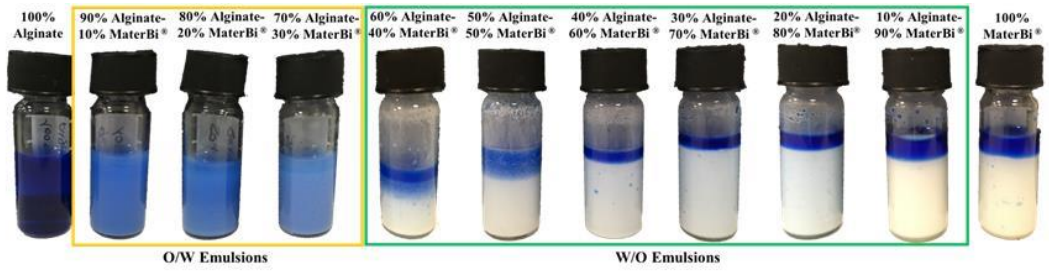

Figure 2.6: Dye test: The addition of Acid Blue, a hydrophilic dye, allows the determination of the water phase within the emulsion. The dye is well dispersed in the O/W emulsions, were the water is the predominant phase (90 wt%, 80 wt%, and 70 wt% of Alginate), while it separates when the organic phase is the predominant one (W/O emulsions).

2.3.2. Morphology of alginate – MaterBi® films

MaterBi® is a commercial hydrophobic biodegradable polymer composite, comprising PCL and thermoplastic starch, obtained by a proprietary compound extrusion method[28,71]. It has been actively marketed as sustainable food packaging material, as well as biodegradable material for perishable food containers[72]. Although beyond the scope of this study, formation of stable surfactant-free emulsions between alginate and MaterBi® can be attributed to the well-known emulsion stabilization properties of starches. Morphological attributes of certain composite films were investigated by SEM and AFM measurements as seen in Fig. 2.7 and 2.8. SEM images (Fig. 2.7a-f) illustrated the morphology of the blended films. If compared with pure alginate or pure MaterBi® films, the alginate-MaterBi® composites showed remarkable differences in terms of surface microstructure. In fact, a smooth continuous structure was observed on the surface of the alginate film (Fig. 2.7a), as previously reported in the literature[73]. SEM inspections of pure MaterBi® indicates presence of small starch particulates embedded in the PCL matrix (Fig. 2.7k). In the case of the composite samples (Fig. 2.7b-j) the presence of MaterBi® caused an appreciable change in the surface topography, leading to the

production of films with rough surfaces by increasing its content within the blend. Films dominant in alginate compositions are obtained from oil-in-water emulsions, whereas films dominant in MaterBi® phase are obtained from water-in-oil emulsions.

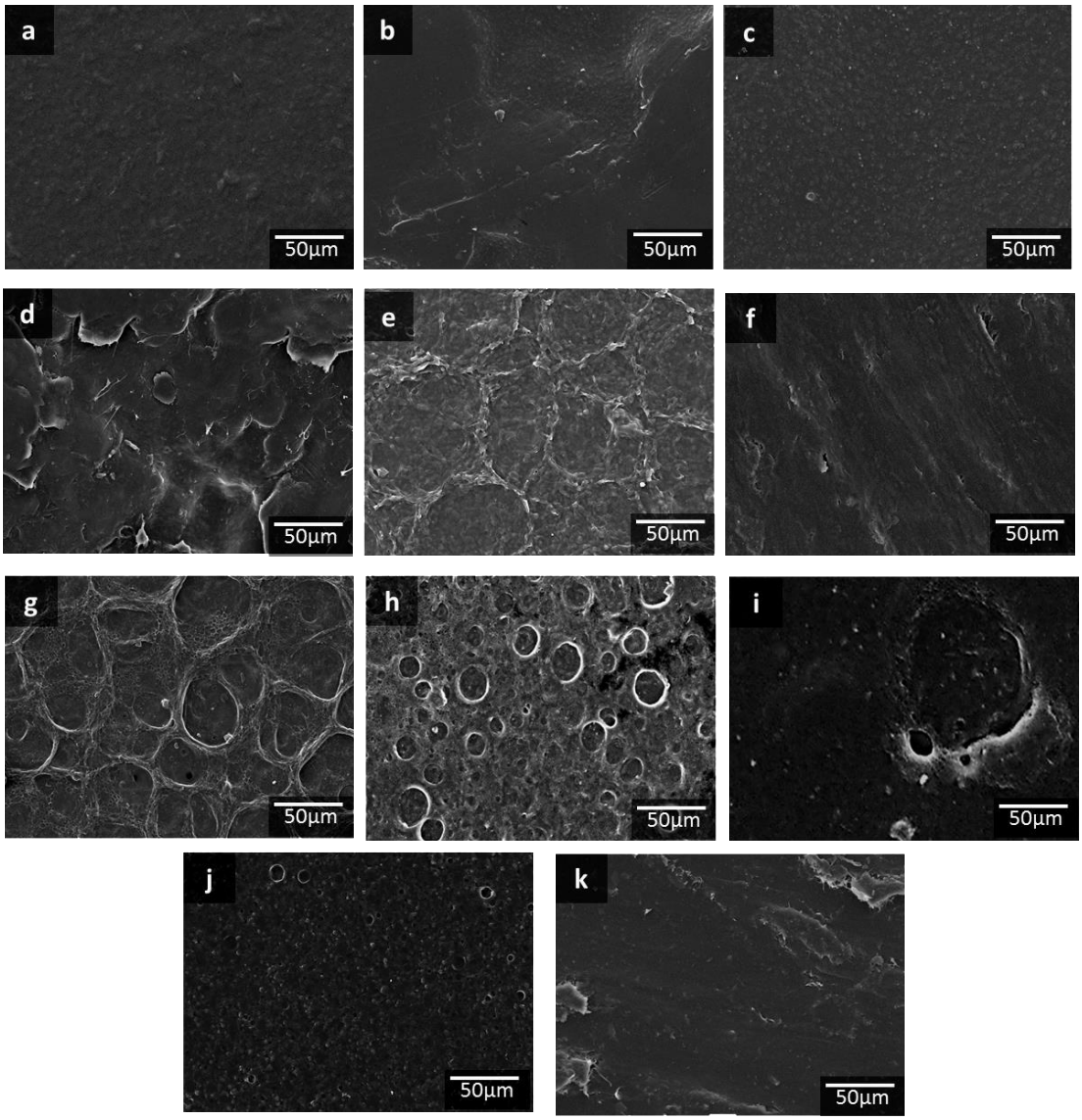

Figure 2.7: SEM surface micrographs of of pure alginate, MaterBi® and composite films.

From the AFM measurements, the composite nature of MaterBi® is reflected by the presence of starch granules, easily detected by the AFM surface scan, shown in Fig. 2.8a, confirming the SEM observations. On the contrary, pure alginate is amorphous and featureless (Fig. 2.8c and d). Surface morphology of the composite films with 50 wt.% alginate content, on the other hand, were found to have foam like cellular features (1 μm on average in size) as shown in Fig. 8e, in addition to valley-like roughness features (dark interconnected zones). The composite film comprising 70 wt.% MaterBi® demonstrates more pronounced cellular surface features and much larger in size (~8 μm), than the composite films having 50 wt.% MaterBi®, as seen in Fig. 2.8g.

These detailed AFM measurements indicated that indeed the cellular surface morphology in the films is dominant in water-in-oil emulsions, whereas surface morphology of films obtained from oil-in-water emulsions bears features similar to pure alginate film surface topography. In all the cases, however, the composite films were uniform blends with no macroscopic phase separated features.

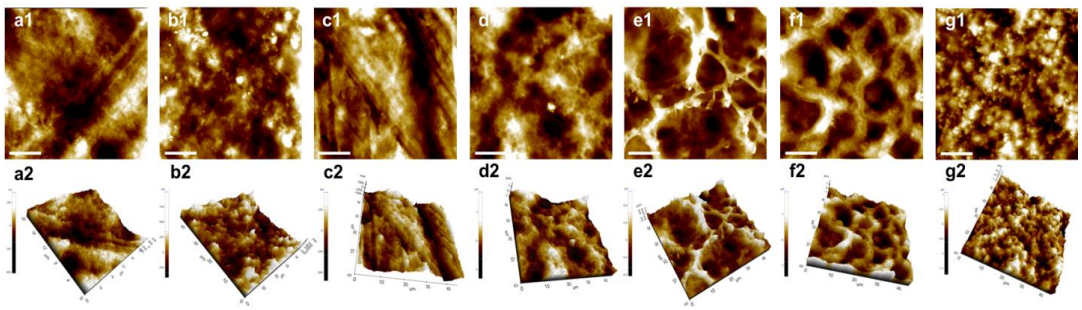

Figure 2.8: Atomic Force Microscope images depicting the surface topography of the fabricated matrices in 2D (series 1, top panel) and in 3D (series 2, bottom panel): (a) 100% alginate, (b) 70 wt.% alginate – 30wt.% MaterBi®, (c) 60wt.% alginate – 40wt.% MaterBi®, (d) 50wt.% alginate - 50 wt % MaterBi®, (e) 40 wt % alginate - 60 wt % MaterBi®, (f) 30 wt % alginate - 70 wt % MaterBi®, and (g) 100% MaterBi®. Scale bar 10 μm.

2.3.3. Chemical characterization

Potential chemical interactions between sodium alginate and MaterBi® in the films were investigated by FTIR spectroscopy as well (Fig.2.9). For pure alginate films, several characteristic bonds were identified such as asymmetric COO- stretching vibrations at 1600 cm^{-1}, overlapping symmetric COO- stretching and O-H bending vibrations at 1410 cm^{-1} and C-O-C stretching at 1030 cm^{-1}. On the other hand, in the pure MaterBi® spectrum (Fig. 2.9b) the characteristic peaks of polycaprolactone (PCL) corresponding to the C=O lactone stretching vibrations at 1720 cm^{-1} and C-O again lactones stretching vibrations at 1180 cm^{-1} are found. In the FTIR spectra of the composite films comprising respectively 30 wt. % alginate (Fig. 2.9c) and 50 wt.% alginate (Fig. 2.9d), no new peaks or shifts in peaks were measured indicating absence of any new covalent bonds within the composites. As such, the emulsion-cast films were simply polymer blends rather than an interacting solid polymer solution.

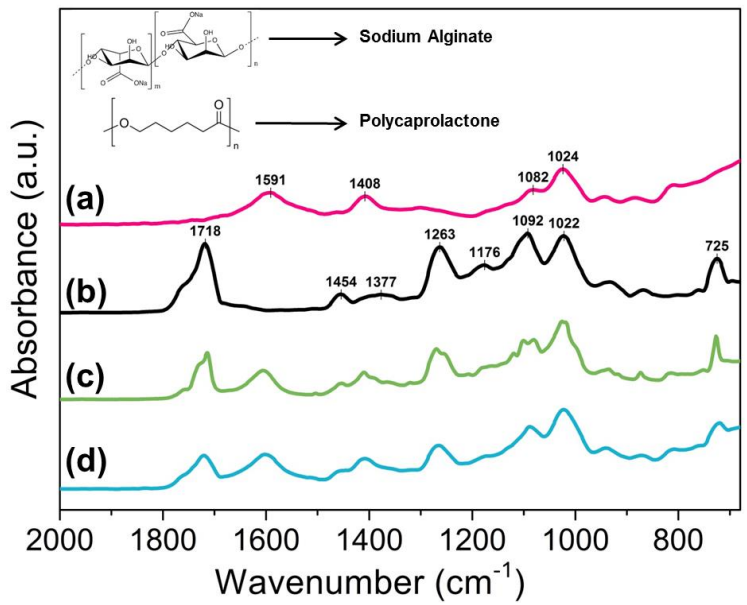

Figure 2.9: FTIR spectra of selected films: (1) 100 % alginate, (2) 100% MaterBi®, (3) 30wt.% alginate – 70wt.% MaterBi® and (4) 50wt.% alginate – 50wt.% MaterBi®.

2.3.4. Thermo-mechanical characteristics

Mechanical properties and thermal degradation characteristics of the films are discussed next. Figures 2.10a and 2.10b demonstrate stress-strain, while Figures 2.10c and 2.10d shows thermal degradation curves of un-crosslinked and crosslinked films, respectively. Summary of the mechanical measurements are also shown in Table2.2. Clearly, MaterBi® is a soft biopolymer whereas alginate is a hard, natural polymer, with no practical elongation capability. It has a very high Young's modulus of about 5GPa compared to MaterBi® (213 MPa). Crosslinking alginate by calcium extrusion lowers the Young's modulus to about 1.2 GPa (Fig. 2.10b). This can be attributed to the formation of interstitial hydrogen composites demonstrate intermediate moduli and elongation values set between pure alginate and MaterBi®. Although, comprehensive mechanical characteristics of these films are beyond the scope of this work, both Figures 2.10a and 1-b and Table 2.2 demonstrates that calcium ion liquid extrusion or crosslinking reduces Young's modulus in all the samples studied.

Thermal degradation characteristics of the films are shown in Figures 2.10c (un-crosslinked) and 2.10d (crosslinked). In the case of pure alginate films (Fig. 2.10c), a weight loss about 8% occurs up to and at 100 °C, which is a consequence of the film dehydration due to the adsorbed water at the surface. Water loss continues until 220 °C and reaches to 15%, after which degradation of alginate starts. This secondary water loss is most likely due the further evaporation of the hydrogen bonded water molecules surrounding the alginate polymeric chains within the bulk[74]. Around 275 °C half of the alginate degrades. Composite films lose less water due to MaterBi® presence as seen in Figure 2.10c; MaterBi® in the composites also extends the 50% weight loss temperatures to 350 °C. Thermal degradation behavior of crosslinked alginate appears similar to the un-crosslinked one (Fig. 2.10d) except that around 220 °C somewhat less water loss (~10%) was measured. Interestingly, crosslinked composite films degradation profiles up to 220 °C become very similar to alginate as seen in Figure 2.10d. Although the reason is not obvious, it could be

due to water uptake of the starch in MaterBi® during the aqueous salt immersion process [75-76]. Finally, in the case of pure MaterBi® (Fig. 2.10c), much less significant weight loss was observed until 100 °C; typical of a thermoplastic. Further degradation steps could be identified as starch degradation (around 320 °C) and polycaprolactone degradation (around 400 °C) [7].

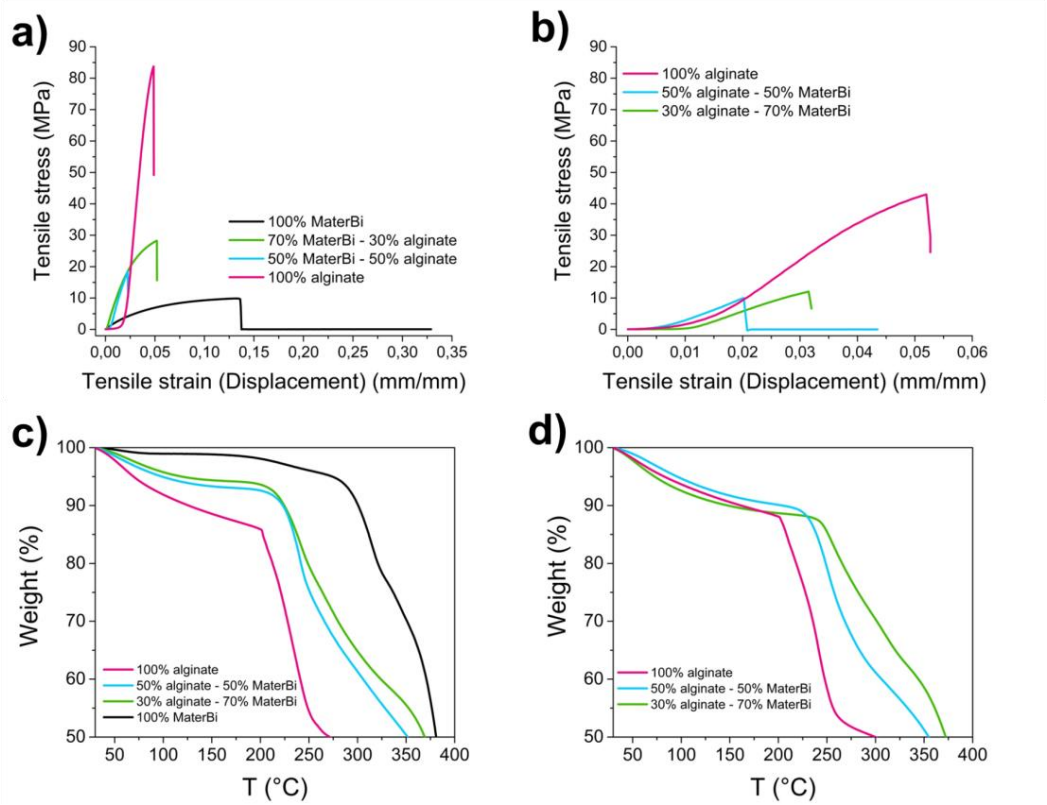

Figure 2.10 Stress-strain curves of emulsion cast pure polymer and composite films (a), stress-strain curves of emulsion cast composite films and pure alginate after cross linking (b), thermal degradation weight loss curves for pure polymers and composites (c) and thermal degradation weight loss curves of alginate and composites after crosslinking (d).

Table 2.2. Summary of Young's Modulus and ultimate tensile stress (UTS) values of un-crosslinked and crosslinked films.

Sample	*Young Modulus (MPa)*	*UTS (MPa)*
100% MaterBi®	213 ± 14	9.5 ± 0.7
70% MaterBi® - 30% alginate	1039 ± 59	21 ± 8
50% MaterBi® - 50% alginate	1403 ± 134	20.3 ± 1
100% alginate	5206 ± 1952	97.7 ± 15
70% MaterBi® - 30% alginate crosslinked	719 ± 52	10 ± 2
50% MaterBi® - 50% alginate crosslinked	767 ± 40	6.5 ± 2
100% alginate crosslinked	1211 ± 100	42 ± 0.6

2.3.5. Incorporation of hydrophilic cutaneous antiseptic Neomercurocromo®

2.3.5.1. Release kinetics

Drug release studies were carried out to examine the suitability of the various alginate-MaterBi® films to act as controlled drug delivery systems, and to check whether MaterBi® could retain the drug encapsulated.

Note that the emulsification process described in this study yielded stable emulsions between MaterBi® and the hydrophilic cutaneous antiseptic in the absence of sodium alginate (Emulsion E11, Table 2.1), which was otherwise impossible to attain using pure PCL polymer[24-26]. As such, MaterBi® can be used as a slower release matrix that does not suffer from water induced excessive swelling, erosion or disintegration compared to many other hydrophilic pharmaceutical polymers that would encapsulate such hydrophilic cutaneous antiseptic[78-80]. As will be discussed next, emulsification with sodium alginate not only allows acceleration of the release

but also permits further control of the delivery profile by calcium crosslinking. As hydrophilic cutaneous antiseptic we used the commercial Neomercurocromo®, containing propylene glycol, since the latter can act as a plasticizer for alginate[81-82], in addition to its other pharmaceutical properties, such as being an emollient for softening and smoothing in skin care [83]. Note that identical emulsions could be produced with aqueous eosin solutions containing no propylene glycol. Films obtained from Neomercurocromo®-alginate-MaterBi® emulsions are able to release the antiseptic (eosin) in a sustained manner as shown in Fig. 2.11a.

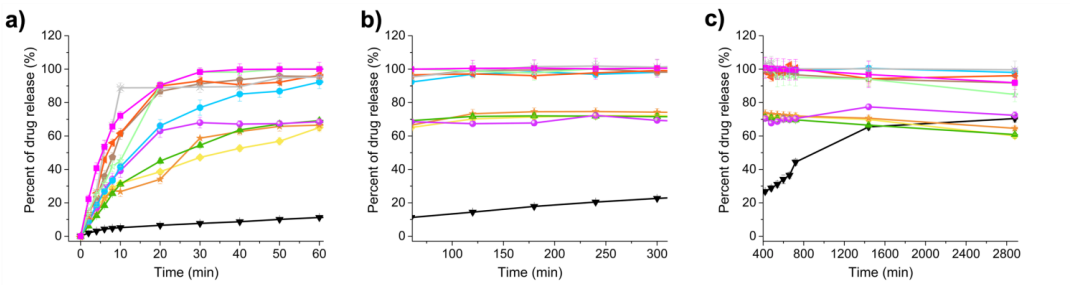

Figure 2.11: Antiseptic drug release profiles from various alginate-MaterBi® matrices, for release periods of (a) 60 minutes, (b) 5 hours, and (c) 2 days. Each data point is an average of at least triplicate measurements.

Release experiments were conducted up to 7 days in order to carefully asses both short and long-term release dynamics, as well as the capability of the films to retain the antiseptic. As seen in Fig. 2.11a, at the end of 60 min only about 10% of the antiseptic is released in vitro from the MaterBi® matrix. The release rate steadily but slowly increases to about 23% at the end of 5 h, as seen in Fig. 2.11b. Interestingly, after this period, antiseptic release from pure MaterBi® film starts to accelerate, reaching close to 44% at the end of 12 h (Fig. 2.11c). This could be attributed to swelling of some starch granules by diffusion of water into regions near the film surface and releasing adsorbed antiseptic. At the end of 24 h, 66% of the medicine is released in vitro (Fig. 2.11c). After this point, no more hydrophilic antiseptic release was measured until the end of the observation period. It may be argued that part of the antiseptic retained within the MaterBi® matrix could be due

to the fact that starch granules can uptake a certain amount of the hydrophilic antiseptic during emulsification[84]. During drying and film forming by self-assembly, most of the starch particles are embedded within the hydrophobic PCL matrix. This can severely prevent diffusion of water towards starch granules embedded in the bulk of the films to swell them and enable diffusion of the antiseptic back towards the liquid medium. Schlesinger *et al.*[85] showed that some portions of both hydrophilic and hydrophobic drugs were retained by the PCL even after long periods of in vitro monitoring. They attributed this to the potential bonding interactions, such as hydrogen bonding or Van der Waals interactions, between the drug molecules and the polymer matrix, as well as to the molecular weight of the drugs. Drug release from such polymers is known as diffusion-controlled systems, as the matrix does not degrade in the release medium during its therapeutic life[86]. Cutaneous antiseptic release from pure alginate films on the other hand was much faster, and in 30 min 100% of the loaded drug was in the release medium, as seen in Fig. 2.11a. More than 70% of the antiseptic was released in a steady fashion in the first 10 min. Since sodium alginate was not crosslinked or gelled, the release was enabled by the *swelling-erosion-dissolution* mechanism of alginates in aqueous media [87]. Release profiles from films obtained by alginate-MaterBi® emulsions also display relatively rapid antiseptic release profiles, as seen in Fig. 2.11a. Effect of drug retaining nature of PCL is clearly evident in the films made with alginate-MaterBi® emulsions. Namely, at the time when 100% antiseptic is released in vitro from pure alginate (~40 min), only between 50-70% of the antiseptic is released from the composite films comprising 90-60 wt% MaterBi®, as seen in Fig. 2.11a, and at the end of 1 h about 70% of the antiseptic was released (Fig. 2.11b). No further release was measured from this membrane until the end of 50 h of monitoring (Fig. 2.11c), and beyond (7 days).

On the other hand, the antiseptic release from the composite films comprising 50-10 wt% MaterBi® was faster, thanks to the presence of the hydrophilic polymer, and a very persistent drug release up to about 100% was possible after 5 h, compared

to 30 min in the case of pure alginate matrix. The fact that membranes containing 90-60 wt.% MaterBi® never reached 100% drug release indicates that MaterBi® can encapsulate part of the alginate polymer (during self-assembly and drying), somehow partially preventing erosion and dissolution, which are known to cause high loads of drug release from alginate[88].

Finally, the AFM and SEM inspection of the topological features of 100 wt.% MaterBi® film and alginate-MaterBi® films with 50 wt.% alginate at the end of 1 h of release, as reported in Fig.2.12, shows presence of pitting features that indirectly indicates occurrence of erosion. dissolution, and escape of the antiseptic from the films or membranes.

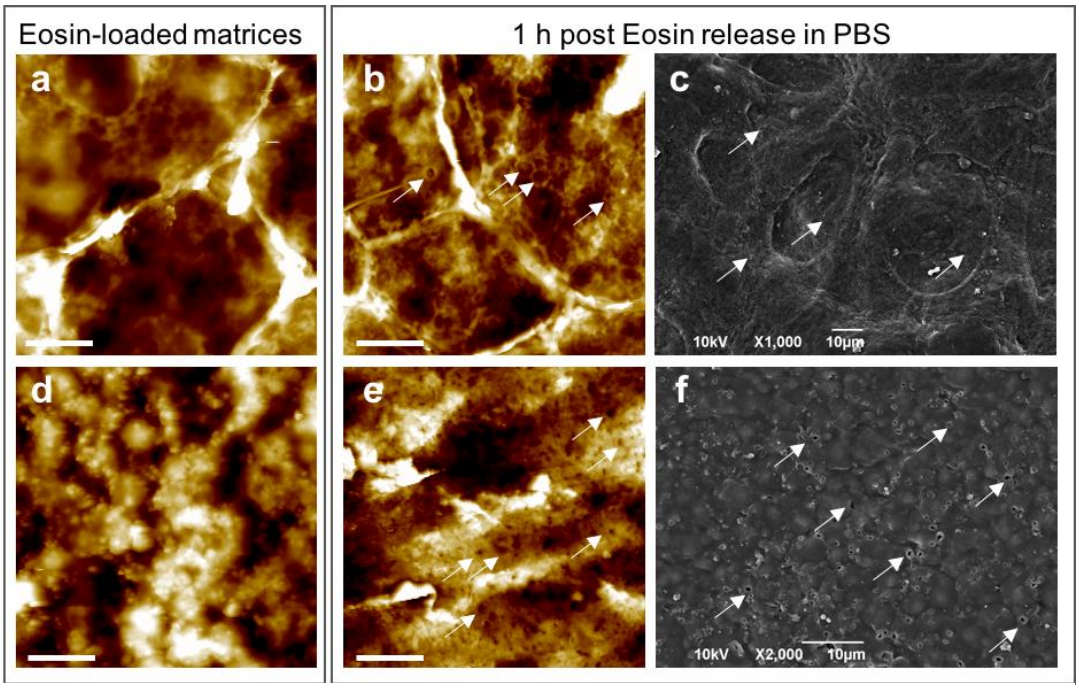

Figure 2.12: Atomic Force Microscope images depicting the surface topography of eosin-loaded fabricated matrices, before the drug release experiment (a, d) and after 1 hour of release in PBS (b, e). SEM images shown in (c, f) confirm formation of pits seen in (b, e). The reported matrices were composed of (a-c) 50wt.% alginate – 50wt.% MaterBi® and (d-f) 100% MaterBi®· White arrows are indicating the "pitting" phenomenon, suggesting the liberation of the drug from the matrices. Scale bar 10 μm.

The morphology of the films which underwent drug release was also investigated after 1 week of dissolution in PBS, via SEM (Fig. 2.13). From the analysis, a change in the morphology with an increase of the porosity was observed for each of the analyzed samples, which appeared to have holes and cracks in the structure. This is probably due to the fact that the starch, the alginate and the drug contained inside the various materials were dissolved fully or partially from each blend.

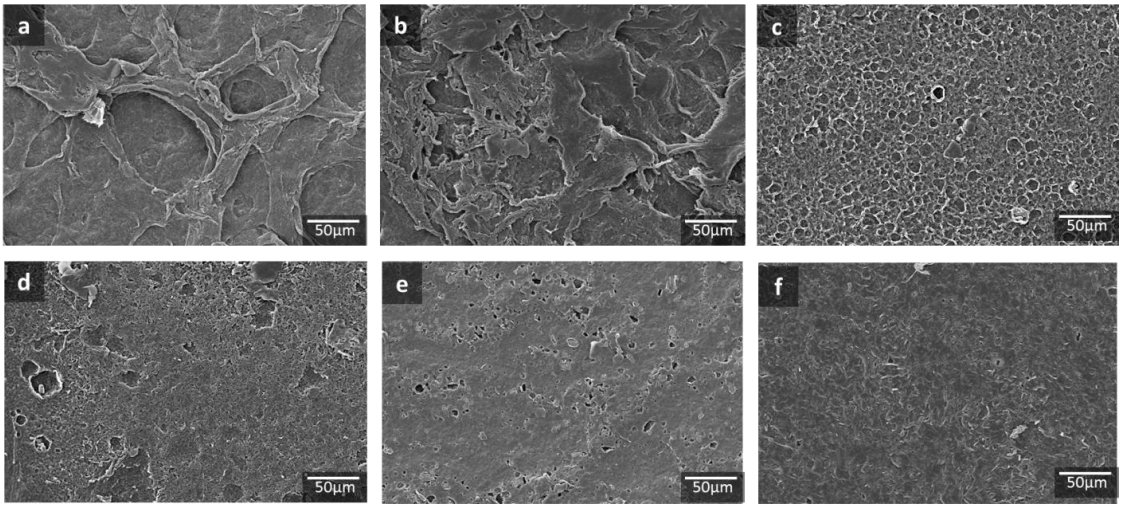

Figure 2.13: SEM images of (a) 100% MaterBi®, (b) 90wt.% MaterBi® – 10wt.% alginate, (c) 80wt.% MaterBi® – 20wt.% alginate, (d) 70wt.% MaterBi® – 30wt.% alginate, (e) 60wt.% MaterBi® – 40wt.% alginate and (f) 50wt.% MaterBi® – 50wt.% alginate after 1 week.

2.3.5.2. Optimization protocol of calcium ion cross-linking

The drug release profile of pure alginate systems can be tuned by increasing the material water stability via cross-linking or gelation process in aqueous solutions containing calcium salts. In order to achieve these properties an optimized crosslinking protocol was developed using pure alginate films encapsulating the hydrophilic model drug, investigating the effect of calcium chloride concentration (1%, 3%, 5% and 15% w/v) and the time of dipping into these solutions (2, 5 and 10

minutes). However, due to the high hydrophilicity of the Neomercurocromo®, a dipping time selected was 2 minutes was fixed, in order to ensure that the antiseptic does not permeate into the salt solution during the gelation process. On the other hand, once fixed the dipping time, the effect of calcium chloride concentration on the drug release was evaluated, as shown in Figure 2.14. The obtained results showed that, compared to the not treated films, by increasing the calcium chloride concentration it is possible to better tune the drug release profile. Therefore, we set 15 wt% $CaCl_2$ aqueous solution (1.4 M) as best condition. The obtained protocol was also applied to the composite films.

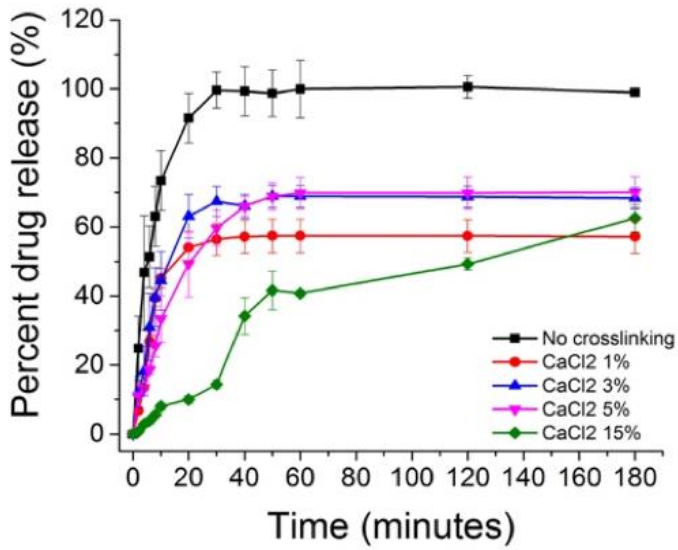

Figure 2.14: Effect of Calcium Chloride concentration on drug release (%) of the hydrophilic model drug from pure alginate films.

2.3.5.3. Effects of calcium ion cross-linking

In order to delay the release from alginate matrices, Aslani and Kennedy[89] suggested a gelling time of at least 10 minutes with a $CaCl_2$ salt solutions with less than 1 M, in order to reduce drug permeability from the alginate film or membrane.

For concentrations above 1 M, they demonstrated a similar effect within only a few minutes (2–5 minutes) of gelling time. In the present case, in order to ensure that the antiseptic molecule does not permeate into the salt solution during gelation, we picked a 1.4 M $CaCl_2$ aqueous solution (15 wt%) and a dipping/gelling time of 2 minutes. Fig. 2.15 shows the temporal evolution of percent reduction of drug release from the three films due to calcium crosslinking, with respect to the not crosslinked films. In this plot, zero percent reduction means no effect of crosslinking on release. According to Fig. 2.15, reduction in release from pure alginate films increases sharply within the first 10 minutes and reaches 75% at around 40 min. The reduction in release slows down to about 40% after two hours and remains stable afterwards. The sudden reduction indicates formation of a good barrier against erosion/dissolution-induced burst release[77,90]. In the case of alginate-MaterBi® films with 50 wt.% of alginate content, the reduction in release is lower and not as sharp as in pure alginate and maximizes at around 40% at 40 min. In fact, after the first five minutes, more drug molecules start to release from this composite compared to pure alginate. The trend, however, is similar to pure alginate and the reduction slows down to about 25% at the end of two hours. At this point, the composite film still releases 15% more drug than pure alginate. The decrease in release trend for alginate-MaterBi® films with 30 wt.% of alginate content is almost identical to the films with 50 wt.% within the first 20–30 minutes. Afterwards, the decrease in release due to cross-linking reaches 50% at 40 minutes. At the completion of two hours, a slightly lower percent decrease in release is observed at around 17%, and, the end of three hours, this film is observed to release the highest quantity of antiseptic, with a percent decrease at 10% with respect to the un-crosslinked film. No further changes were observed in the release profiles after 3 h and at the end of one day of monitoring. Similar observations shown in Fig. 2.15 were also reported on other model drug release from calcium crosslinked PLA-alginate fibers obtained from emulsions[15]. While not all of the drugs incorporated within materials such as PCL and PLA are released fully at the end of a prolonged release test [91], drug retaining capacity of these

biopolymer-based films present several other advantages, such as sustaining bacteriostatic activity, until they degrade if they are used as implants[91]. Comparisons between un-crosslinked and cross-linked films (pure alginate, alginate-MaterBi® films with 30 wt% and 50 wt% alginate) time release profiles are shown in Figure 2.16.

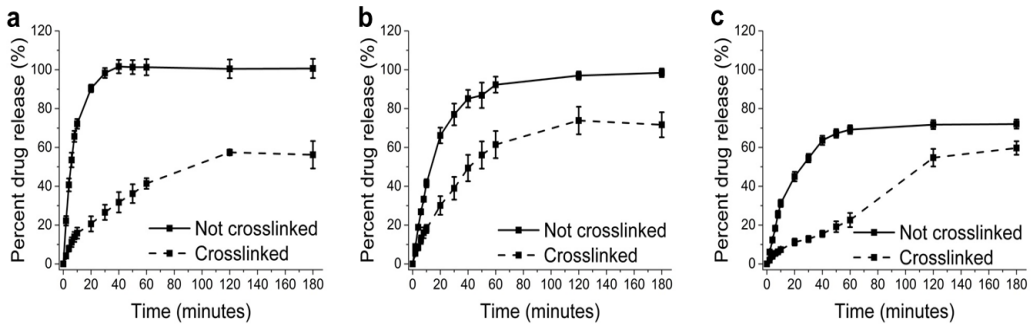

Figure 2.15: Effect of the crosslinking on 100% alginate, 50 wt.% alginate–50 wt.% MaterBi® and 30 wt.% alginate–70 wt.% MaterBi® films. Increase in percent decrease in release due to cross-linking indicates slower and lower amount release. The decline in percent decrease in release after reaching its maximum indicates that the release rate starts to catch up with the un-crosslinked films. If the percent decrease in release does not decline but remains steady after reaching the maximum, the crosslinked matrix could not release more than the un-crosslinked film. Each data point is an average of at least triplicate measurements.

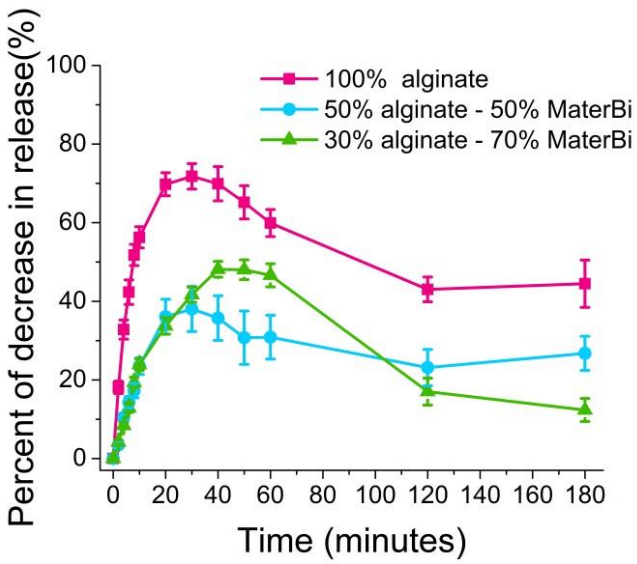

Figure 2.16: Effect of the calcium crosslinking treatment on the hydrophilic, antiseptic drug (eosin) release from (a) 100% alginate film, (b) 50wt.% alginate – 50wt.% MaterBi®, and (c) 30wt.% alginate – 70wt.% MaterBi® matrices.

Hydrophilic drug release profiles obtained for the case of pure alginate films are presented in Figure 2.16a. Sodium alginate film completely delivers the drug in 30 minutes, due to a sudden swelling of the matrix and its subsequent disintegration/dissolution in water. Upon gelation/crosslinking with calcium salt solution, at the end of 30 minutes, only 27% of the antiseptic initially loaded was dispensed and, after 180 min (3 hours), only up to 56% of the drug was detected in the media. More interestingly, a delayed release of the cutaneous antiseptic was observed for the case of the composite emulsions. In such films, calcium salt gelation caused strong resistance to antiseptic permeability *in vitro*. For example, in the case of membranes containing 50 wt.% of alginate, and cross-linked with 1.4 M calcium salt solution, at the end of 1 hour, only about 60% of the antiseptic was dispensed, compared to about 90% release with no crosslinking (Fig. 2.16b). Furthermore, after 3 hours of experiment, only up to 72% of the antiseptic was found in the release media while un-crosslinked films reached 98% of release. Increasing the MaterBi®

content in the emulsions (30 wt.% alginate, Fig. 2.16c), the cross-linking effect was still observable, leading to a 22% of antiseptic release after 1 hour of experiment, with respect to about 70% observed for the un-crosslinked films. Moreover, as expected, after 3 hours, only about 60% of the loaded hydrophilic drug was released from the crosslinked films, while 72% was detected for the un-crosslinked matrices.

3.3.6. Incorporation of hydrophobic drug (Curcumin)

3.3.6.1. Dynamics of release

Curcumin is known to be effective against cutaneous, chronic and excisional wounds, accelerating the healing process[92-95]. It dissolves in aqueous solutions at pH values above 7, and hence becomes highly susceptible to hydrolytic degradation[95]. Therefore, there have been only a few reports on the release of curcumin from alginate beads prepared in aqueous media. Previously, curcumin was introduced in sodium alginate solution by either dissolving it in ethanol[96] or using multiple surfactants such as Tween and Span[97]. Due to very limited solubility of curcumin in water or in PBS (~1 ng/mL)[83-85,98], some modifications to the release medium were required to quantify the in vitro release without significantly altering the pH level of PBS. For this purpose, release medium of 10% ethanol in 0.2 M PBS containing 0.5% Tween 80 was formulated according to earlier reports[66]. Similar to MaterBi®-hydrophilic antiseptic emulsions with no alginate, as shown in Fig. 2.11a, emulsions with alginate-hydrophobic curcumin with no MaterBi® were also fabricated, to investigate potential release kinetics (Fig. 2.17a). Indeed, sodium alginate films can uptake curcumin and release it into the modified media via erosion/dissolution. In fact, within 10 min, alginate films completely degrade and the entire hydrophobic drug escapes into the release media. Fig. 2.17a also shows the release of curcumin from films produced by drying alginate- MaterBi® emulsions. Release of curcumin from solvent-cast pure MaterBi® films occurs in two stages. In the first stage, within the first 10 min, 20% of curcumin is released; afterwards, the release rate slows down

and at the end of one hour about 50% of curcumin could be release into the modified PBS solution (Fig. 2.17a). This is a significant release rate and quantity compared to most of the values reported in literature[86-87] on curcumin release from pure PCL matrices but rather resembling dynamics from hydrophilic polymer grafted PCL matrices[99]. We attribute this to the presence of starch within the PCL matrix and its interaction (swelling and partial dissolution) with the modified aqueous PBS. In fact, release of curcumin from MaterBi® films continues to increase steadily and stabilizes at around 80% after 5 h (Fig. 2.17b), while no further release could be measured.

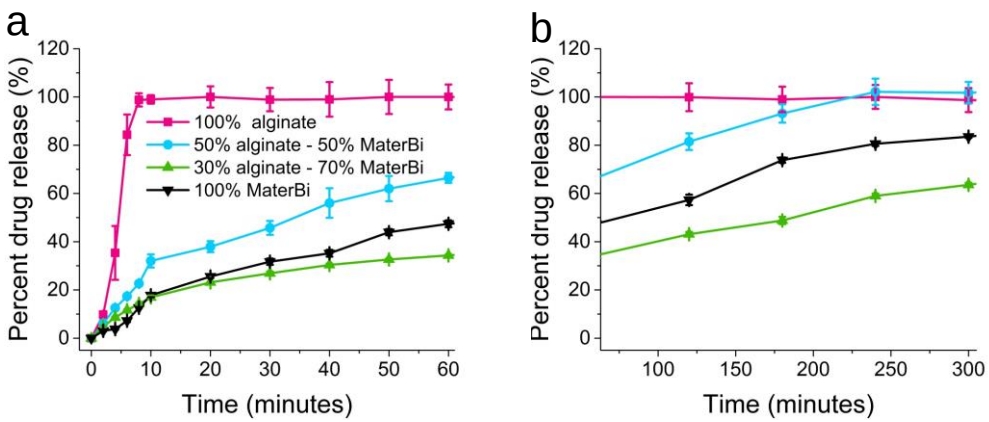

Figure 2.17: Hydrophobic drug (curcumin) release profiles for 60 minutes (a) and 5 hours (b). The release profile is divided in two plots in order to aid inspection of the initial release period. Each data point is an average of at least triplicate measurements.

The release of curcumin from alginate-MaterBi® films with 30 wt% alginate appears somewhat similar to the release from pure during the first 40 min as seen in Fig. 16a. However, for longer time point, the release slows down with respect to the one from the MaterBi® matrix and about 50% release is achieved at the end of one hour. The reduction in release is more significant afterwards up until five hours, at the end of which only about 60% curcumin release can be measured (Fig. 2.17b). Alginate-MaterBi® films with 50 wt% alginate, however, release more curcumin than pure MaterBi® with faster initial state corresponding to the first ten minutes, at the

end of which 35% curcumin is released. Afterwards, the release slows down still increasing while remaining above pure MaterBi® levels and reaches close to 70% release at the end of one hour (Fig. 2.17a). More interestingly, this composite film releases all the cur- cumin at the end of 4h as seen in Figure 2.17b. Due to emulsification and subsequent self-assembly of alginate-MaterBi® films with 30 wt.% alginate, a significant portion of the alginate domains can be encapsulated into MaterBi®. These encapsulated alginate domains may also contain curcumin that would otherwise be dispersed in MaterBi® matrix as schematically shown in Fig. 2.18a. Collectively, hydrophobic barrier around alginate due to the MaterBi® can slow down the release rate of curcumin. This does not by any means should be taken as an indication that alginate in 70wt% MaterBi® composite contains more curcumin than 50%. In the case of alginate- MaterBi® films with 50 wt% alginate, however, in addition to domains in which alginate is encapsulated by MaterBi®, a significant portion of the emulsion can also contain domains (droplets) in which alginate encapsulates MaterBi®, instead (Fig. 2.18b). This should, naturally lead to more curcumin release compared to pure MaterBi® film but still lower and slower than pure alginate film as seen in Fig. 2.17. Therefore, composite films obtained from drying emulsions can readily be used to tune hydrophobic drug release depending on the desired application.

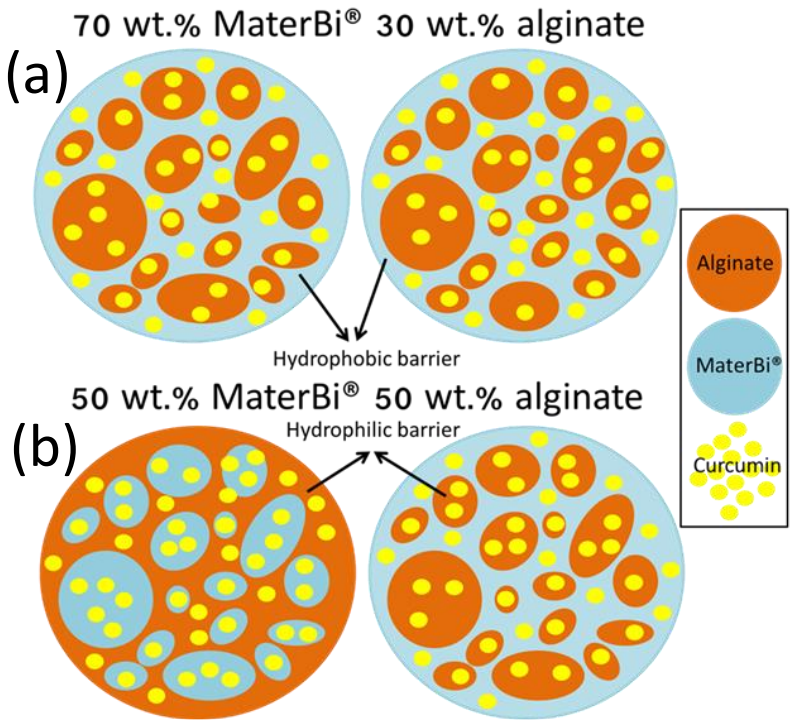

Figure 2.18: Schematic representation of composite films comprising (a) 30 wt.% alginate-70 wt.% MaterBi® and (b) 50 wt.% alginate-50 wt.% MaterBi®. In the latter, the alginate domains encapsulating curcumin can be easily eroded by the release media allowing more release of curcumin compared to pure MaterBi® or to 30 wt.% alginate-70 wt.% MaterBi®.

2.3.6.2. Effects of calcium ion crosslinking

The effects of crosslinking on the alginate matrix by calcium ions was evaluated next (Fig. 2.19). Original release profiles are given in Fig. 2.20. As previously seen for the hydrophilic drug in Fig. 15, also in this case the crosslinking strategy appears to significantly decrease the burst release from the sodium alginate matrix, due to erosion/dissolution processes arising within the first 10 minutes (Fig. 2.20). The decrease in release starts to reduce after the first 20 minutes and, at the end of three hours, it reaches to 20%, a lower value compared to hydrophilic cutaneous antiseptic (Fig. 2.15). This can be attributed to the fact that the modified PBS solution has a lower surface tension than water due to the presence of ethanol

(10wt%) and the surfactant can penetrate deeper into the bulk of the crosslinked film. In the case of alginate-MaterBi® with 50 wt.% alginate, a sharp increase in percent decrease in curcumin release is observed in the first ten minutes, afterwards the increase in percent decrease slows down and reaches about 50% at the end of three hours, indicating that a much slower release of curcumin is achieved from this composite matrix. Alginate-MaterBi® films with 30 wt% alginate, follow a similar trend in which the percent decrease in curcumin release does not exceed 20% at the end of three hours. More interestingly, comparing Figures 2.15 and 2.19 the following observations and conclusions can be drawn pertaining to release from composite films: for the hydrophilic drug, cross link-induced percent decrease in release curves are all hump-shaped similar to pure alginate (Fig. 2.15). This means that crosslinking has stronger effects in the early stages of the delivery process (0–30 min), while for longer times the effect of crosslinking diminishes significantly. For the hydrophobic drug, however, percent decrease in release curves are not hump-shaped but rather resemble the original release curves much like a logarithmic increase. This means that although not as strong, effect of cross-linking is more sustained throughout the whole release process.

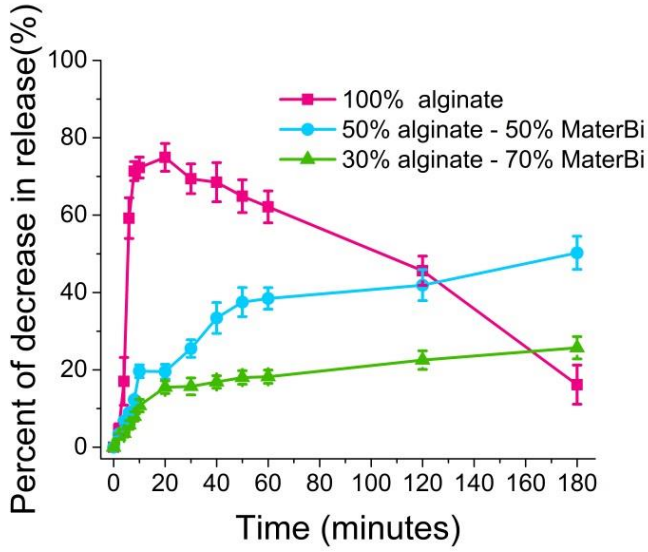

Figure 2.19: Effect of the crosslinking on 100% alginate, 50 wt.% alginate-50 wt.% MaterBi® and 30 wt.% alginate-70 wt% MaterBi® films containing curcumin. Increase in percent decrease in release due to cross-linking indicates slower and lower amount release. The decline in percent release after its maximum indicates that the release rate starts to catch up with the un-crosslinked films. If the percent of decrease does not decline but remains steady after reaching the maximum, the crosslinked matrix could not release more than the un-crosslinked film. See Fig. 2.20 for a schematic demonstration. Each data point is an average of at least triplicate measurements.

Figure 2.20 schematically illustrates this effect. Further monitoring of these films up to 48 h indicated that almost all the curcumin is released from pure crosslinked alginate films, whereas composite films with 50 wt.% and 30 wt.% alginate contents still retain about 10% and 20% of initially loaded curcumin, respectively.

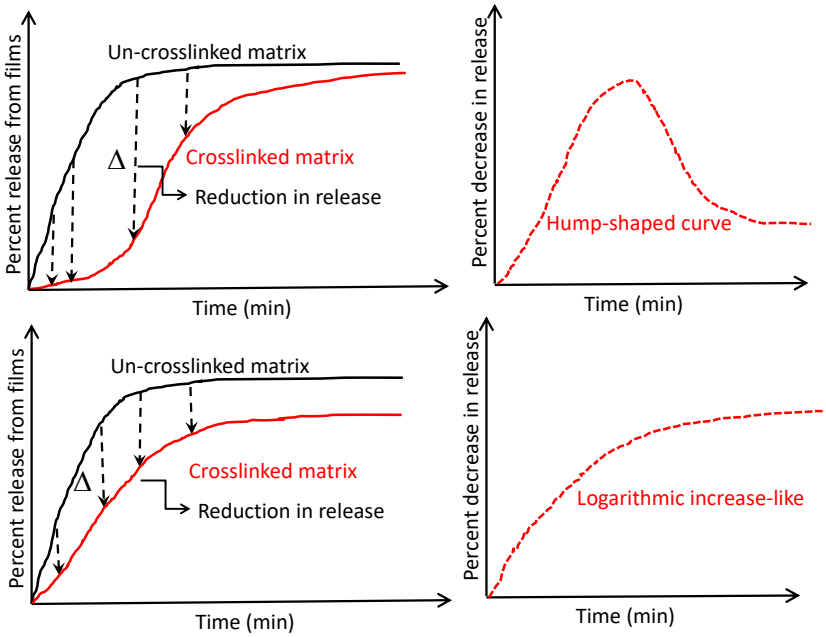

Figure 2.20: Effect of the crosslinking treatment on hydrophilic (top panel) and hydrophobic (bottom panel) drug delivery profile from alginate-MaterBi® films, expressed in terms of percent decrease in release.

Comparisons between un-crosslinked and crosslinked films (pure alginate, alginate-MaterBi® films with 30 wt.% and 50 wt.% alginate) release profiles are shown in Figure 2.21. As previously reported for eosin loaded-alginate films (Fig. 2.16a), the matrices incorporating curcumin demonstrated the possibility to delay the active molecule release, thanks to the gelation strategy, based on the use of calcium salt solution. Figure 2.21a shows that, after 30 minutes, only 35% of curcumin was released from the crosslinked alginate films, compared to the 100% liberated from the un-crosslinked ones. Moreover, at the end of 3 hours of experiment, the treated samples were only able to release up to 86% of the hydrophobic compound. Matrices composed of 50 wt.% alginate-50 wt.% MaterBi® (Fig. 2.21b) released only about 28% of curcumin at the end of 1 hour, compared to 62% of initial drug delivered from the un-crosslinked samples. In addition, at the end of 3 hours, only about 42% of the hydrophobic drug was released, while, when no crosslinking was implemented, about 93% of the active molecule was found in the media. Similarly,

for the 30 wt.% alginate - 70 wt.% MaterBi® films crosslinking caused lower amounts of curcumin release (Fig. 2.21c) and, at the end of 3 hours, only up to 23% of the loaded curcumin was delivered, compared to the 49% released from untreated matrices.

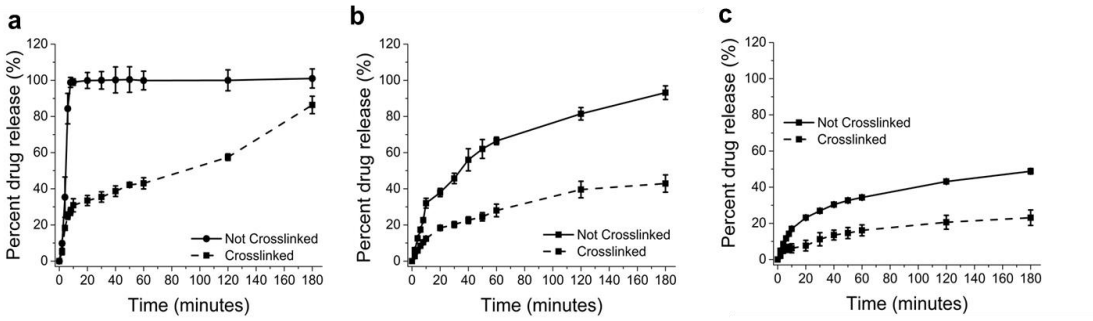

Figure 2.21: Effect of calcium crosslinking treatment on the hydrophobic drug (curcumin) release from (a) 100% alginate film, (b) 50% alginate - 50% MaterBi®, and (c) 30% alginate - 70% MaterBi® matrices.

2.3.7. Dynamics of dual drug release

In order to demonstrate the capability of the films to release both drugs at the same time, we considered three of the samples studied above: namely, pure MaterBi®, alginate-MaterBi® films with 50 wt.% and 30 wt.% alginate fractions, respectively. We adopted a modified PBS solution as release medium, to monitor the hydrophobic curcumin molecules. Fig. 2.22 reports all the release measurements, including the effect of calcium ion crosslinking. Additionally, Table 1 compares release from all films at the end of a three-hour period with or without crosslinking including both individual and dual release experiments. Based on Table 2.3, at the end of three hours of release, MaterBi® matrix releases more hydrophilic cutaneous drug, when it is loaded with both drugs, presenting curcumin release as practically unaltered. When un-crosslinked 50 wt.% alginate films are loaded with both drugs, both drugs were released lower than their individual counterparts. On the other hand, when un-crosslinked 30 wt.% alginate films are loaded with both drugs, the delivery

of the hydrophilic molecules increases, whereas the hydrophobic component release appears to decline. Table 2.3 indicates that crosslinking of films containing dual drugs ensures decline in the release of both drugs, however in the case of 30 wt% alginate films, effect of crosslinking on eosin release is less pronounced.

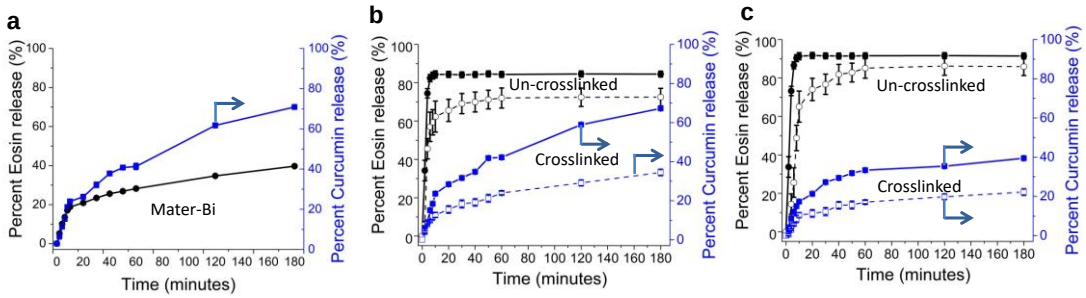

Figure 2.22: (a) Dual drug release from 100% MaterBi®; (b) comparison of the dual release from un-crosslinked and crosslinked 50 wt.% alginate -50 wt.% MaterBi® film and (c) 30 wt.% alginate-70 wt.% MaterBi®. Each data point is an average of at least triplicate measurements.

Table 2.3. Comparison of individual and dual drug release from un-crosslinked and crosslinked films at the end of three hours of monitoring.

Matrix	Individual Release				Dual Release			
	Un-crosslinked		Crosslinked		Un-crosslinked		Crosslinked	
	Eosin	Curcumin	Eosin	Curcumin	Eosin	Curcumin	Eosin	Curcumin
Alginate	100	100	56	86	100	100	92	90
MaterBi®	18	74	n/a	n/a	40	70	n/a	n/a
50/50	98	93	72	43	86	67	73	34
30/70	72	49	60	23	92	40	86	22

Finally, comparing crosslinked films with individual and dual drug loadings in Table 2.3 we noticed that, when less alginate is present in the composite film (30/70), the dual drug loading leads to more hydrophilic drug release while curcumin release is practically unaffected. One the other hand, when more alginate is present (50/50), the dual drug loading causes less curcumin delivery, maintaining the eosin

profile almost unaffected. As such, our initial observations indicate that not only tuning the relative alginate – MaterBi® ratios allows for a control of each individual component delivery, but also the dual drug loading was noticed to affect the release profiles. This rather complex phenomenon would require future experiments and further characterization for a more detailed explanation.

2.3.8. Biocompatibility of MaterBi® and composite films

The biocompatibility of pure MaterBi® and the composite films with 30 and 50 wt.% alginate contents, respectively, was evaluated using HDFa cells as an *in vitro* model. Figure 2.24a shows cell proliferation reagent WST-1 outcomes after 1, 3 and 5 days for the samples studied in drug release experiments. The results demonstrated that the cells treated with the polymer extraction medium were healthy and had very strong proliferation levels (Fig. 2.23a). After one day of treatment no significant differences ($p < 0.05$) were observed in the viability of the treated cells in comparison with the control. However, a significant increase ($p < 0.01$) in their proliferation, with respect to the control, was observed after 3 days of incubation in the polymer extraction medium. Moreover, we did not find significant differences ($p < 0.05$) in the viability between the treated cells and the control samples up to 5 days of culture. Confocal images displayed in Figure 2.23b–e indeed shows that all cellular components appeared rather healthy, revealing how MaterBi® itself can be considered a human cell-friendly soft matrix that can be safely utilized for wound management related applications.

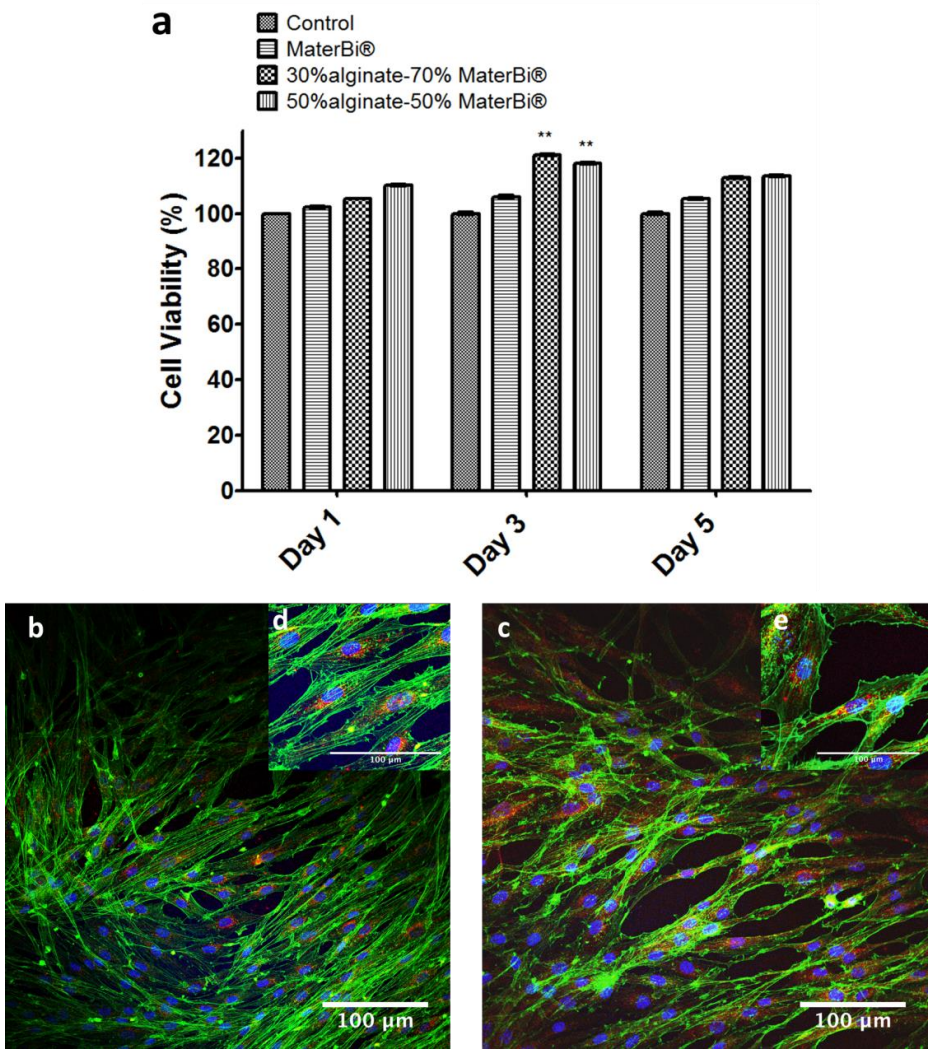

Figure 2.23: (a) Cell viability assay on different films. (b-e) Confocal microscopy images highlighting the overall cell morphology after 3 days of culture for control cells (b, d) and cells grown in the presence of MaterBi® extract (c, e). Actin is stained in green (Alexa Fluor Phalloidin 488), while nuclei are highlighted in blue (DAPI), and mitochondria in red (MitoTracker Red). Note that images in (d) and (e) are insets.

2.4 Conclusions

Partially taken from Setti, Chiara, et al. "Investigation of in vitro Hydrophilic and Hydrophobic Dual Drug Release from Polymeric Films Produced by Sodium alginate-MaterBi® Drying Emulsions." European Journal of Pharmaceutics and Biopharmaceutics (2018).

In this study, we demonstrated for the first time ultrasonic-assisted self-emulsification between two biopolymers, namely a hydrophobic PCL/starch composite (MaterBi®) and sodium alginate. The emulsions remain stable for several days and can be cast into solid films upon drying. MaterBi®-alginate fractions in the films can be tuned during the emulsification process, leading to systems able to incorporate two model drugs, one being a commercial eosin-based cutaneous antiseptic (Neomercurocromo®) and the other hydrophobic curcumin. In *vitro* release studies demonstrated the ability of the composite film matrices to release the two model drugs individually or simultaneously in a sustained manner. Due to the presence of embedded starch granules, MaterBi® films have been found to release more drugs, both hydrophilic and hydrophobic, compared to pure PCL polymer. Individual drug release rates can be delayed by calcium crosslinking of the films by simple salt solution immersion. Calcium crosslinking is also efficient in delaying release rates of both drugs during dual release action. Detailed cell viability assay studies also confirmed that the films are highly biocompatible and ideal for superficial cell proliferation. These films can have a number of pharmaceutical applications as potential wound care materials or hygienic packaging of pharmaceutical products.

2.5. References

1. T.W. Yeung, E.F. Üçok, K.A. Tiani, D.J. McClements, D.A. Sela, Microencapsulation in Alginate and Chitosan Microgels to Enhance Viability

of Bifidobacterium longum for Oral Delivery., Front. Microbiol. 7 (2016) 494.

2. S. Johnson, Boren K, Topical and oral administration of essential oils - safety issues, 22 (2013) 43–48.
3. W. Yu, E.S.T. do Egito, G. Barratt, H. Fessi, J.P. Devissaguet, F. Puisieux, A novel approach to the preparation of injectable emulsions by a spontaneous emulsification process, Int. J. Pharm. 89 (1993) 139–146.
4. K. Hippalgaonkar, S. Majumdar, V. Kansara, Injectable lipid emulsions-advancements, opportunities and challenges., AAPS PharmSciTech. 11 (2010) 1526–40.
5. L. Liu, F. Wu, X.-J. Ju, R. Xie, W. Wang, C. Hui Niu, L.-Y. Chu, Preparation of monodisperse calcium alginate microcapsules via internal gelation in microfluidic-generated double emulsions, J. Colloid Interface Sci. 404 (2013) 85–90.
6. C.-X. Zhao, Multiphase flow microfluidics for the production of single or multiple emulsions for drug delivery, Adv. Drug Deliv. Rev. 65 (2013) 1420–1446.
7. S. Pallandre, E.A. Decker, D.J. McClements, Improvement of Stability of Oil-in-Water Emulsions Containing Caseinate-Coated Droplets by Addition of Sodium Alginate, J. Food Sci. 72 (2007) E518–E524.
8. S.H. Yuk, S.H. Cho, H.B. Lee, pH-sensitive drug delivery system using OW emulsion, J. Control. Release. 37 (1995) 69–74.
9. C. de C. Spadari, L.B. Lopes, K. Ishida, Potential Use of Alginate-Based Carriers As Antifungal Delivery System, Front. Microbiol. 8 (2017) 97.
10. Y. Baimark, Y. Srisuwan, Preparation of alginate microspheres by water-in-oil emulsion method for drug delivery: Effect of Ca2+ post-cross-linking, Adv. Powder Technol. 25 (2014) 1541–1546.
11. Z. Zhang, R. Zhang, L. Zou, L. Chen, Y. Ahmed, W. Al Bishri, K. Balamash, D.J. McClements, Encapsulation of curcumin in polysaccharide-based

hydrogel beads: Impact of bead type on lipid digestion and curcumin bio-accessibility, Food Hydrocoll. 58 (2016) 160– 170.

12. J.P. Paques, E. Van Der Linden, C.J.M. Van Rijn, L.M.C. Sagis, Preparation methods of alginate nanoparticles, Adv. Colloid Interface Sci. 209 (2014) 163–171.
13. K.Y. Lee, D.J. Mooney, Alginate: Properties and biomedical applications, Prog. Polym. Sci.37 (2011) 106–126.
14. A. Ribeiro, Microencapsulation of lipophilic drugs in chitosan-coated alginate microspheres, Int. J. Pharm. 187 (1999) 115–123.
15. W.T.K. Stevenson, M.V. Sefton, Graft copolymer emulsions of sodium alginate with hydroxyallsyl methacrylates for microencapsulation, Biomaterials. 8 (1987) 449–457.
16. S.H. Ching, N. Bansal, B. Bhandari, Rheology of emulsion-filled alginate microgel suspensions, (2016).
17. H. Qi, P. Hu, J. Xu, A. Wang, Encapsulation of Drug Reservoirs in Fibers by Emulsion Electrospinning: Morphology Characterization and Preliminary Release Assessment, (n.d.).
18. W. Xu, R. Shen, Y. Yan, J. Gao, Preparation and characterization of electrospun alginate/PLA nanofibers as tissue engineering material by emulsion eletrospinning, (2016).
19. I.S. Bayer, Thermomechanical Properties of Polylactic Acid-Graphene Composites: A State-of-the-Art Review for Biomedical Applications., Mater. (Basel, Switzerland). 10 (2017).
20. Y. Hu, S. Ma, Z. Yang, W. Zhou, Z. Du, J. Huang, H. Yi, C. Wang, Facile fabrication of poly(L-lactic acid) microsphere-incorporated calcium alginate/hydroxyapatite porous scaffolds based on Pickering emulsion templates, Colloids Surfaces B Biointerfaces. 140 (2016) 382–391.
21. C.-H. Zheng, J.-Q. Gao, Y.-P. Zhang, W.-Q. Liang, A protein delivery system: biodegradable alginate–chitosan–poly(lactic-co-glycolic acid)

composite microspheres, Biochem. Biophys. Res. Commun. 323 (2004) 1321–1327.

22. T. Chandy, R.F. Wilson, G.H.R. Rao, G.S. Das, Changes in Cisplatin Delivery Due to Surface-Coated Poly (Lactic Acid)–Poly(ε-Caprolactone) Microspheres, J. Biomater. Appl. 16 (2002) 275–291.
23. S.E. Friberg, Phase diagram approach to evaporation from emulsions with n oil compounds.,J.Phys. Chem. B. 113 (2009) 3894–900.
24. Timgren, M. Rayner, M. Sjöö, P. Dejmek, Starch particles for food-based Pickering emulsions, Ital. Oral Surg. 1 (2011) 95–103.
25. A. Yusoff, B.S. Murray, Modified starch granules as particle-stabilizers of oil-in-water emulsions, Food Hydrocoll. 25 (2011) 42–55.
26. S. Tesch, C. Gerhards, H. Schubert, Stabilization of emulsions by OSA starches, J. Food Eng. 54 (2002) 167–174.
27. C. Bastioli, V. Bellotti, L. Del Giudice, G. Gilli, Mater-Bi: Properties and biodegradability, J. Environ. Polym. Degrad. 1 (1993) 181–191.
28. C. Bastioli, Properties and applications of Mater-Bi starch-based materials, Polym. Degrad. Stab. 59 (1998) 263–272.
29. E. Malikmammadov, T.E. Tanir, A. Kiziltay, V. Hasirci, N. Hasirci, PCL and PCL-based
    materials in biomedical applications, J. Biomater. Sci. Polym. Ed. (2017) 1–31.
30. T.F. Tadros, Applications of Surfactants in Emulsion Formation and Stabilisation, 2005.
31. J.K. Lee, D.B. Kim, J. Il Kim, P.Y. Kim, In vitro cytotoxicity tests on cultured human skin fibroblasts to predict skin irritation potential of surfactants, Toxicol. Vitr. 14 (2000) 345– 349.
32. J. Demetrulias, T. Donnelly, V. Morhenn, B. Jessee, S. Hainsworth, P. Casterton, L. Bernhofer, K. Martin, D. Decker, Skin2 - an in vitro human

skin model: the correlation between in vivo and in vitro testing of surfactants., Exp. Dermatol. 7 (1998) 18–26.

33. T. Welss, D. a Basketter, K.R. Schröder, K.R. Schroder, In vitro skin irritation: facts and future. State of the art review of mechanisms and models., Toxicol. In Vitro. 18 (2004) 231– 243.
34. I. Effendy, H.I. Maibach, Surfactants and experimental irritant contact dermatitis, Contact Dermatitis. 33 (1995) 217–225.
35. E. Lémery, S. Briançon, Y. Chevalier, C. Bordes, T. Oddos, A. Gohier, M.A. Bolzinger, Skin toxicity of surfactants: Structure/toxicity relationships, Colloids Surfaces, A Physicochem. Eng. Asp. 469 (2015) 166–179.
36. H. Heerklotz, Interactions of surfactants with lipid membranes, Q. Rev. Biophys. 41 (2008) 205–264.
37. T. Cserháti, E. Forgács, G. Oros, Biological activity and environmental impact of anionic surfactants, Environ. Int. 28 (2002) 337–348.
38. R. Ernst, J. Arditti, P. Healey, Biological effects of surfactants, New Phytol. 70 (1971) 457–475.
39. T. Sakai, Surfactant-free emulsions, Curr. Opin. Colloid Interface Sci. 13 (2008) 228–235.
40. Kirsner RS, Eaglstein WH. The wound healing process. Dermatol Clin. 1993 Oct;11(4) 629-640.
41. Broughton G, Janis JE, Attinger CE. The basic science of wound healing. Plast Reconstr Surg. 2006 Jun;117(7 Suppl) 12S-34S.
42. S. Guo, L.A. Dipietro Factors affecting wound healing J Dent Res, 89 (2010), pp. 219–229
43. Velnar, T., Bailey, T. and Smrkolj, V. (2009). The wound healing process: an overview of the cellular and molecular mechanisms. J. Int. Med. Res. 37, 1528-1542.
44. Dhivya S, Padma VV, Santhini E. Wound dressings - a review. Biomedicine (Taipei). 2015;5(4):22.

45. Simões, D., Miguel, S. P., Ribeiro, M. P., Coutinho, P., Mendonça, A. G., & Correia, I. J. (2018). Recent advances on antimicrobial wound dressing: A review. European Journal of Pharmaceutics and Biopharmaceutics.
46. Naseri-Nosar, Mahdi, and Zyta Maria Ziora. "Wound dressings from naturally-occurring polymers: A review on homopolysaccharide-based composites." Carbohydrate polymers (2018).
47. Jones V, Grey JE, Harding KG. Wound dressings. BMJ. 2006;332(7544):777-80.
48. Ovington, Liza G. Advances in wound dressings. Clinics in dermatology 25.1 (2007): 33-38.
49. Murphy, Patrick S., and Gregory RD Evans. Advances in wound healing: a review of current wound healing products. Plastic surgery international 2012 (2012).
50. Mayet, Naeema, et al. A comprehensive review of advanced biopolymeric wound healing systems. Journal of pharmaceutical sciences 103.8 (2014): 2211-2230.
51. Sun, Bryan K., Zurab Siprashvili, and Paul A. Khavari. Advances in skin grafting and treatment of cutaneous wounds. Science 346.6212 (2014): 941-945.
52. Bruch M K. Chloroxylenol: an old-new antimicrobial. In: Ascenzi J M, editor. Handbook of disinfectants and antiseptics. New York, N.Y: Marcel Dekker, Inc.; 1996. pp. 265–294.
53. Russell A D, Furr J R. The antibacterial activity of a new chloroxylenol formulation containing ethylenediamine tetra acetic acid. J Appl Bacteriol. 1977;43:253–260
54. "WHO Model List of Essential Medicines (19th List)" World Health Organization. April 2015.

55. Contardi, Marco, et al. Polyvinylpyrrolidone/hyaluronic acid-based bilayer constructs for sequential delivery of cutaneous antiseptic and antibiotic. Chemical Engineering Journal 358 (2019): 912-923.
56. Strimpakos, Alexios S., and Ricky A. Sharma. Curcumin: preventive and therapeutic properties in laboratory studies and clinical trials. Antioxidants & redox signaling 10.3 (2008): 511-546.
57. Hewlings SJ, Kalman DS. Curcumin: A Review of Its' Effects on Human Health. Foods. 2017;6(10):92. Published 2017 Oct 22. doi:10.3390/foods6100092
58. Goel, Ajay, Ajaikumar B. Kunnumakkara, and Bharat B. Aggarwal. Curcumin as "Curecumin": from kitchen to clinic. Biochemical pharmacology 75.4 (2008): 787-809.
59. Hatcher, H., Planalp, R., Cho, J., Torti, F. M., & Torti, S. V. (2008). Curcumin: from ancient medicine to current clinical trials. Cellular and molecular life sciences, 65(11), 1631-1652.
60. Maheshwari, R. K., Singh, A. K., Gaddipati, J., & Srimal, R. C. (2006). Multiple biological activities of curcumin: a short review. Life sciences, 78(18), 2081-2087.
61. Joe, B., Vijaykumar, M., & Lokesh, B. R. (2004). Biological properties of curcumin-cellular and molecular mechanisms of action. Critical reviews in food science and nutrition, 44(2), 97-111.
62. Shehzad, A., & Lee, Y. S. (2010). Curcumin: Multiple molecular targets mediate multiple pharmacological actions: A review. Drugs Fut, 35(2), 113.
63. Akbik, D., Ghadiri, M., Chrzanowski, W., & Rohanizadeh, R. (2014). Curcumin as a wound healing agent. Life sciences, 116(1), 1-7.
64. Mohanty, Chandana, and Sanjeeb K. Sahoo. Curcumin and its topical formulations for wound healing applications. Drug Discovery Today (2017).

65. Cheppudira, B., Fowler, M., McGhee, L., Greer, A., Mares, A., Petz, L., ... & Clifford, J. L. (2013). Curcumin: a novel therapeutic for burn pain and wound healing. Expert opinion on investigational drugs, 22(10), 1295-1303.
66. X. Li, J. Qin, J. Ma, Silk fibroin/poly (vinyl alcohol) blend scaffolds for controlled delivery of curcumin., Regen. Biomater. 2 (2015) 97–105.
67. I. Romano, F. Ayadi, L. Rizzello, M. Summa, R. Bertorelli, P.P. Pompa, F. Brandi, I.S. Bayer, A. Athanassiou, Controlled antiseptic/eosin release from chitosan-based hydrogel modified fibrous substrates, Carbohydr. Polym. 131 (2015) 306–314.
68. G. Conzatti, D. Faucon, M. Castel, F. Ayadi, S. Cavalie, A. Tourrette, Alginate/chitosan polyelectrolyte complexes: A comparative study of the influence of the drying step on physicochemical properties, Carbohydr. Polym. 172 (2017) 142–151.
69. N. Pramanik, T. Mitra, M. Khamrai, A. Bhattacharyya, P. Mukhopadhyay, A. Gnanamani, R.K. Basu, P.P. Kundu, Characterization and evaluation of curcumin loaded guar gum/polyhydroxyalkanoates blend films for wound healing applications, RSC Adv. 5 (2015)
70. S. Mondal, S. Ghosh, S.P. Moulik, Stability of curcumin in different solvent and solution media: UV–visible and steady-state fluorescence spectral study, (2016).
71. C. Bastioli, Mater-Bi: Biodegradable Material for Various Applications, in: A.Steinbüchel (Ed.), Biopolym. Online, Wiley-VCH Verlag GmbH & Co. KGaA, Weinheim, Germany, 2005.
72. G. Lo Re, M. Morreale, R. Scaffaro, F.P. La Mantia, Biodegradation paths of Mater-Bi®/kenaf biodegradable composites, J. Appl. Polym. Sci. 129 (2013) 3198–3208.
73. A. Hambleton, F. Dé, R. Debeaufort, A. Bonnotte, A.E. Voilley, Influence of alginate emulsion-based films structure on its barrier properties and on the protection of microencapsulated aroma compound.

74. R. Russo, M. Malinconico, G. Santagata, Effect of cross-linking with calcium ions on the physical properties of alginate films, Biomacromolecules. 8 (2007) 3193–3197.
75. V. Paşcalau, V. Popescu, G.L. Popescu, M.C. Dudescu, G. Borodi, A. Dinescu, I. Perhaiţa, M.Paul, The alginate/k-carrageenan ratio's influence on the properties of the cross-linked composite films, in: J. Alloys Compd., 2012.
76. B.Y. Shin, S. Il Lee, Y.S. Shin, S. Balakrishnan, R. Narayan, Rheological, mechanical and biodegradation studies on blends of thermoplastic starch and polycaprolactone, Polym. Eng. Sci. 44 (2004) 1429–1438.
77. G. Li, B.D. Favis, Morphology Development and Interfacial Interactions in Polycaprolactone/Thermoplastic-Starch Blends, Macromol. Chem. Phys. 211 (2010) 321– 333.
78. A. Awadhiya, S. Tyeb, K. Rathore, V. Verma, Agarose bioplastic-based drug delivery system for surgical and wound dressings, Eng. Life Sci. 17 (2017) 204–214.
79. U. Turaga, V. Singh, A. Gibson, S. Maharubin, C. Korzeniewski, S. Presley, E. Smith, R.J. Kendall, S.S. Ramkumar, C. To, Functionalized Antimicrobial Electrospun Poly (vinyl alcohol) Nanowebs, J. Eng. Fiber. Fabr. 60 (n.d.).
80. S. Nagarajan, L. Soussan, M. Bechelany, C. Teyssier, V. Cavaillès, C. Pochat-Bohatier, P. Miele, N. Kalkura, J.-M. Janot, S. Balme, Novel biocompatible electrospun gelatin fiber mats with antibiotic drug delivery properties, J. Mater. Chem. B. 4 (2016) 1134–1141.
81. R. Mishra, P. Joshi, T. Mehta, Formulation, development and characterization of mucoadhesive film for treatment of vaginal candidiasis., Int. J. Pharm. Investig. 6 (2016) 47– 55.
82. A. Paraskevopoulou, Stabilization of olive oil lemon juice emulsion with polysaccharides, Food Chem. 90 (2005) 627–634.

83. J.O. Funk, H.I. Maibach, Propylene glycol dermatitis: re-evaluation of an old problem, Contact Dermatitis. 31 (1994) 236–241.
84. J. Mulhbacher, P. Ispas-Szabo, M.A. Mateescu, Cross-linked high amylose starch derivatives for drug release. II. Swelling properties and mechanistic study., Int. J. Pharm. 278 (2004) 231–8.
85. E. Schlesinger, N. Ciaccio, T.A. Desai, Polycaprolactone thin-film drug delivery systems: Empirical and predictive models for device design, Mater. Sci. Eng. C. 57 (2015) 232–239.
86. W.B. Liechty, D.R. Kryscio, B. V Slaughter, N.A. Peppas, Polymers for drug delivery systems., Annu. Rev. Chem. Biomol. Eng. 1 (2010) 149–73.
87. C.-S.Wu, Enhanced antibacterial activity, antioxidant, and in vitro biocompatibility of modified polycaprolactone-based membranes, Int. J. Polym. Mater. Polym. Biomater. 65 (2016) 872–880.
88. J. Sujja-areevath, D.L. Munday, P.J. Cox, K. Khan, Relationship between swelling, erosion and drug release in hydrophillic natural gum mini-matrix formulations, Eur. J. Pharm. Sci. 6 (1998) 207–217.
89. P. Aslani, R.A. Kennedy, Studies on diffusion in alginate gels. I. Effect of cross-linking with calcium or zinc ions on diffusion of acetaminophen, J. Control. Release. 42 (1996) 75–82.
90. J.-W. Rhim, Physical and mechanical properties of water-resistant sodium alginate films, LWT - Food Sci. Technol. 37 (2004) 323–330.
91. X.-Z. Bi, W.-H. Pan, X.-P. Yu, Z.-M. Song, Z.-J. Ren, M. Sun, C.-H. Li, K.-H. Nan, Application of 5-Fluorouracil-Polycaprolactone Sustained-Release Film in Ahmed Glaucoma Valve Implantation Inhibits Postoperative Bleb Scarring in Rabbit Eyes, PLoS One. 10 (2015) e0141467.
92. D. Akbik, M. Ghadiri, W. Chrzanowski, R. Rohanizadeh, Curcumin as a wound healing agent, Life Sci. 116 (2014) 1–7.
93. R.K. Maheshwari, A.K. Singh, J. Gaddipati, R.C. Srimal, Multiple biological activities of curcumin: A short review, (2006).

94. C. Mohanty, S.K. Sahoo, Curcumin and its topical formulations for wound healing applications, Drug Discov. Today. 22 (2017) 1582–1592.
95. B. Cheppudira, M. Fowler, L. McGhee, A. Greer, A. Mares, L. Petz, D. Devore, D.R. Loyd, J.L. Clifford, Curcumin: a novel therapeutic for burn pain and wound healing, Expert Opin. Investig. Drugs. 22 (2013) 1295–1303.
96. A.B. Hegge, R.B. Schüller, S. Kristensen, H.H. Tønnesen, In vitro release of curcumin from vehicles containing alginate and cyclodextrin. Studies of curcumin and curcuminoides. XXXIII., Pharmazie. 63 (2008) 585–92.
97. S. Song, Z. Wang, Y. Qian, L. Zhang, E. Luo, The Release Rate of Curcumin from Calcium Alginate Beads Regulated by Food Emulsifiers, J. Agric. Food Chem. 60 (2012) 4388–4395.
98. H.H. Tønnesen, M. Másson, T. Loftsson, Studies of curcumin and curcuminoids. XXVII. Cyclodextrin complexation: solubility, chemical and photochemical stability, Int. J. Pharm. 244 (2002) 127–135.
99. C. Mohanty, S. Acharya, A.K. Mohanty, F. Dilnawaz, S.K. Sahoo, Curcumin-encapsulated MePEG/PCL diblock copolymeric micelles: a novel controlled delivery vehicle for cancer therapy, Nanomedicine. 5 (2010) 433–449.

Chapter 3

Anthocyanin-rich extract release from alginate-Beeswax emulsion gel beads.

3.1. Introduction

Anthocyanins (ACNs) are water soluble pigments (red, blue, purple and orange) that color the fruits and flowers of many plants. They are phenolic compounds belonging to the class of flavonoids, which are secondary metabolites synthesized by higher plants. The aglycon form of ACNs, as reported in Fig.3.1, called anthocyanidin, is structurally based on the flavylium ion or 2-phenylbenzopyrilium. ACNs consist of an aromatic ring A bonded to a heterocyclic ring C, that contains oxygen. In turn, the C ring is also connected by a carbon-carbon bond to third aromatic ring B[1-2].

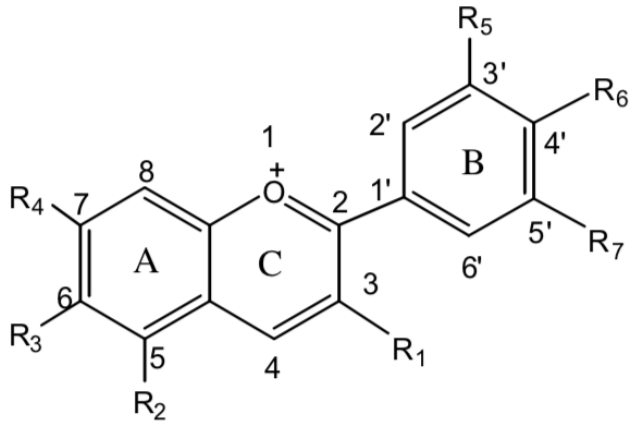

Figure 3.1: General Anthocyanins structure[1]

The main differences between the individual ACNs found in nature are the number of hydroxyl and methoxyl groups, the nature and the number of bonded sugars to their structure, the aliphatic or aromatic carboxylates residues bonded to the sugar in the molecule, and the position of these functional groups[3]. The hydroxyl groups on the aglycone may be substituted by sugar moieties (i.e. rhamnose, glucose, galactose, arabinose and xylose) or acylated with organic aromatic (i.e. p-coumaric, caffeic or ferulic acid) or aliphatic acids (i.e. acetic, malic, malonic, oxalic and succinic acids). Both glycosylation and acylation can affect the physicochemical properties of ACNs[4].

The most common anthocyanidins in higher plants are: pelargonidin (Pg), peonidin (Pn), cyanidin (Cy), malvidin (Mv), petunidin (Pt) and delphinidin (Dp), and, among them, the glycosides of three non-methylated anthocyanidins (Cy, Dp and Pg) are the most abundant in nature[1]. Due to their ionic nature, anthocyanins have the unique property to reversibly transform their structures in a pH-dependent manner. In water solutions they co-exist as four main equilibrium species: flavylium cation, quinonoidal base, carbinol pseudobase, and chalcone C. At low pH (below 2) the predominant specie is the red flavylium cation. As the pH increases ranging from 2 to 4, the flavylium cation undergoes conversion to the blue quinonoidal base. When

the pH ranges from 3 to 6, rapid hydration of flavylium cation generates the colourless carbinol pseudobase and chalcone. When the pH is higher than 7 degradation can occur[5-6].

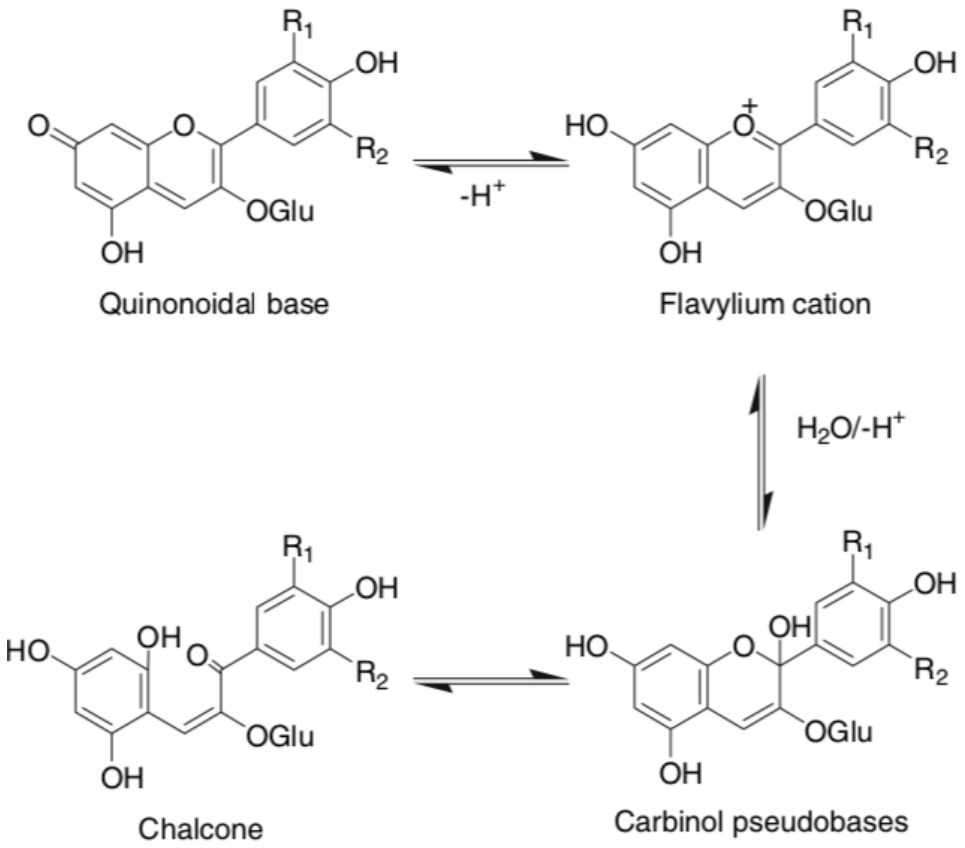

Figure 3.2: Chemical transformations of anthocyanins[6]

In addition to their colorant properties, ACNs gained a great interest for their multiple health benefits to humans, such as anti-inflammatory, anti-carcinogenic, antioxidant, anti-aging, cardioprotective, antidiabetic properties, improved eye health, and play a vital role in the prevention of degenerative diseases without toxicity[6-9]. For these reasons, they are considered potent nutraceutical and pharmaceutical ingredients. As a nutraceutical, the bioavailability of anthocyanin is the key factor for maintaining good health and for prevention of diseases[9].

Researchers have shown that, when orally administrated, the ACNs passing through the gastrointestinal tract (GIT) can be modified both by different pH and different microbial populations[10-11]. These studies demonstrated that ACNs are absorbed in the upper GIT (stomach and upper intestine) and this could explain their rapid appearance in the blood stream after administration. In general, they are stable in the stomach, due to the low pH (1-2), which should ensure that anthocyanins are maintained as the flavylium cation. In this organ their absorption is mediated by an organic anionic carrier, the bilitranslocase [12]. An insufficient retention of ACNs in the upper GIT could limit their absorption and contribute to degradation due to both high pH values found in the intestines[13-14] and to metabolic process[15-17].

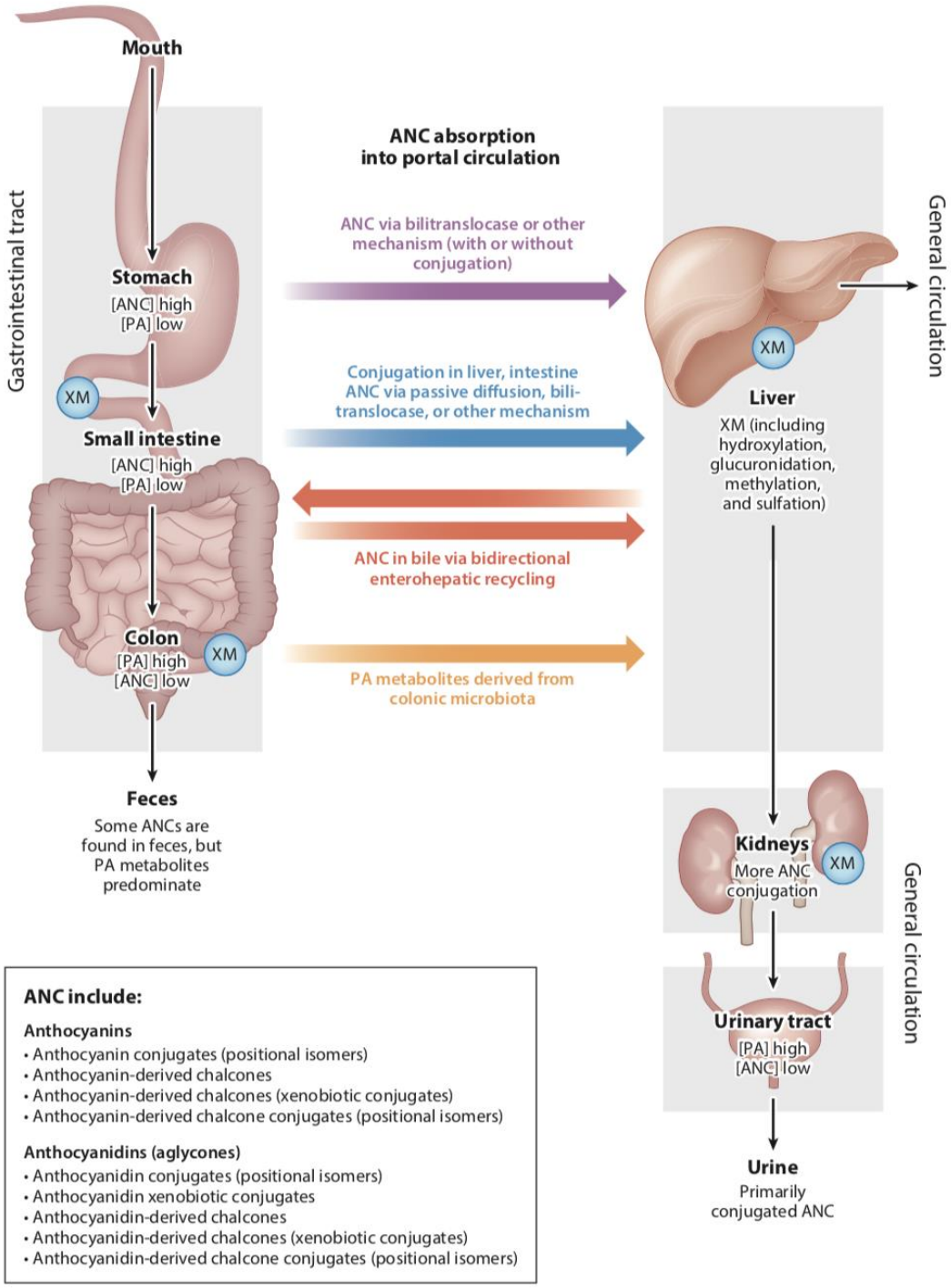

Figure 3.3: Translocation of anthocyanins and their metabolites within the human body[10].

Nevertheless, ACNs are highly unstable and it has been reported that they are very susceptible to several environmental conditions such as pH, Temperature, light, oxygen, presence of other compounds (enzymes, metal ions, phenolic compounds), which may subsequently reduce their *bioactivity* and *bioavailability*[18-19]. To circumvent these drawbacks, these compounds have been encapsulated with the aim to provide protective mechanisms from adverse environmental conditions, to maintain these compounds active until the time of consumption and deliver them to the physiological target. A wide range of technologies have been developed to encapsulate ACNs, including spray drying, micelles, nanoparticles, freeze- drying, liposomes coacervation, co-crystallization, emulsions and yeast encapsulation[20-21]. Among these, ***emulsion-encapsulation***, including single, multiple and nano-emulsions, is regarded as one of the most promising techniques for encapsulation and delivery of polyphenols. These systems have evidenced to be useful in entrapping anthocyanins, thanks to a high loading efficiency, maintenance of the stability of the cargo molecules and controlled release capacity. In addition, some polyphenols encapsulated within emulsions have shown a higher biological activity than free molecules[23].

In this study we used *Prunus mahaleb L. (P. mahaleb)* fruit concentrated extract (*mcfe*), which exhibits a high concentration of anthocyanins. *Prunus mahaleb L.* is a deciduous tree from the Rosaceae subfamily Prunoideae, native to the Mediterranean region, Iran and Central Asia. The fruit exists both in wild and cultivated forms for seed production. *P. mahaleb* is a tree species commonly used as rootstock for sweet cherry in well-drained soils in Italy, particularly in the Apulia Region.

Figure 3.4: Botanical characteristics of *Prunus mahaleb*. From top left to right: leaf, tree habit, ripe fruits, bark, flower, bud, branch with ripe fruits[23].

Its extract has been characterized to determine the amounts of sugars, organic acids and phenolic compounds by HPLC method (Tab.3.1). In *mcfe* a high concentration of bioactive compounds (especially ACNs) have been identified, exhibiting strong antioxidant capacities[23-24] and multiple biological activities, including anti-proliferative, anti-inflammatory and anti-mutagenic properties[25].

Table 3.1: HPLC characterization of *mfce*[25].

Compounds	
Sugars (g/ml)	
Glucose	0.177 ± 0.007
Fructose	0.160 ± 0.006
Sorbitol	0.132 ± 0.0046
Organic acids (g/ml)	
Tartaric acid	0.075 ± 0.003
Malic acid	0.033 ± 0.003
Succinic acid	0.015 ± 0.001
Citric acid	0.064 ± 0.003
Anthocyanins (mgKE/ml)*	15.060 ± 0.773
Flavonols (μg/ml)	
Quercetin	120.244 ± 1.403
Quercetin-3-O-glucoside	500.736 ± 27.196
Rutin	512.034 ± 35.853

Among many biopolymers used so far for ACNs encapsulation, alginate (see Chapter 1, section 1.2) has been commonly applied as material for microencapsulation of bioactive compounds, because it can protect them from adverse environmental conditions, providing controlled release of the encapsulant[26-29]. Various methods exist for production of alginate delivery systems and calcium-alginate beads represent one of the most widely used carriers[30-32]. Calcium ions were commonly used as a cross linking agent for gelling of alginate and obtaining hard droplets, by simply adding dropwise a dispersion of the polysaccharide and drug to be encapsulated into a calcium chloride bath[33-34]. The obtained crosslinked microspheres exhibit controlled release properties due to the sensitivity of Ca^{2+}/COO_2 linkage to pH and other ions[35].

Alginate microspheres can be prepared by ionotropic gelation along with extrusion method which represent an easy, low-cost and effective technique suitable for the encapsulation of both hydrophilic and hydrophobic compounds[36-37].

Dried forms of microbeads usually have greater stability and mechanical stiffness compared with hydrogel forms thus they are preferable for utilization in

foods and pharmaceuticals products[38]. In particular, alginate has been used in recent years as a unique vehicle for oral drug delivery[39], mostly in the form of gel particles and several techniques have been developed and optimized to prepare alginate-based microparticles[40].

Recently, many works reported the use of calcium alginate beads for the encapsulation of natural polyphenolic compounds, some of them include cocoa extract[41] , stevia extract[42], yerba mate extract[43], dandelion (*Taraxacum officinalis* L.) extract[44], Hibiscus extract[45] , pomegranate peel's polyphenol extract[46], Tamarind Seed Extracts[47], mulberry fruits extract[48] and harskap berries (*Lonicera caerulea* L.) rich extract[49]. The physical properties of calcium-alginate beads can be modified by the incorporation of insoluble substances, such as waxes[50-51] that could increase drug entrapment efficiency and retard drug release from the beads.

In this study, Beeswax was used as insoluble material, with the aim to develop composite alginate-based emulsion gel beads able to encapsulate and release in a controlled manner the *Prunus mahaleb L.* anthocyanin-rich fruit extract. Beeswax is a natural and edible material used in pharmaceutical, cosmetics, food and other industries. It is produced by the bee *Apis millifera L.* It is classified as GRAS (Generally Recognized as Safe) material and employed as additive, with other waxes (carnauba and candelilla), in the European Union (E901-903)[52-53]. It consists in a mixture of both saturated and unsaturated linear and complex monoesters, hydrocarbons, free fatty acids, free fatty alcohols, and other minor exogenous substances. Beeswax has a melting point range of 62-65 °C and it is practically insoluble in water, sparingly soluble in ethanol and soluble in chloroform and other oils[1]. Its advantages include good stability at different pHs and moisture content, biocompatibility, with no immunogenicity due to its water insoluble nature, slight effects of food in the GI tract, chemical inertness and no dose dumping[54]. All these characteristics make Beeswax a safe material for oral application in humans and suggest a high potential for pharmaceutical uses. Specifically, waxes are used to

encapsulate various types of drugs[55-62] and are mostly exploited as release retardant in the design of sustained release systems, including beads, tablets, suspensions, implants and microparticles[52].

Considering the above-mentioned premises and the physicochemical characteristics of the material system under study, we formulated the following hypotheses.

- ***Hypothesis (a):*** the combination of alginate and Beeswax via emulsion gelation method can lead to the development of a new biodegradable material with controlled drug release properties.
- ***Hypothesis (b):*** The presence of Beeswax within the material matrix can influence the physico-chemical properties and will sustain the drug release profile over time under simulated gastrointestinal conditions, preserving its antioxidant activity.
- ***Hypothesis (c):*** The presence of pores within the microbeads structure can accelerate the release process thanks to higher exposure of the molecule to the fluids.

In order to test our hypotheses, various formulation strategies and characterization methods have been implemented, as presented in detail in the following sections of this Chapter.

3.2. Materials and methods

3.2.1. Materials

Sodium alginate powder, Beeswax and Calcium Chloride were supplied by Sigma Aldrich (St. Louis, MO, USA). Soy lecithin powder (90%) was purchased from Alfa Aesar. Prunus mahaleb rich extract (*mcfe*) was a gift of Dr. Carmela Gerardi from Institute of Science of Food Production, CNR, Territorial Unit Lecce.

3.2.2. Preparation of conventional Calcium Alginate (CaAlg) beads and Emulsion gel beads

Conventional CaAlg beads were prepared by ionotropic gelation technique. Briefly, an aqueous solution of sodium alginate (1 gr; 4% w/v) was extruded through a 15G syringe needle into calcium chloride (2% w/v) under gentle agitation at room temperature. The dropping rate was kept 5 mL/min. Calcium ions crosslinked the alginate molecules, allowing the formation of bead-structures. The obtained gel beads were allowed to harden in calcium chloride solution for 2 minutes under stirring (500 rpm), separated by sieve, and washed twice with distilled water, in order to remove the excess of calcium chloride. Beads were oven dried at 40 °C overnight or freeze dried. CaAlg-Beeswax emulsion gel beads were prepared by emulsion gelation method, blending and emulsifying different alginate to Beeswax ratio by weight, 100:0; 85:15 and 50:50 respectively. Briefly, appropriate amounts of sodium alginate aqueous solution (4% w/v) were heated up to 65°C ± 10 °C, which corresponds to the melting temperature for the Beeswax (62-67 °C). Various amounts of wax were then added and melted into the hot alginate solution, and the mixture was homogenized with a vortex to obtain homogeneous pre-emulsions. The pre-emulsions were probe sonicated for 3 min (cycles of 30s on and 30s off) with 40% Amplitude. Finally, the emulsions were extruded through a 15G syringe needle into calcium chloride (2% w/v), cooled at 5 °C, and treated in the same manner as conventional CaAlg beads.

3.2.2. Optimization of the formulation and Encapsulation Efficiency

To prepare drug-loaded beads anthocyanins-rich extract (*mcfe*) was added dropwise into sodium alginate aqueous solution or into the hot alginate-Beeswax aqueous mixture, and then homogenously dispersed by vortex mixing. Upon emulsification by ultrasonic processing for 3 minutes (30s on and 30s off) with 40% Amplitude, the emulsions were loaded into a plastic syringe and the *mcfe*-

incorporating emulsion gel beads were obtained by emulsion gelation method, as previously described. In order to examine the effect of some formulation and processing parameters on drug entrapment efficiency, the following variables were investigated:

- Hardening time (2, 5 and 10 min)
- Amount of surfactant, Soy Lecithin (0%,0,5%,1,5%,3%,5% and 10% w/v)

All experiments were made in triplicates.

Drug entrapment efficiency was measured spectrophotometrically and calculated indirectly, by determining the non- entrapped drug present in the calcium chloride solution. More specifically, the following equation was used:

$$\mathrm{EE\%} = \frac{(\mathrm{M1} - \mathrm{M2})}{\mathrm{M1}} \times 100$$

where M_1 is the drug content initially added during the batch preparation and M_2 is the drug content recovered in the aqueous solutions after beads curing time. *Mcfe* content was then calculated using a pre-constructed calibration curve. Each result is reported as mean of at least three separate experiments.

3.2.3. Surface Morphology

Scanning Electron Microscopy (SEM) was used to determine particle size distribution, surface topography and to examine the internal structure of the beads by cutting them in half with a steel blade. SEM studies were carried out by using JEOL JSM-6490LA scanning electron microscope, with an accelerating voltage of 10 kV. The beads were mounted on stubs with double sided adhesive carbon tape and coated with gold (10 nm). The samples were then randomly scanned, and photomicrographs were taken at different magnifications.

3.2.4. Thermogravimetric analysis

The thermal degradation behavior of the beads was investigated by a standard thermogravimetric analysis (TGA) method using a TGA Q500 from TA Instruments. Measurements were performed on samples in an aluminum pan under inert N_2 atmosphere with a flow rate of 50 mL/min**.**

3.2.5. Swelling studies

Swelling properties were investigated to assess their pH-dependency by soaking the beads in Simulated Gastric Fluid (SGF, NaCl 2 gr, 7 mL HCL and water up to 1 L, with a pH=1.2) or Simulated Intestinal Fluid (SIF, Potassium monobasic 6 gr, 77 mL NaOH 0.2N and water up to 1 L, with a pH=6.8) for 8 hours. In addition, a similar experiment was conducted by immersing the beads in SGF for the first 2 hours and in SIF for the following 6 hours. Samples (60 mg) were accurately weighed in the dry state and immersed in 50 mL Falcon Tubes filled with 20 mL of simulated gastrointestinal media, at 37 °C. At pre-defined time intervals, the beads were retrieved from the media, blotted to remove the excess of water using blotting paper, and immediately weighted. The swelling degree (SD) was calculated as follow:

$$\text{Swelling degree (SD)} = (W_t - W_0) / (W_0) \times 100\%$$

where W_t and W_0 are the wet weight at time t and the initial dry weight of the beads. The SD of the beads in terms of weight was expressed as percentage (%) versus time.

3.2.6. Fourier Transform Infrared (FTIR) spectroscopy

FTIR spectra of loaded and unloaded beads were obtained by using an attenuated total reflectance (ATR) accessory (MIRacle ATR, PIKE Technologies) coupled to a Fourier transform infrared (FTIR) spectrometer (Equinox 70 FT-IR, Bruker). The beads were powdered prior to perform the analysis, and all spectra were

scanned over the range of 4000 to 600 cm^{-1}, with 4 cm^{-1} resolution (accumulating 64 scans).

3.2.7. Porosity

Mercury intrusion porosimetry was performed with Pascal 140 Evo and Pascal 240 Evo mercury porosimeters (Thermo Fisher Scientific). A double run in the Pascal 140 Evo module was required in order to break the particle aggregates. The results were obtained combining the second run of the Pascal 140 Evo module with the run obtained from the high-pressure module. The pressure of mercury intrusion was set at 0.0136 MPa and was continuously increasing up to 200 MPa, with a rate of 6 - 14 $MPa \cdot min^{-1}$. The contact angle of mercury with the samples and the surface tension of pure mercury were assumed to be 140° and 0.48 $N \cdot m^{-1}$, respectively. Washburn equation was used to calculate the pore size from the applied pressure, assuming that the pores are of spherical shape. The analysis was performed using a CD6/P dilatometer (sample holder) for heterogeneous solid samples and powders, in which were placed around 3 g for each sample.

3.2.8. XRD analysis

XRD measurements were carried out on a 'Xpert Panalytical diffractometer in reflection mode using CuKα radiation (λ=1.5406 Å) with 0.05° step size in the range 10-70° 2θ.

3.2.9. Mechanical properties

The stiffness of the beads was measured by uniaxial compression on an Instron dynamometer equipped with a 500 N load cell. The diameter of each sample was measured by optical observations, then samples were loaded on the compression anvil and tested with the rate of 1 mm/min, until 50% deformation. The clamp position at the beginning of the test, identified with a small preload, defined the sample height. At least five specimens were tested for each material/condition.

The Young's modulus was extracted from the initial portion of stress-strain curves, approximating the beads to cylinders. Such approximation, albeit an underestimation, is considered reasonable for the low aspect ratio of the beads. Results are presented as average, the error as standard deviation.

3.2.10. Antioxidant activity

Antioxidant capacity of the films was determined by the standard DPPH free radical scavenging method. Briefly, 15 mg of beads were placed into 1.5 mL of SGF. At pre-determined time points, the solution was added to 1.5 mL of 0.2 mM solution of DPPH radical in ethanol and it was kept in the dark. After 10min, the absorbance (A_1) was determined at 517 nm by UV– Vis spectrophotometer. Meanwhile, a control absorbance value (A_2) was also measured from a mixture of 1.5 mL SGF and 1.5 mL of 0.2 mM DPPH free radical solution in ethanol. The percentage of antioxidant activity was calculated by following formula:

$$\%\text{antioxidant activity} = A_1\text{-}A_2/A_2$$

where A_1 is the absorbance of the solution containing the extract and DPPH radical, A_2 refers to the absorbance of DPPH control solution All the absorbance values were determined at 517 nm. Each result is the mean of three repetitions.

3.2.11. In vitro drug release

Drug release studies were conducted mimicking the gastrointestinal fluids. Briefly, dried samples (150 mg) were placed in capped polypropylene tubes filled with 50 mL of releasing medium, either SGF or SIF, and maintained under shaking (100 rpm) at 37 °C, for 8 hours. At specific time points (every 15, 30, 45 and 60 minutes for the first hour and then every hour), aliquots of 0.5 mL were collected and replaced with the same amount of fresh medium. The amount of drug released at a given time was determined spectrophotometrically at λ_{max} (515 nm) which corresponds to characteristic peak detected for the anthocyanins present within the

extract. Prior to the studies, a standard curve was acquired. In addition, release studies were also performed following an alternative procedure: first, the samples (150 mg) were placed for 2 hours into the SGF medium; subsequently, the pH of the medium was adjusted and kept at 6.8; the samples were incubated in the SIF for 6 additional hours. Aliquots of the release media (0.5 mL) were collected every 15, 30, 45 and 60 mins in SGF and every hour in SIF, replaced with fresh medium, and analyzed by UV-Vis spectrophotometer at λ_{max} (515 nm) to determine the amount of drug released. All the experiments were performed in triplicates.

3.3. Results and discussion

3.3.1. Particle size and morphology of the beads

The macroscopical appearance of CaAlg-Beeswax microbeads, produced by emulsion-gelation method is presented in Fig.3.5a-c, where in the wet state the beads revealed a spherical shape. In addition, freshly-prepared beads (Fig.3.5a-c), showed color differences, such as transparent for pure alginate samples (Fig.3.5a), and white in the samples comprising 15% wt. (Fig.3.5b) and 50% wt. (Fig.3.5c) of Beeswax. However, during drying, the beads shrank, due to the evaporation of the internal water, reducing their size. Particle size analysis showed that the dimensions were in the range of 2.3 ± 0.2 mm for alginate beads, while for the samples comprising 15% and 50% w/w Beeswax were in the range of 1.6 ± 0.17 mm. A decrease in size was observed when Beeswax was present into the bead matrix. The external surface and internal structures of CaAlg-Beeswax beads were examined by SEM. From micrographs, it is clear that, after the drying process of the micro-particles, the initial spherical shape (Fig.3.5a-c) is lost, and a more irregular shape is acquired, as confirmed by Fig.3.5d-i. The conventional CaAlg beads (Fig.3.5a and g), with an aspect ratio value of 0.6, were *red blood cell*-like shaped, with a smooth external surface. On the other hand, the inclusion of Beeswax in the matrix led to a *drop*-like shape and a rough surface. These features appeared more defined by increasing the

amount of wax from 15% (Fig.3.5e and h) to 50% w/w (Fig.3.5f and i), which also led to an aspect ratio of 0.5 and 0.8, respectively. The analysis of the cross-sections unraveled a rougher internal matrix, due to an increasing amount of Beeswax, from 0 to 50% w/w (Fig.3.5l-n). From this observation it was possible to say that the presence of Beeswax into the bead matrix can influence the size, shape and external and internal structure of the particles.

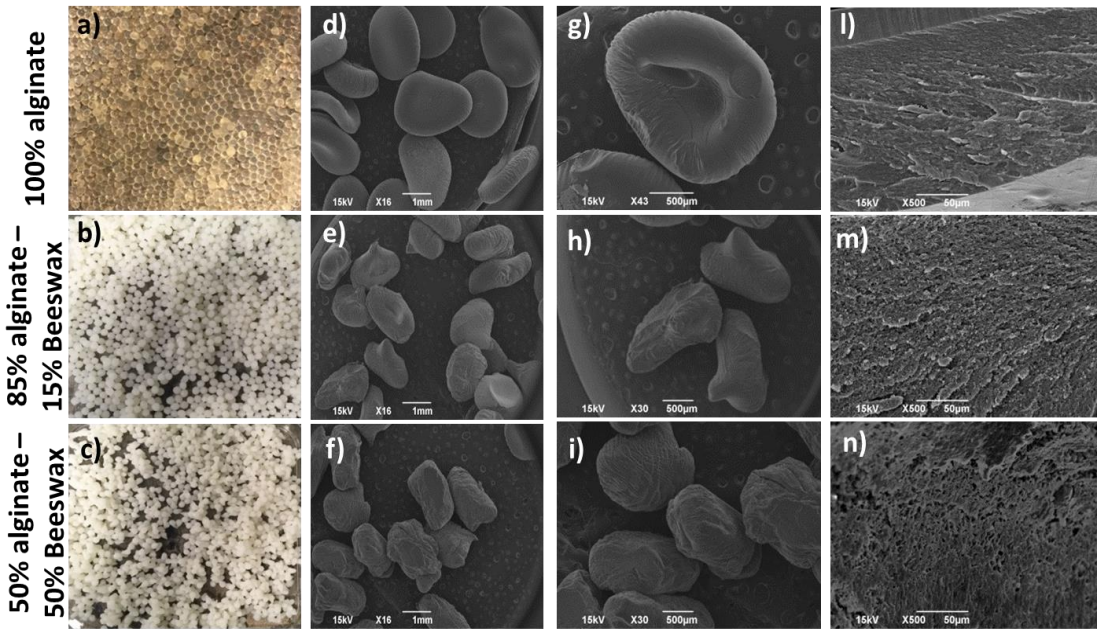

Figure 3.5: Morphological features at a macro-scale (a-c) and SEM micrographs of surface (d-i) and cross-section (l-n) of CaAlg-Beeswax microbeads.

3.3.2. Physico-chemical properties

Figure 3.6a shows the FTIR-ATR spectra of the beads containing alginate or alginate-Beeswax inside their matrix (85% CaAlg-15% Beeswax and 50% CaAlg-50% Beeswax). Beeswax represents a complex organic mixture of numerous compounds (fatty acids and fatty alcohols, long- chain hydrocarbons, and free fatty acids) and its main peaks are reported in Fig.3.6a (black spectra)[63]. The peak at 3333 cm^{-1} corresponds to O-H stretching. The peaks at 2916 and 2848 cm^{-1} were assigned

to the asymmetric and symmetric C–H stretching vibrations of the fatty acid chains. The C = O stretching in the carboxylic groups of cholesterol ester was observed at 1737 cm^{-1} . The peaks at 1462 and 1376 cm^{-1} were attributed to and the $C–H_2$ and $C–H_3$ bending in alkanes, respectively. Finally, the peak at 1171 cm^{-1} was associated with the ketone groups, specifically with the stretching vibrations of the –C–O ester groups, while the peak at 1096 cm^{-1} corresponded to the symmetric C-C stretching vibrations. The FTIR spectrum of calcium alginate (Fig.3.6a red spectra) showed peaks at 3333, 1593 and 1415 cm^{-1}, indicating the O-H stretching, the asymmetric and symmetric COO^- stretching, respectively. The peak at 1303 cm^{-1} was attributed to C-O stretching vibrations, while 1081 cm^{-1} was related to the C-O, C-C and C-O-C stretching vibrations. In the FTIR spectrum of alginate-beeswax beads, comprising 15% (Fig.3.6a blue spectra) and 50% (Fig.3.6a green spectra) of wax, various characteristic peaks of alginate and Beeswax were appeared without any significant shifting of these peaks. This suggests that there were no interactions between the two materials.

The diffractograms in the Fig.3.6b are related to the pure sodium alginate powder and two different blends in presence of Beeswax. Two main peaks appear between 20 and 25° present in the three compositions, compatible with the sodium alginate reflections [64]. With the increasing beeswax content, the occurrence of low intensity peaks below 30° presumably due to the beeswax component arises[65]. The presence of the bands (marked with a star) at 32, 45 and 56° can be ascribed to the silicon substrate background signal.

The Thermal behavior of the samples was evaluated by TGA, as reported in Fig.3.6c. For pure CaAlg beads two weight loss steps at ~ 200°C (weight loss of 18%) and at 300°C (weight loss of 50%) were reported. The first step is a consequence of the water loss, while the second one is attributed to the degradation of alginate backbone [66] . The inclusion of Beeswax into the bead matrices improved their thermal stability, extending the 50% weight loss temperature to ~300°C, proportionally to the amount of wax present inside the samples.

Fig.3.6d shows the Young's modulus of dry beads as function of Beeswax content. The results demonstrated that the Young's modulus slightly increased when Beeswax was added into the bead matrix and its value ranged from 84 MPa for pure CaAlg beads to 88 and 103 MPa for the beads comprising 15% wt. and 50% wt. of Beeswax respectively.

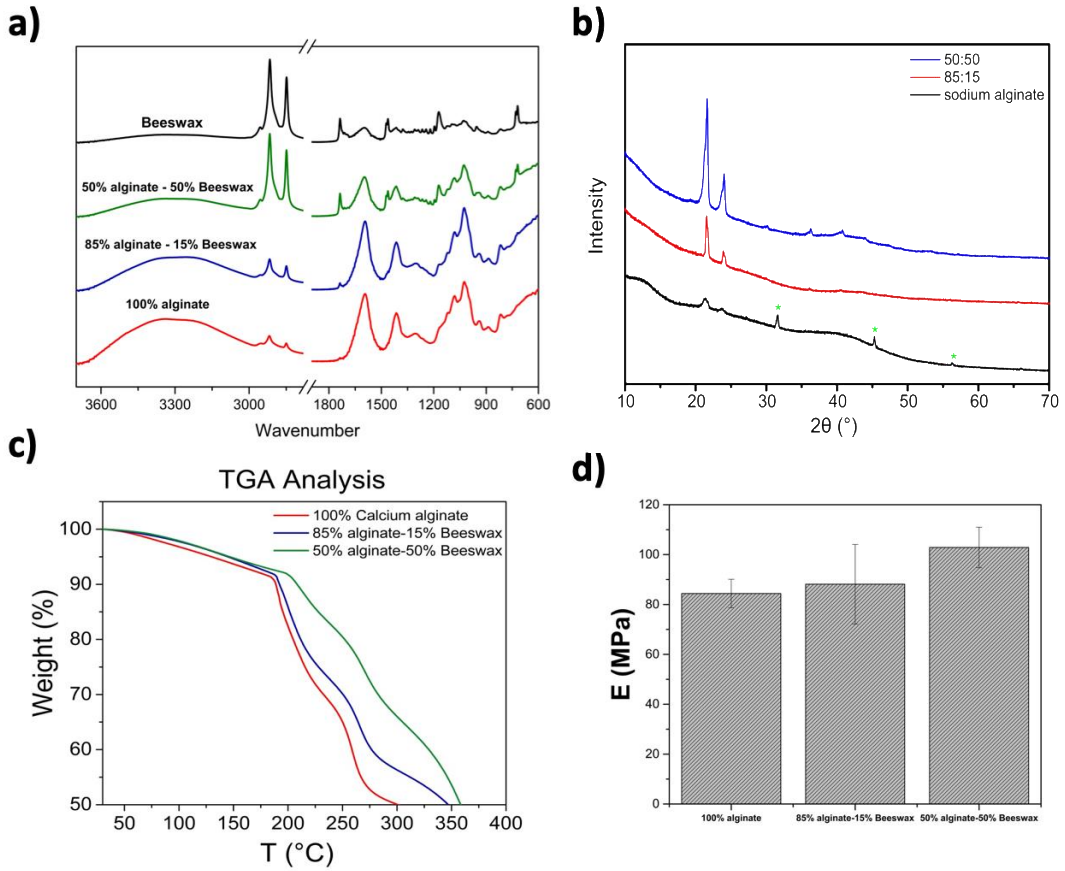

Figure 3.6: FTIR analysis (a), XRD patterns (b), Thermogravimetric analysis (c) and Mechanical properties of CaAlg and CaAlg-Beeswax microbeads.

3.3.3. Swelling and mechanical properties of Calcium alginate-Beeswax beads

Swelling is the major factor which influences the drug release of any encapsulated compound from polymeric beads which require to be re-hydrated before usage. This process is very complex in alginate hydrogels, because it

depends on the pH of the solution in which the beads are placed and the osmotic pressure gradient that exist between the gel and the environment acts as important factor in the swelling process[67]. As shown in Fig.3.7, water swelling ability of the CaAlg-Beeswax beads was influenced both by the pH of the solution and by the particle's composition after rehydration, by incubating the beads in SGF (Fig.3.7a) and in SIF (Fig.3.7b). In both swelling media it was observed that the water uptake capability of the beads decreased as the amount of Beeswax increased. Under acidic conditions (Fig.3.7a), no significant changes in the weight of the particles were recorded, due to the formation of alginic acid in this medium, neither changes in the turbidity of SGF were appreciated[68-69]; moreover, the maximum swelling values remained constant until the end of the experiment (8 h). This phenomenon is due to the reduction of the of the electrostatic repulsion among the carboxylate groups, minimizing the degree of swelling.

On the other hand, when the beads were immersed in SIF (Fig.3.7b), whose pH is near neutrality (6.8), their swelling capability enhanced, and an increase in their weight was recorded. Responsible for this phenomenon is the anionic nature of alginate. At neutral pH, the ionization of the carboxylate groups of the alginate backbone, generates a net negative charge, leading to repulsive forces between these charges which cause a rapid relaxation in the polysaccharide network.

This relaxation improves the insertion of water molecule in to the bead network structure. In addition, the presence of phosphate ions into SIF act as calcium sequestrant, leading to a very fast swelling of the particles and the recovery of their initial, spherical shape. The turbidity of this solution can also be attributed to the formation of calcium phosphate due to the ionic exchange between the Ca^{2+} in the egg-box structure of the beads and the Na^{+} contained in the medium[68]. Together with the pH-effect. Also the Beeswax content appears to influence the process: the more amount of Beeswax is present within the bead matrix, the less is the water uptake capability.

The mechanical properties of the microbeads were also investigated after submersion in SIF or SGF as reported in Fig.3.7c. The results show a dramatic decrease of the modulus, attributed to the hydration of alginate, compared to those measured for the dried samples (Fig.3.6d). In detail, particles in SIF reached 1 MPa after 1h submersion, and kept the same value after 24h, with no variation as a function of the beeswax content. In SGF, similarly, no significant difference was detected as a function of time, whereas the amount of beeswax plays a role, decreasing the modulus fairly linearly as a function of concentration. Interestingly, values of pure alginate beads are about three time as high as the same beads in SIF, which suggest lower swelling thereof. When beeswax is added, values converge to the 2 or 1 MPa for samples comprising 15% and 50% wt. of wax respectively

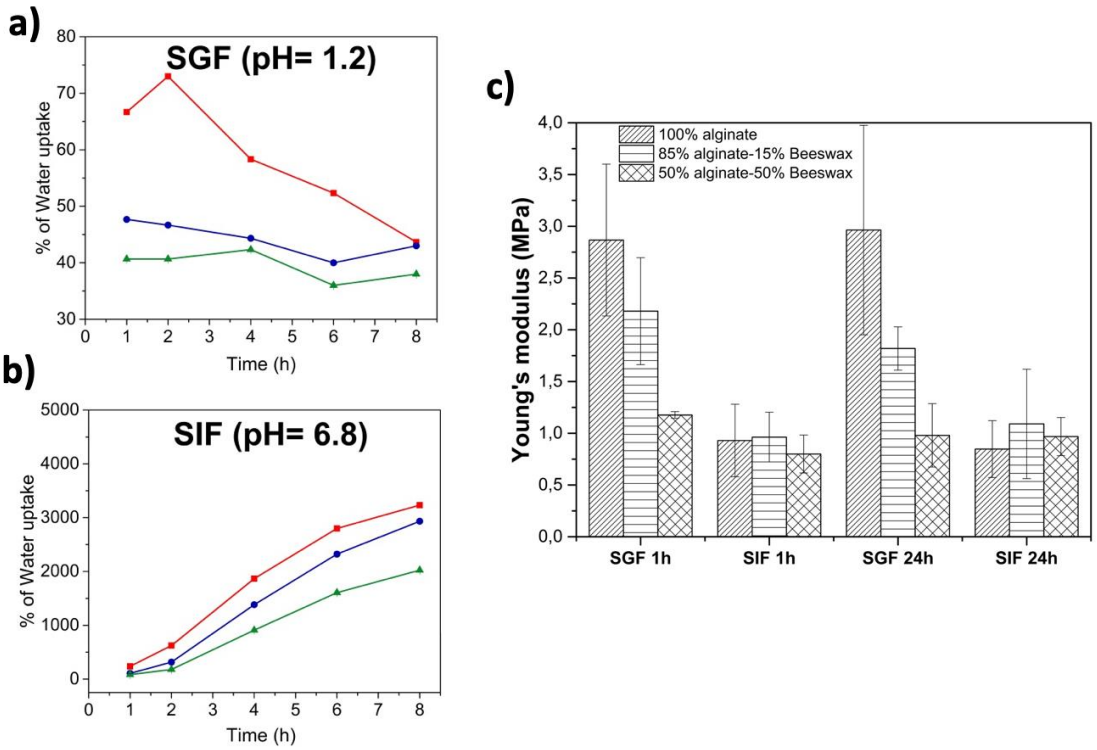

Figure 3.7: Swelling profiles of 100%CaAlg (red line); 85%CaAlg-15%Beeswax (blue line) and 50%CaAlg-50%Beeswax (green line) in SGF (a) and SIF (b). Mechanical properties of emulsion gel beads after immersion in SGF or SIF (c).

Morphological analysis of the beads after 8 hours of experiment showed that, under acidic conditions, the shape of the particles was maintained, with some signs of erosion on their surface (Fig.3.8a-f). At this pH the system appears stable and does not undergo any type of disintegration. On the other hand, when in neutral environment, the beads were completely destroyed as consequence of the rupture of the cross-linked structure.

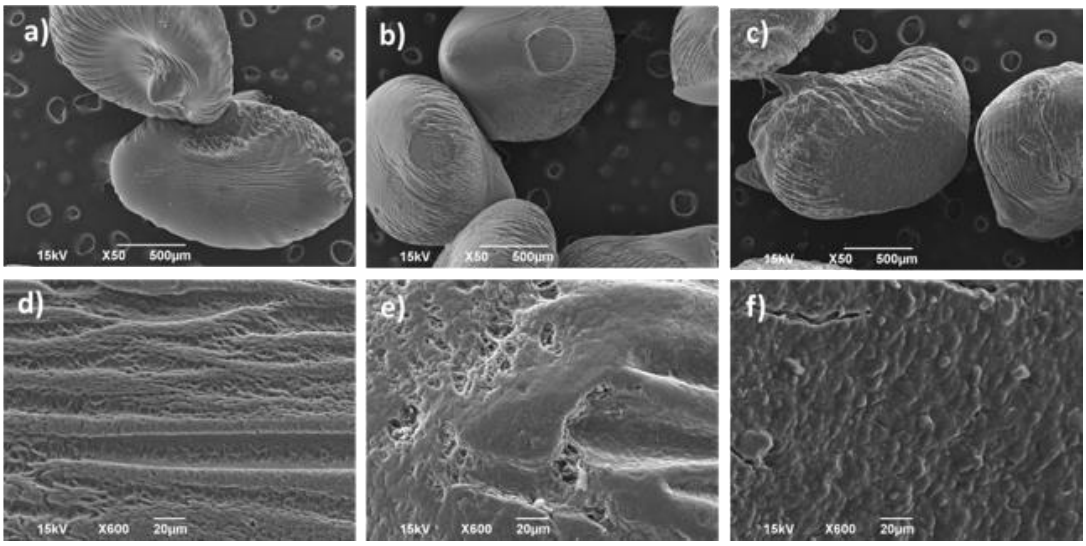

Figure 3.8: SEM micrographs of 100% CaAlg (a-d); 85% CaAlg - 15% Beeswax (b-e) and 50% CaAlg - 50% Beeswax (c-f) after 8h in SGF.

In order to simulate the real gastrointestinal transit, the swelling experiments were performed also by placing the beads for 2h in SGF and for the following 6h in SIF (Fig.3.9a). The results revealed a water uptake of about ~ 50% in acidic pH, due to alginate shrinking. A weight gain of ~ 30 times higher occurs when the pH becomes alkaline, with erosion but without any sign of disintegration for all the formulations (Fig. 3.9b-d).

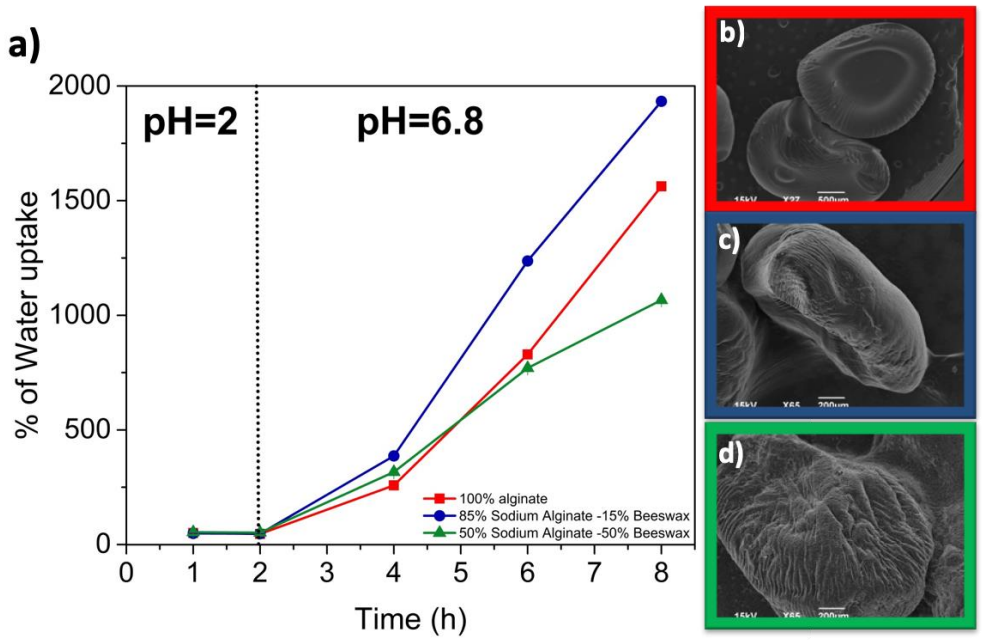

Figure 3.9: Swelling profiles (a) and SEM micrographs of 100% CaAlg (b), 85% CaAlg - 15% Beeswax (c) and 50% CaAlg - 50% Beeswax (c) after 8h under simulated gastrointestinal conditions.

3.3.4. Encapsulation of anthocyanin

Various formulation and process variables were investigated to maximize the encapsulation efficiency (EE%) of the anthocyanin inside the micro-particles. The EE% of *mcfe*, as a function of hardening time before separation of the beads from the gelation medium ($CaCl_2$ at 2% w/v) is reported in Tab.1. It was noticed that, prolonging the curing time from 2 to 10 min, a reduction in the encapsulation efficiency was recorded. In fact, due to its high solubility, the drug diffuses out of the beads into the calcium chloride solution. For this reason, a hardening time of 2 min was selected for further investigations.

Table 3.2: Effect of hardening time on the Encapsulation Efficiency of *mcfe*.

Curing time (min)	***100% CaAlg (EE%)***	***85% CaAlg -15% Beeswax (EE%)***	***50% CaAlg -50% Beeswax (EE%)***
2	94,5±0,005	93±0,004	81±0,006
5	89±0,005	86±0,005	74±0,004
10	80±0,001	81±0,006	70±0,003

A different formulation strategy to enhance the active molecule encapsulation efficiency was based on the addiction of a natural surfactant, soy lecithin. As lecithin consists of a glycerol backbone esterified with two fatty acids and a phosphate group, it has an excellent emulsifying property and it is widely applied as an emulsifier in food-grade emulsions [70-71]. As reported in Fig.3.10, increasing the amount of lecithin within the formulation leads to an increasing in the EE% values. The best surfactant concentration was found to be 5% w/w of polymer, while for higher concentrations of soy lecithin the encapsulation efficiency remained practically unvaried. With the addiction of 5% w/w soy lecithin the EE% values increased from 94.5% to 98 % for 100% alginate beads; from 93 % to 98 % for 85:15 samples and from 81% to 96% for 50:50 beads.

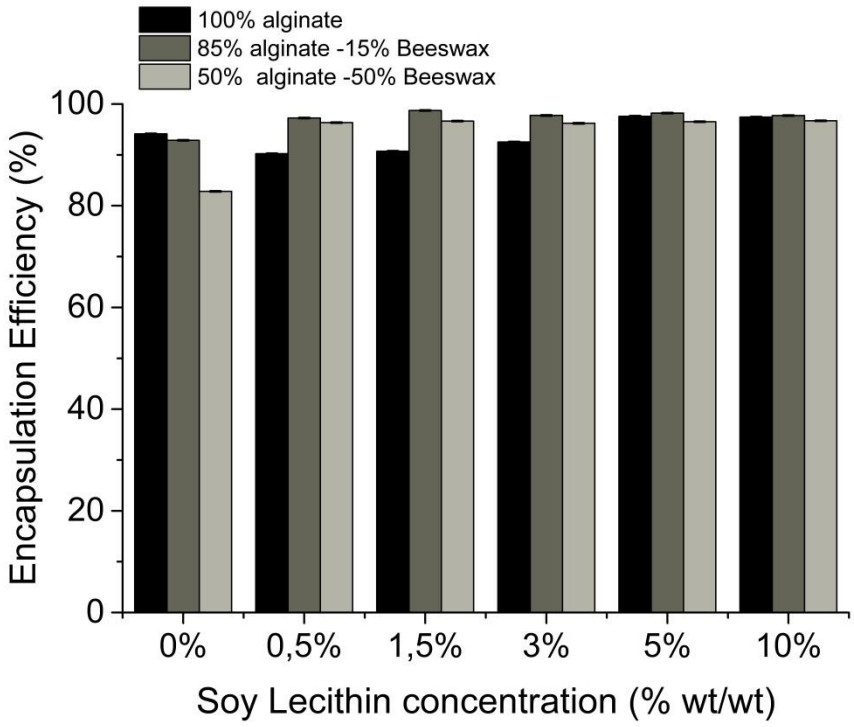

Figure 3.10: Effect of soy lecithin concentration on *mcfe* encapsulation efficiency.

3.3.5. In vitro release and antioxidant activity of mcfe from CaAlg-Beeswax emulsion gel beads

Drug release studies were carried out to examine the suitability of the CaAlg -Beeswax microparticles as an oral delivery system for *mcfe,* and to check whether Beeswax could retain the drug encapsulated. The release characteristic of *mcfe* was examined in simulated gastrointestinal fluids, SGF and SIF respectively. Fig.9 shows the cumulative release of the anthocyanin from CaAlg (conventional) beads and emulsion gel beads holding 15% or 50% w/w Beeswax. Under gastric condition (Fig.3.11a) the percentage of cumulative release from CaAlg or CaAlg - Beeswax, 85:15 and 50:50, microbeads within 2h was in the range of 53%, 59%, and 61% respectively, due to the insoluble alginic acid formation. This first phase of the delivery was followed by a second, slower drug release phase, after 4 hours and up

to 8 hours, where all the samples reached a plateau. In SGF the release of the anthocyanin was driven only by diffusion into the acidic medium. However, when the release was performed in SIF (Fig.3.11b) within 2h the percentage of cumulative release from alginate or alginate-Beeswax, 85:15 and 50:50, microbeads, was equal to 53%, 53%, and 50%, respectively. At the end of the experiment all the beads were completely rehydrated, and an opposite trend was observed starting from 4h, by increasing the amount of alginate within the beads also the amount of drug liberated increased. In SIF, the polymeric matrix is eroded thanks to the alkaline pH, and *mcfe* was released by both diffusion and erosion of the bead matrix. At the end of the experiment, all the beads were completely re-hydrated, and an opposite trend was observed starting from 4 hours. By increasing the amount of alginate within the beads, the amount of drug released also increased. In SIF, the polymeric matrix is eroded thanks to the alkaline pH, and *mcfe* was released by both diffusion and erosion of the matrix.

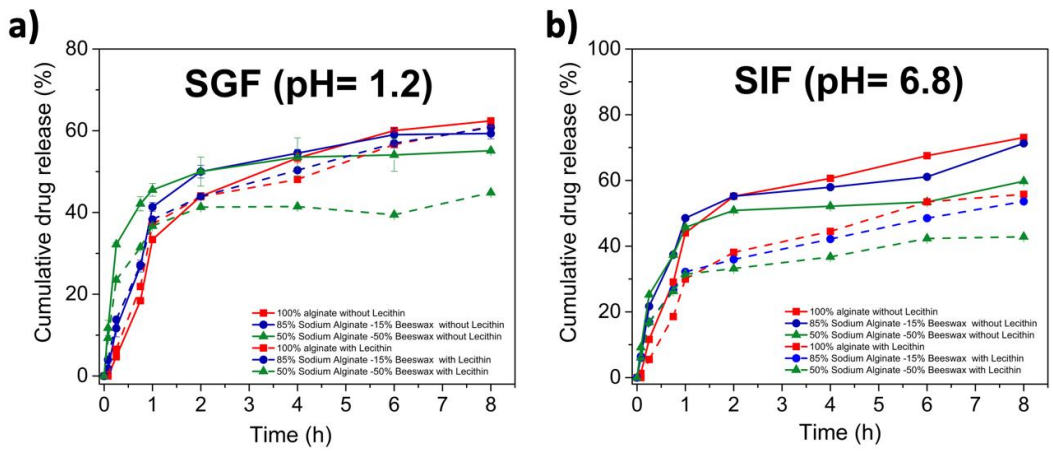

Figure 3.11: In vitro drug release studies in SGF (a) and SIF (b) up to 8h from emulsion gel beads with (Dash lines) and without (Solid lines) soy lecithin

In addition, the dissolution studies were carried by incubating the beads into the two different fluids, such as acidic medium and 6.8 phosphate buffer medium for a period of 2h and 8 h, at 37 °C under 100 rpm, to have a sequential release of the *mcfe*

simulating the real gastric transit (Fig.3.12a). In this case, within the first 2 h, 28–37 % of the drug was released in SGF from all the formulations. Specifically, 33%, 37% and 28% of *mcfe* was released from CaAlg (conventional), 85:15 and 50:50 beads, respectively. The rest of the entrapped drug was released in the SIF, lasting for up to 8 h with a sustained release, reaching 36-56% of the amount of drug released. Specifically, conventional alginate beads were able to release a further 23% of the molecule, resulting in a cumulative release of 56% after 8h. In contrast, for samples containing Beeswax a further release of 11% and 8% was measured, causing a cumulative release equal to 48% and 36% for beads comprising 15% and 50% of wax, respectively.

Under the same experimental conditions, antioxidant activity of the anthocyanin was also investigated. However, because anthocyanins can undergo conversion from the stable form of flavylium cation into unstable forms (quinonoidal base, carbinol pseudobase and chalcone C) by increasing the pH, we tested the formulation antioxidant activity only at low pH values. As seen in Fig.3.12b, the antioxidant can be released in a controlled manner, thanks to the presence of Beeswax into the bead matrix. The anthocyanin extract diffuses gradually in the surrounding media, prolonging the activity of the encapsulated anthocyanin. Particularly, at the end of 2h, *mcfe* activity was 94% for CaAlg beads and 86% and 78% for the particles comprising 15% and 50% of Beeswax, respectively. For instance, the composition of the microbeads and especially the content of wax can be considered as a control factor of the diffusion of the anthocyanin in the medium, maintaining its antioxidant properties.

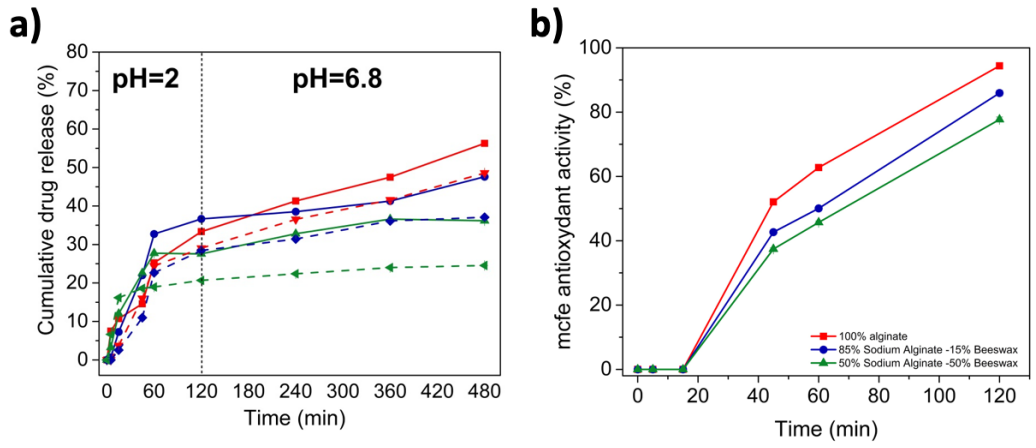

Figure 3.12: In *vitro* drug release of *mcfe* from the microparticles (a) without (solid lines) and with soy lecithin (Dash lines); (b) antioxidant properties of the anthocyanin released within the media. The first 2h of the experiment were performed at pH = 2 in SGF, while the next 6h at pH = 7 in SIF. The two media were prepared as described in the experimental section.

The whole release profiles may reflect the outcome of two contributing factors: the pH dependence of alginate, which is stable in acidic solution but swells and degrades under higher pH values, and the presence of Beeswax within the bead matrix that could retard the release from emulsion gel beads. Beeswax may confer hydrophobicity to the matrix, consequently delaying the diffusion of the drug from the beads. The addiction of the natural surfactant during the fabrication process demonstrated its function either in increasing the encapsulation efficiency of the natural extract or in delaying its delivery profile, as reported in Figs.3.11 (a-b) and 3.12 (a).

3.3.6. Effect of Porosity

3.3.6.1. Morphological analysis of freeze-dried beads and porosity examination

The surface and internal morphology of the lyophilized beads is reported in Fig.3.13(a.i). The freeze-dried beads displayed a slightly shrunk and rough surface. The cross-sectional view of these beads exhibited a spongy texture, with numerous open channel-like structures, which render them brittle to touch. The pores were formed when water molecules slowly sublimated from the polymeric network during the freezing step[72]. Notably, the three types of beads exhibited different pore morphology, although a microporous structure was observed in all of them. The beads comprising Beeswax within their matrix revealed smaller pore structures than the pure CaAlg beads, proportional to the amount of wax present.

Porous beads show in general, expectedly, lower values of Young's modulus and larger scatter in the results (standard deviation), as shown in Fig.3.13l . This is attributed to the inhomogeneity added by the freeze-thaw process, and to the variable amount of porosity, which make the stress states inhomogeneous. Nonetheless, the behavior of dry beads is similar to the non-porous ones, meaning that the addition of beeswax acts as a stiffener (from ≈0.5 to 2 Mpa).

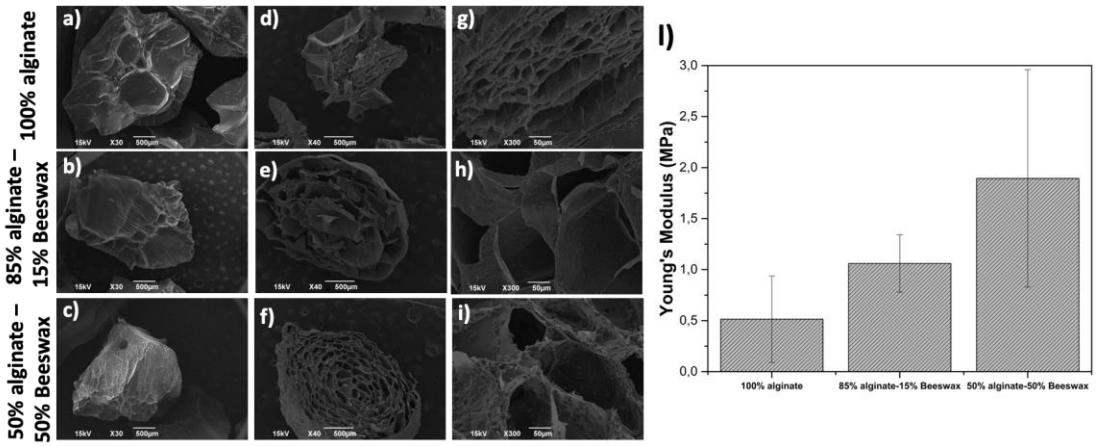

Figure 3.13: SEM micrographs of surface(a-c) and cross-sections (d-i) of calcium alginate-Beeswax emulsion gel beads and mechanical properties in the dry state (l).

A more quantitative analysis of the bead porosity was carried out via mercury intrusion porosimetry. Figure 3.14 shows the penetration plots, which represent the cumulative penetrated mercury volume that is intruded inside the sample under increasing pressure (up to 200 MPa). The penetration pressure is inversely proportional to the pore and particle size. The particle size distribution is not completely described by the mercury intrusion measurements, due to the average diameter of the beads exceeding 580 μm (the maximum particle size detectable by the instrument). It is possible to observe a remarkably different behavior for the two sets of prepared samples. Specifically, the porous samples exhibit a total intruded volume of mercury higher than the one measured for the non-porous beads. The values of total intruded volume achieved by the different samples are summarized in the Table 3.3. In fact, in addition to the penetration of the mercury inside the inter-particle voids, at higher pressure the mercury is also forced to intrude the intra-particle voids present in the porous beads. By increasing the amount of alginate inside the matrix it is possible to induce an enhancement of the system porosity. From the extrusion curves of the porous samples (Fig.3.14, red dash lines), it is

possible to infer the presence of an interconnected porous system, considering the amount of entrapped mercury within the porous beads after the measurements. On the other hand, the extrusion curves (Fig.3.14, black dash line) of the non-porous beads are similar to the intrusion curves[73], so no porosity is present in their structure. Further studies are needed in order to understand the total open pore volume for the accurate calculation of the pore size distribution. For this reason, the measurement of the material real density by a helium pycnometer is required to exclude any effect of sample compression during the analysis. The real density is independent on the particle aggregation degree and it is related to the real volume occupied by the material, if all the porosity is accessible by the helium. Thanks to this information it will be possible to define the intra-pore size distribution.

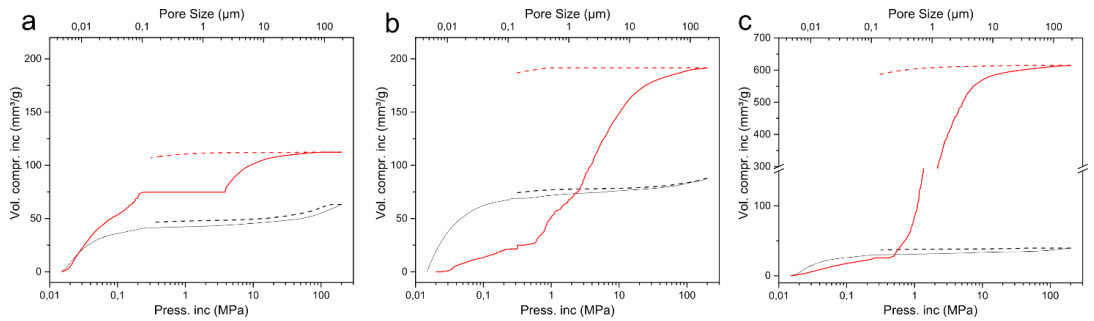

Figure 3.14. Mercury intrusion (solid line)/extrusion (dash line) curves of (a) 50/50, (b) 85/15 and (c) 100 of the non-porous (black) and porous (red) beads.

Table 3.3. Total intruded volume measured by mercury porosimetry.

	Total intruded volume (mm^3/g)	
Sample	**Non-porous**	**porous**
50/50	63.3	112.37
85/15	78.83	187.79
100	39.63	609.56

3.3.6.2. Swelling behavior and mechanical properties

As in the case of the oven dried beads, also for the lyophilized ones, the swelling degree was investigated. Due to their porous structure and larger size, freeze-dried beads showed higher water uptake capacity. In SGF (Fig.3.15a), the swelling degrees for all the hydrogels was quite low due to the proton-calcium exchange forming alginic acid regions, as the media penetrates into the bead gel network. However, in comparison to the oven dried samples, the lyophilized beads showed marginal swelling with a weight gain 5-fold higher (~ 200%), probably due to the penetration of the fluid through the pores.

However, in SIF (Fig.3.15b) freeze-dried samples had a weight gain, within the first 2h, of about 5-10 times higher according to the matrix composition. Subsequently, the bead structure started quickly to disaggregate, leading to the dissolution of the swollen beads at the end of 8h.

The mechanical properties of the freeze-dried samples in the wet state was also investigated (Fig.3.15c). Beads in SIF follow similar trends as the non-porous ones, with roughly constant values, although some stiffening is visible after 24h. Beads in SGF, similarly, resemble the non-porous ones, but in this case after 24h they are less stiff than at 1h.

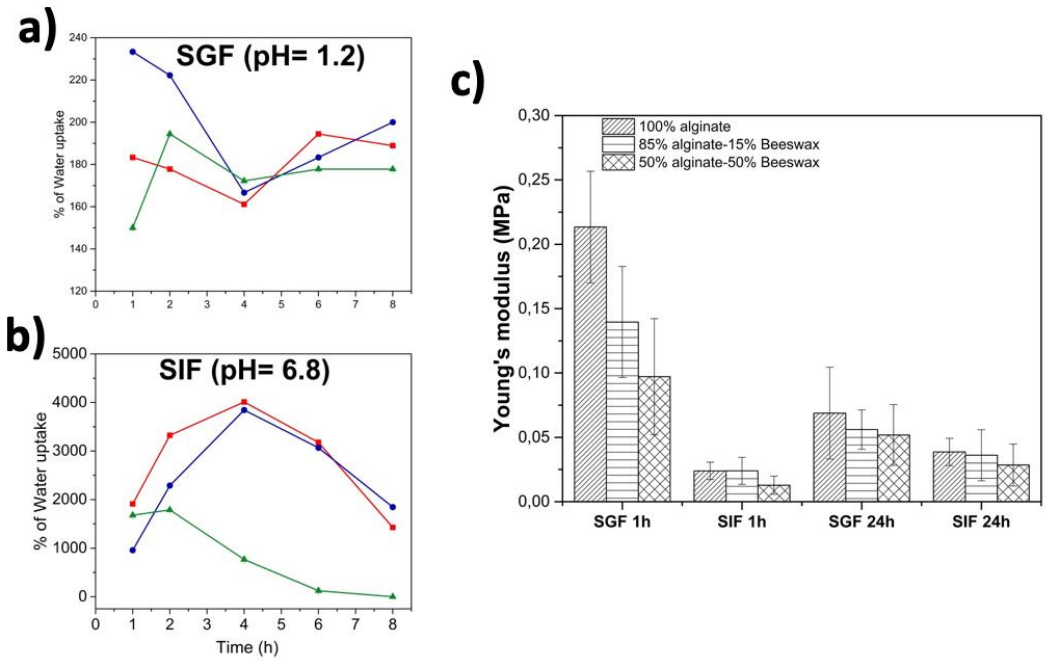

Figure 3.15: Swelling profiles of 100%CaAlg (red line); 85%CaAlg-15%Beeswax (blue line) and 50%CaAlg-50%Beeswax (green line) in SGF (a) and SFI (b). Mechanical properties of emulsion gel beads after immersion in SGF or SIF (c).

The swelling degree of calcium alginate-Beeswax microbeads in simulated gastric fluid (SGF) for 2h followed by simulated intestinal fluid (SIF) for 8h is shown in Fig. 3.16. Beads were found swollen in the gastric medium 4-time more respect to the non-porous beads. When they are subsequently transferred to the intestinal fluid, the beads began to disintegrate starting from 4h.

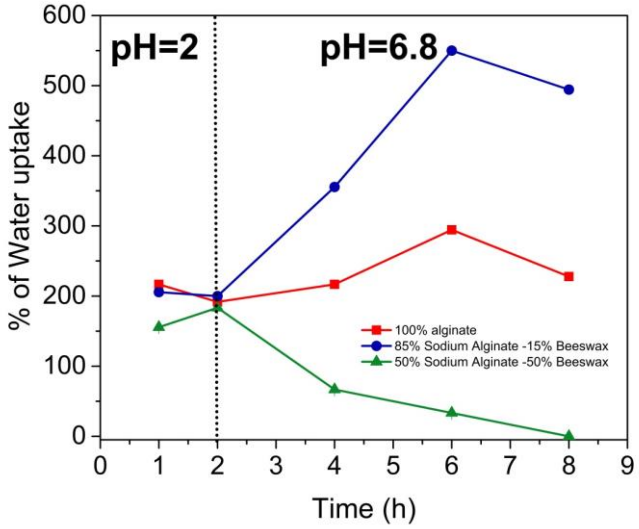

Figure 3.16: Swelling behavior of porous beads under sequential passage from SGF (2h) and SIF (8h).

3.3.6.3. In vitro drug release

The presence of pores within the microbeads structure is also able to influence the drug release properties of these matrices. As reported in Fig.3.17a, thus using the same material composition, the changes in beads morphology improved *mcfe* relase, making it faster. As reported in Fig. 3.17a, in SGF at the end of 2h was detected a 2-fold higher amount of anthocyanin, equal to 64%, 59% and 46% for 100% CaAlg, 85% CaAlg - 15% Beeswax and 50% CaAlg - 50% Beeswax respectively, in comparison to the quantity of drug released from not porous beads within this fluid. When the samples were subsequently incubated into SIF the amount of *mcfe* released was equal to 72%, 67% and 41% for 100% CaAlg, 85% CaAlg -15% Beeswax and 50% CaAlg - 50% Beeswax, respectively. The results suggested the potentiality of freeze-dried beads to accelerate the release of the anthocyanin, due to a higher exposure of the active molecule to the gastrointestinal fluids. Furthermore, also in the lyophilized samples, the presence of soy lecithin

(Fig.3.17b) was able to delay the amount of drug released of about half, in comparison with the beads without the emulsifying agent.

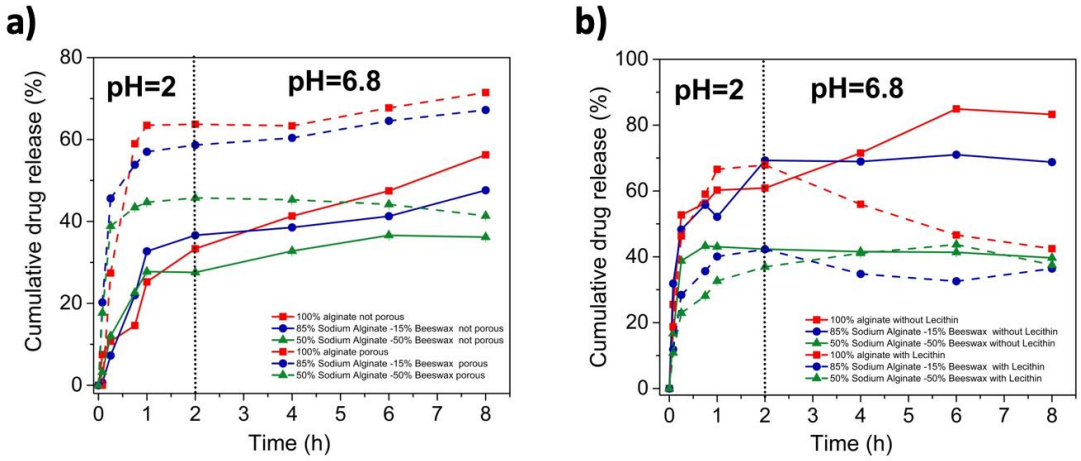

Figure 3.17: (a) In vitro drug release of *mcfe* from porous microbeads (dash lines) vs not porous beads (solid lines); (b) in vitro drug release profiles of *mcfe* from porous microbeads without (solid lines) and with soy lecithin (dash lines).

3.4. Conclusions

Prunus mahaleb L. anthocyanin-rich fruit extract (*mcfe*) was entrapped in calcium alginate-Beeswax emulsion gel beads prepared by emulsion gelation method, using calcium chloride as cross-linking agent. The beads were evaluated for their physico-chemical properties, morphology, drug entrapment efficiency, and drug release characteristics in enzyme free Simulated Gastric Fluid and Simulated Intestinal Fluid. The drug entrapment was optimized by decreasing the curing time into calcium chloride solution, due to the hydrophilicity of the active compound, and by adding the natural surfactant soy lecithin. Incorporation of Beeswax into the beads influenced the drug release. Therefore, an increased amount of wax favored an extended release of the anthocyanin from emulsion gel beads. In addition, *mcfe* appeared to be chemically stable and antioxidant activity was preserved upon encapsulation. Freeze-dried beads exhibited significant high release capability compared to the oven-dried forms due to a higher exposure of the molecule to the

fluids. We therefore suggested the application of calcium alginate-Beeswax emulsion gel beads, using a modified ionotropic gelation technique, as microcarrier to enhance the efficiency and control the delivery of the natural anthocyanin and improving its stability and bioavailability.

3.5. References

1. Castaneda-Ovando, A., de Lourdes Pacheco-Hernández, M., Páez-Hernández, M. E., Rodríguez, J. A., & Galán-Vidal, C. A. (2009). Chemical studies of anthocyanins: A review. Food chemistry, 113(4), 859-871.
2. Delgado-Vargas, Francisco, A. R. Jiménez, and O. Paredes-López. Natural pigments: carotenoids, anthocyanins, and betalains—characteristics, biosynthesis, processing, and stability. Critical reviews in food science and nutrition 40.3 (2000): 173-289.
3. Kong, J. M., Chia, L. S., Goh, N. K., Chia, T. F., & Brouillard, R. (2003). Analysis and biological activities of anthocyanins. Phytochemistry, 64(5), 923–933.
4. Clifford, M. N. (2000). Anthocyanins – nature, occurrence and dietary burden. Journal of the Science of Food and Agriculture, 80(7), 1063–1072.
5. Bongue-Bartelsman M, Phillips DA (1995) Nitrogen stress regulates gene expression of enzymes in the flavonoid biosynthetic pathway of tomato. Pl Physiol Biochem 33:539–546
6. de Pascual-Teresa, Sonia, and Maria Teresa Sanchez-Ballesta. Anthocyanins: from plant to health. Phytochemistry reviews 7.2 (2008): 281-299.
7. Khoo HE, Azlan A, Tang ST, Lim SM. Anthocyanidins and anthocyanins: colored pigments as food, pharmaceutical ingredients, and the potential health benefits. Food Nutr Res. 2017;61(1):1361779.
8. Pojer, E., Mattivi, F., Johnson, D., & Stockley, C. S. (2013). The case for anthocyanin consumption to promote human health: a

review. Comprehensive Reviews in Food Science and Food Safety, 12(5), 483-508.

9. Bagchi, D., Sen, C. K., Bagchi, M., & Atalay, M. (2004). Anti-angiogenic, antioxidant, and anti-carcinogenic properties of a novel anthocyanin-rich berry extract formula. Biochemistry (Moscow), 69(1), 75-80.
10. Lila, M. A., Burton-Freeman, B., Grace, M., & Kalt, W. (2016). Unraveling anthocyanin bioavailability for human health. Annual review of food science and technology, 7, 375-393.
11. Felgines, C., Texier, O., Besson, C., Lyan, B., Lamaison, J. L., & Scalbert, A. (2007). Strawberry pelargonidin glycosides are excreted in urine as intact glycosides and glucuronidated pelargonidin derivatives in rats. British Journal of Nutrition, 98(6), 1126-1131.
12. McGhie, Tony K., and Michaela C. Walton. The bioavailability and absorption of anthocyanins: towards a better understanding. Molecular nutrition & food research 51.6 (2007): 702-713.
13. Liu, Y., Zhang, D., Wu, Y., Wang, D., Wei, Y., Wu, J., et al. (2014). Stability and ab- sorption of anthocyanins from blueberries subjected to a simulated digestion process. International Journal of Food Science and Nutrition, 65, 440e448.
14. McDougall, G. J., Dobson, P., Smith, P., Blake, A., & Stewart, D. (2005). Assessing potential bioavailability of raspberry anthocyanins using an in vitro digestion system. Journal of Agricultural and Food Chemistry, 53, 5896e5904.
15. Czank, C., Cassidy, A., Zhang, Q., Morrison, D. J., Preston, T., Kroon, P. A., et al. (2013). Human metabolism and elimination of the anthocyanin, cyanidin-3-glucoside: a ^{13}C-tracer study. American Journal of Clinical Nutrition, 97,995e1003.

16. Ferrars, R. M., Czank, C., Zhang, Q., Botting, N., Kroon, P. A., Cassidy, A., et al. (2014). The pharmacokinetics of anthocyanins and their metabolites in humans. British Journal of Pharmacology, 171, 3268e3282.
17. Fleschhut, J., Kratzer, F., Rechkemmer, G., & Kulling, S. E. (2006). Stability and biotransformation of various dietary anthocyanins in vitro. European Journal of Nutrition, 45, 7e18.
18. Kopjar M, Orsolic M, Pilizota V. Anthocyanins, phenols, and anti- oxidant activity of sour cherry puree extracts and their stability during storage. Int J Food Prop. 2014;17:1393–1405.
19. Chung C, Rojanasasithara T, Mutilangi W, et al. Enhanced stability of anthocyanin-based color in model beverage systems through whey protein isolate complexation. Food Res Int. 2015;76:761–768.
20. Fang, Zhongxiang, and Bhesh Bhandari. Encapsulation of polyphenols–a review. Trends in Food Science & Technology21.10 (2010): 510-523.
21. Munin, Aude, and Florence Edwards-Lévy. Encapsulation of natural polyphenolic compounds; a review. Pharmaceutics 3.4 (2011): 793-829.
22. Lu, Wei, Alan L. Kelly, and Song Miao. Emulsion-based encapsulation and delivery systems for polyphenols. Trends in food science & technology 47 (2016): 1-9.
23. Blando, F., Albano, C., Liu, Y., Nicoletti, I., Corradini, D., Tommasi, N., ... & Kitts, D. D. (2016). Polyphenolic composition and antioxidant activity of the under-utilised Prunus mahaleb L. fruit. Journal of the Science of Food and Agriculture, 96(8), 2641-2649.
24. Gerardi, C., Tommasi, N., Albano, C., Blando, F., Rescio, L., Pinthus, E., & Mita, G. (2015). Prunus mahaleb L. fruit extracts: a novel source for natural food pigments. European Food Research and Technology, 241(5), 683-695.
25. Gerardi, C., Frassinetti, S., Caltavuturo, L., Leone, A., Lecci, R., Calabriso, N., ... & Mita, G. (2016). Anti-proliferative, anti-inflammatory and anti-

mutagenic activities of a Prunus mahaleb L. anthocyanin-rich fruit extract. Journal of Functional Foods, 27, 537-548.

26. Madziva, H., Kasipathy Kailasapathy, and Michael Phillips. Evaluation of alginate–pectin capsules in Cheddar cheese as a food carrier for the delivery of folic acid. LWT-Food Science and Technology 39.2 (2006): 146-151.
27. Anbinder, P. S., Deladino, L., Navarro, A. S., Amalvy, J. I., & Martino, M. N. (2011). Yerba mate extract encapsulation with alginate and chitosan systems: interactions between active compound encapsulation polymers. Journal of Encapsulation and Adsorption Sciences, 1(04), 80-87.
28. Goh, Cheong Hian, Paul Wan Sia Heng, and Lai Wah Chan. Alginates as a useful natural polymer for microencapsulation and therapeutic applications. Carbohydrate Polymers 88.1 (2012): 1-12.
29. Gombotz, Wayne R., and Siow Fong Wee. Protein release from alginate matrices. Advanced drug delivery reviews 64 (2012): 194-205.
30. Sarmento, B., Ferreira, D., Veiga, F., & Ribeiro, A. (2006). Characterization of insulin-loaded alginate nanoparticles produced by ionotropic pre-gelation through DSC and FTIR studies. Carbohydrate Polymers, 66(1), 1-7.
31. Leonard, M., De Boisseson, M. R., Hubert, P., Dalencon, F., & Dellacherie, E. (2004). Hydrophobically modified alginate hydrogels as protein carriers with specific controlled release properties. Journal of controlled release, 98(3), 395-405.
32. Chen, S. C., Wu, Y. C., Mi, F. L., Lin, Y. H., Yu, L. C., & Sung, H. W. (2004). A novel pH-sensitive hydrogel composed of N, O-carboxymethyl chitosan and alginate cross-linked by genipin for protein drug delivery. Journal of Controlled Release, 96(2), 285-300.
33. Østberg, Tone, Ellen Marie Lund, and Christina Graffner. Calcium alginate matrices for oral multiple unit administration: IV. Release characteristics in different media. International Journal of Pharmaceutics 112.3 (1994): 241-248.

34. Sugawara, Shinya, Teruko Imai, and Masaki Otagiri. The controlled release of prednisolone using alginate gel. Pharmaceutical Research 11.2 (1994): 272-277.
35. Zheng, H., Zhou, Z., Chen, Y., Huang, J., & Xiong, F. (2007). pH-sensitive alginate/soy protein microspheres as drug transporter. Journal of applied polymer science, 106(2), 1034-1041.
36. Stojanovic, R., Belscak-Cvitanovic, A., Manojlovic, V., Komes, D., Nedovic, V., & Bugarski, B. (2012). Encapsulation of thyme (Thymus serpyllum L.) aqueous extract in calcium alginate beads. Journal of the Science of Food and Agriculture, 92(3), 685-696.
37. Đorđević, V., Balanč, B., Belščak-Cvitanović, A., Lević, S., Trifković, K., Kalušević, A., Kostić, I., Komes, D., Bugarski, B., & Nedović, V. (2015). Trends in encapsulation technologies for delivery of food bioactive compounds. Food Engineering Reviews, 7(4), 452-490. 2015.
38. Nedovic, V., Kalusevic, A., Manojlovic, V., Levic, S., & Bugarski, B. (2011). An overview of encapsulation technologies for food applications. Procedia Food Science, 1, 1806-1815.
39. Alejandro Sosnik, Alginate Particles as Platform for Drug Delivery by the Oral Route: State-of-the-Art, ISRN Pharmaceutics, vol. 2014, Article ID 926157, 17 pages, 2014.
40. Tiwari, Ritesh Kumar, Lalit Singh, and Vijay Sharma. Alginate micro-beads in novel drug delivery system: an overview. IJPT 5.1 (2013): 1-13.
41. Kim, M. S., Park, G. D., Jun, S. W., Lee, S., Park, J. S., & Hwang, S. J. (2005). Controlled release tamsulosin hydrochloride from alginate beads with waxy materials. Journal of pharmacy and pharmacology, 57(12), 1521-1528.
42. Lupo, B., Maestro, A., Porras, M., Gutiérrez, J. M., & González, C. (2014). Preparation of alginate microspheres by emulsification/internal gelation to encapsulate cocoa polyphenols. Food Hydrocolloids, 38, 56-65.

43. Arriola, D.A., Chater, P.I., Wilcox, M., Lucini, L., Rocchetti, G., Dalmina, M., Pearson, J.P., de Mello Castanho Amboni, R.D., Encapsulation of Stevia rebaudiana Bertoni aqueous crude extracts by ionic gelation – Effects of alginate blends and gelling solutions on the polyphenolic profile, Food Chemistry (2018).
44. Deladino, L., Anbinder, P. S., Navarro, A. S., & Martino, M. N. (2008). Encapsulation of natural antioxidants extracted from Ilex paraguariensis. Carbohydrate Polymers, 71, 126e134.
45. Belščak-Cvitanović, A., Bušić, A., Barišić, L., Vrsaljko, D., Karlović, S., Špoljarić, I., Vojvodić, A., Mršić, G., Komes, D., Emulsion templated microencapsulation of dandelion (Taraxacum officinale L.) polyphenols and ß-carotene by ionotropic gelation of alginate and pectin, Food Hydrocolloids (2016).
46. de Moura, S.C.S., Berling, C.L., Germer, S.P.M., Alvim, I.D., Hubinger, M.D., Encapsulating anthocyanins from Hibiscus sabdariffa L. calyces by ionic gelation: Pigment stability during storage of microparticles, Food Chemistry (2017).
47. Zam, W., Bashour, G., Abdelwahed, W., & Khayata, W. (2014). Alginate-pomegranate peels' polyphenols beads: Effects of formulation parameters on loading efficiency. Brazilian Journal of Pharmaceutical Sciences, 50, 741-748.
48. Soradech, S., Petchtubtim, I., Thongdon-A, J., & Muangman, T. (2016). Development of Wax-Incorporated Emulsion Gel Beads for the Encapsulation and Intragastric Floating Delivery of the Active Antioxidant from Tamarindus indica L. Molecules, 21(3), 380.
49. Yamdech, Rungnapha, Pornanong Aramwit, and Sorada Kanokpanont. Stability of Anthocyanin in Mulberry Fruits Extract Adsorbed on Calcium Alginate Beads. International Conference Chulalongkorn University, Bangkok Thailand. 2012.

50. Celli, Giovana Bonat, Amyl Ghanem, and Marianne Su-Ling Brooks. Optimized encapsulation of anthocyanin-rich extract from haskap berries (Lonicera caerulea L.) in calcium-alginate microparticles.Journal of Berry Research 6.1 (2016): 1-11.
51. Pongjanyakul, Thaned, and Satit Puttipipatkhachorn. Xanthan–alginate composite gel beads: molecular interaction and in vitro characterization. International Journal of Pharmaceutics 331.1 (2007): 61-71.
52. R. Bodmeier, J. Herrmann: Waxes, in: Encyclopedia of Pharmaceutical Technology, volume 16 (editors, J. Swarbrick, J.C. Boylan), Marcel Dekker, 335-361 (1997).
53. Milanovic, J., Manojlovic, V., Levic, S., Rajic, N., Nedovic, V., & Bugarski, B. (2010). Microencapsulation of flavors in carnauba wax. Sensors, 10(1), 901-912.
54. Shaki, H., Vasheghani-Farahani, E., Shojaosadati, S. A., & Ganji, F. (2014). Optimizing formulation variables of KCl loaded waxy microspheres. Iranian Journal of Pharmaceutical Sciences, 10(1), 37-54.
55. Mellema, M., Van Benthum, W. A. J., Boer, B., Von Harras, J., & Visser, A. (2006). Wax encapsulation of water-soluble compounds for application in foods. Journal of microencapsulation, 23(7), 729-740.
56. Chitprasert, P., & Sutaphanit, P. (2014). Holy basil (Ocimum sanctum Linn.) essential oil delivery to swine 371 gastrointestinal tract using gelatin microcapsules coated with aluminum carboxymethyl cellulose and beeswax. 372 Journal of agricultural and food chemistry, 62, 12641-12648.
57. Ranjha, N. M., Khan, H., & Naseem, S. (2010). Encapsulation and characterization of controlled release 414 flurbiprofen loaded microspheres using beeswax as an encapsulating agent. Journal of Materials Science: 415 Materials in Medicine, 21, 1621-1630.

58. Haghighat-Kharazi, S., Milani, J. M., Kasaai, M. R., & Khajeh, K. (2018). Microencapsulation of α-amylase in beeswax and its application in gluten-free bread as an anti-staling agent. LWT, 92, 73–79.
59. Gowda, D. V.; Ravi, V.; Shivakumar, H. G.; Hatna, S. Preparation, evaluation and bioavailability studies of indomethacin- bees wax microspheres. J. Mater. Sci. Mater. Med. 2009, 20, 1447− 1456.
60. Giannola, L. I., V. De Caro, and M. C. Rizzo. Preparation of white beeswax microspheres loaded with valproic acid and kinetic study of drug release. Drug development and industrial pharmacy 21.7 (1995): 793-807.
61. Giannola, L. I., V. Stefano Di, and V. Caro De. White beeswax microspheres: a comparative in vitro evaluation of cumulative release of the anticancer agents fluorouracil and ftorafur. Die Pharmazie 48.2 (1993): 123-126.
62. Gifani, A., Taghizadeh, M., Seifkordi, A. A., & Ardjmand, M. (2009). Preparation and investigation the release behaviour of wax microspheres loaded with salicylic acid. Journal of microencapsulation, 26(6), 485-492.
63. Shaltooki, Parisa, and Afshin Farahbakhsh. Encapsulation of material using bees wax. (2015).
64. Svečnjak, L., Baranović, G., Vinceković, M., Prđun, S., Bubalo, D., & Gajger, I. T. (2015). An approach for routine analytical detection of beeswax adulteration using FTIR-ATR spectroscopy. Journal of apicultural science, 59(2), 37-49.
65. Tong, Z., Chen, Y., Liu, Y., Tong, L., Chu, J., Xiao, K., Zhou, Z., Dong, W. & Chu, X. (2017). Preparation, Characterization and Properties of Alginate/Poly (γ-glutamic acid) Composite Microparticles. Marine drugs, 15(4), 91.
66. Lim, J. H., Kim, J. A., Ko, J. A., & Park, H. J. (2015). Preparation and characterization of composites based on polylactic acid and beeswax with improved water vapor barrier properties. Journal of food science, 80(11), E2471-E2477.

67. Soares, J. P.; Santos, J. E.; Chierice, G. O.; Cavalheiro, E. T. G. Thermal behavior of alginic acid and its sodium salt. Ecletica Quim. 2004, 29 (2), 57.
68. Pasparakis G, Bouropoulos N (2006) Swelling studies and in vitro release of verapamil from calcium alginate and calcium alginate–chitosan beads. Int J Pharm 323:34–42
69. Tønnesen, Hanne Hjorth, and Jan Karlsen. Alginate in drug delivery systems. Drug development and industrial pharmacy28.6 (2002): 621-630.
70. Kim, W.-T., Chung, H., Shin, I. I.-S., Yam, K. L., & Chung, D. (2008). Characterization of calcium alginate and chitosan-treated calcium alginate gel beads entrapping allyl isothiocyanate. Carbohydrate Polymers, 71, 566–573.
71. Xu, Q., Nakajima, M., Liu, Z., & Shiina, T. (2011). Soybean-based surfactants and their applications. In Soybean-Applications and Technology. InTech.
72. Machado, A. R., de Assis, L. M., Machado, M. I. R., & de Souza-Soares, L. A. (2014). Importance of lecithin for encapsulation processes. African Journal of Food Science, 8(4), 176-183.
73. Nail, Steven L., and Larry A. Gatlin. Freeze-drying: principles and practice. Pharmaceutical Dosage Forms-Parenteral Medications. CRC Press, 2016. 366-394.
74. Chan, E. S., Wong, S. L., Lee, P. P., Lee, J. S., Ti, T. B., Zhang, Z., Poncelet, D., Ravindra, P., Phan, S.H. & Yim, Z. H. (2011). Effects of starch filler on the physical properties of lyophilized calcium–alginate beads and the viability of encapsulated cells. Carbohydrate Polymers, 83(1), 225-232.

Chapter 4

Conclusions

Due to their biodegradability, biocompatibility, heterogeneity in architecture, chemical tailorability, morphology, and degradation rate, bio-polymers have been widely used for the development of several drug delivery systems. The latter have become very attractive in the biomedical and pharmaceutical fields, because they can overcome issues related to the conventional drug formulations. In fact, they are able to deliver active principles in a controlled and targeted manner, maintaining the drug levels within the therapeutic window, overcoming the risk of over or under dosage, and reducing the frequency of drug administration while increasing the patient compliance.

Herein, two polymeric systems were developed using the same technique of fabrication, ***emulsification***, which is a facile, inexpensive, quick method for *bio-composite fabrication*, and allows the combination of different materials in an *easy-to-scale-up approach*. This technique is very versatile because can be used both for the encapsulation of bioactive compound or to combine materials with different physiochemical properties (hydrophilic and hydrophobic). In both developed systems ***sodium alginate*** was the hydrophilic polymer, widely investigated in the biomedical field due to its natural origin, low cost, biocompatibility, biodegradability, non-toxicity, and non-immunogenicity.

The first system was fabricated by means of *emulsion casting and solvent evaporation method*, with the aim of obtaining *composite solid films with varying MaterBi®-alginate fractions*. MaterBi® is a commercial hydrophobic and biodegradable polymer, consisting of polycaprolactone (PCL) and thermoplastic starch. This bio-polymer, obtained by a proprietary compound extrusion method, is actively marketed as sustainable food packaging material as well as biodegradable material for perishable food containers. However, it has not been applied in the biomedical field so far. In this case, our bio-composite material was design in order *to simultaneously release two selected drugs*, for the treatment of skin wounds. Neomercurocromo®, a commercially available antiseptic agent used topically for the local treatment of wounds, was identified as the hydrophilic component, while Curcumin was selected as lipophilic model drug. This natural yellow pigment has been widely studied as a wound healing agent, able to treat cutaneous, chronic and excisional wounds, and to accelerate the healing process, given its anti-inflammatory, anti-oxidant and anti-infective properties. With our alginate-MaterBi® system ***we demonstrated for the first time the possibility of using MaterBi® also in the pharmaceutical field, as a potential wound care materia[1]***. Our results demonstrated that ultrasonic-assisted self-emulsification between two biopolymers allow us to obtain stable and surfactant-free emulsions. Solid films comprising different alginate: MaterBi® ratios (100% alginate, 50wt.%alginate-50wt.% MaterBi®, 30wt.%alginate-70wt.% MaterBi®, and 100% MaterBi®), were obtained upon casting and solvent evaporation. The morphological analysis revealed a foam-like cellular features for the composite films, while for pure MaterBi® the presence of starch granules embedded within PCL matrix was detected. Although beyond the scope of this study, formation of stable surfactant- free emulsions can be attributed to the emulsion stabilization properties of starches. The presence of MaterBi® affected both the thermal degradation and mechanical properties of the biocomposite films. The emulsions were also able to incorporate two model drugs, namely the hydrophilic antiseptic Neomercurocromo® and the hydrophobic curcumin. Release

studies demonstrated the ability of the composite matrices to release the two model drugs individually or simultaneously and in a sustained manner, either by tuning the polymer fraction in the films during emulsification or by crosslinking sodium alginate fraction of the films by calcium salt solution immersion. Moreover, the films demonstrate excellent cell biocompatibility against human dermal fibroblast, adult cells.

The second construct was prepared via *hot-melt extrusion along with ionotropic gelation,* blending *sodium alginate with Beeswax to obtain emulsion gel beads, encapsulating a concentrated extract from Prunus mahaleb L. fruit (mcfe).* Beeswax is a natural and edible material, with good stability at different pHs and moisture content, biocompatibility, no immunogenicity. In addition, it is non-swellable and water insoluble, features which make it safe for oral application in humans. All these properties suggest a high potential for pharmaceutical applications, such as encapsulation of various types of drugs, and delivery retardant. Anthocyanins (ACNs) are a group of water-soluble natural pigments present in plants with health-promoting, anti-oxidant properties. The extract under study was characterized for its phenolic content, revealing a high concentration of bioactive compounds, especially ACNs, and exhibiting a strong antioxidant capacity. Moreover, it showed biological activities, such as anti-proliferative, anti-inflammatory and anti-mutagenic properties.

The aim of this work was to optimize the encapsulation of *mcfe* in ***calcium alginate-Beeswax emulsion gel microbeads to obtain an all-natural delivery system.*** The final system is envisioned as *gastro-retentive platform* able to increase the residence time and modulate the release of ACNs in the upper gastrointestinal tract, where they are completely released and absorbed. Our results demonstrated that the presence of Beeswax within the bead matrix affects the size, and both the external and the internal morphology of the samples. The morphological analysis revealed a red-blood cell like shape for conventional CaAlg beads and a drop-like

shape for alginate-Beeswax composite beads. The presence of Beeswax affected both the thermal degradation and mechanical properties of the composite beads.
The water swelling ability of conventional CaAlg or alginate-Beeswax composite beads after re-hydration in SGF and SIF, separately or sequentially (2h in SGF and 6h in SIF) revealed that the swelling was influenced both by the pH and the matrix composition.

The pH of the media influenced the release profiles of the *mcfe*-loaded beads, previously optimized in their formulation in terms of hardening time (calcium chloride solution of 2%w/v) and addition of the natural surfactant soy lecithin, evaluating the effect of these parameters on the encapsulation efficiency of the active molecules. Drug release experiments, performed under simulated gastrointestinal conditions, revealed that the incorporation of Beeswax within the bead matrix favored an extended release of the anthocyanin from emulsion gel beads.
The addiction to the formulation of soy lecithin, as surfactant, demonstrated its capability not only to help the EE% of the anthocyanin, but also to slow down the percentage of drug released.

Antioxidant properties of the anthocyanin were also investigated, revealing that its antioxidant activity was preserved upon encapsulation. Change in matrix structure, through the induction of porosity thanks to freeze-drying process, revealed a higher amount of anthocyanin released in comparison to the not-porous beads, due to an high exposure of the bioactive molecule to the fluids. These results suggested the possible application of calcium alginate-Beeswax emulsion gel beads, using a modified ionotropic gelation technique, as microcarrier to enhance the efficiency and control the delivery of the natural anthocyanin.

References

1. Setti, Chiara, et al. "Investigation of in vitro Hydrophilic and Hydrophobic Dual Drug Release from Polymeric Films Produced by Sodium alginate-MaterBi® Drying Emulsions." European Journal of Pharmaceutics and Biopharmaceutics (2018).